

NATIONAL ACADEMY OF SCIENCES OF UKRAINE
B. Verkin INSTITUTE FOR LOW TEMPERATURE PHYSICS
AND ENGINEERING

NATIONAL ACADEMY OF SCIENCES OF UKRAINE
B. Verkin INSTITUTE FOR LOW TEMPERATURE PHYSICS AND
ENGINEERING

Qualification scientific
work printed as manuscript

Bahrova M. Olha

UDK 538.93

DISSERTATION

**ELECTROMECHANICAL PHENOMENA
IN NORMAL AND SUPERCONDUCTING
NANOSTRUCTURES
BASED ON A MOVABLE QUANTUM DOT**

104 — "Physics and Astronomy"

10 — "Natural Sciences"

Submitted for obtaining the Doctor of Philosophy degree

The dissertation contains the results of own research. The ideas, results, and texts of the

other authors are referred accordingly _____ O.M. Bahrova
(candidate's signature)

**Supervisor: Kulinich I. Sergei,
Candidate of Physico-Mathematical Sciences,
Senior Researcher**

Kharkiv – 2023

ABSTRACT

Bahrova O.M. ELECTROMECHANICAL PHENOMENA IN NORMAL AND SUPERCONDUCTING NANOSTRUCTURES BASED ON A MOVABLE QUANTUM DOT. — Manuscript.

Dissertation for a Doctor of Philosophy degree on speciality 104 – Physics and Astronomy. — B. Verkin Institute for Low Temperature Physics and Engineering, NAS of Ukraine, Kharkiv, 2023.

The dissertation is devoted to the study of new fundamental phenomena which emerge due to electromechanical coupling in mesoscopic systems based on movable quantum dot.

In the **introduction** it is briefly justified the relevance of the dissertation topic, defined the purpose and main tasks of the research, as well as objects, subject and research methods. The scientific novelty and practical value of the obtained results are formulated. The information about the publications, the personal applicant's contribution and the approbation of the results of the dissertation are discussed. The information about the structure and volume of the dissertation is also given.

The **chapter 1** is devoted to the review and analysis of the literature related to the topic of the dissertation. The main phenomena which arise in the electron transport through a single-electron transistor, are considered. Namely, Landauer-Büttiker approach and the Coulomb blockade of electron tunneling are introduced. The **subsection 1.1.2** is devoted to the polaronic effects in transport of electrons in molecular transistors. In particular, the origin of the Franck-Condon (polaronic) blockade and polaronic narrowing of the energy level width are discussed as well as non-monotonic temperature dependence of the differential conductance. In addition, in the last part of the **subsection 1.1.2** a special case of a non-equilibrium vibron subsystem is briefly considered.

In contrast to the first part of the **chapter 1**, where influence of the mechanical vibrations of a quantum dot on the electron transport is discussed, in the further parts we alternatively take into account the evolution of the mechanical subsystem under an impact of the tunneling of electrons. Thus, in the **section 1.2** the concept of a driven qubit and Landau-Zener-Stückelberg-Majorana formula for transition probability are introduced. Also, some protocols for quantum error correction codes and its importance in the further consideration are discussed. In

the **section 1.3** nature of the mechanical instability phenomenon and key results are considered.

The **chapter 2** is devoted to the derivation and analysis of polaronic effects which emerge due to the *non-equilibrium* coherent vibron subsystem.

In the **section 2.1** a model device is introduced. A single-molecule transistor consists of a big molecule which is placed between two bulk electrodes biased by a constant voltage. The quantum dot which models the molecule, undergoes quantum oscillations in the direction perpendicular to the electron transport flow. It also gated by the gate voltage in order to control the energy of a single-electron level in the quantum dot.

In the **section 2.2** Hamiltonian of the system under consideration is presented and equations for the density matrix of the electronic subsystem are obtained.

In the **section 2.3** an analytical expression for the electric current through the single-molecular transistor is derived. In the **section 2.4** results of numerical calculations for the current-voltage characteristics (I - V curves) are presented and analysed. The correspondence between the current-voltage curves obtained for the assumption of the vibron subsystem being in coherent (*non-equilibrium*) state and Franck-Condon steps for equilibrated vibrons are drawn. It is demonstrated that in contrast to the Franck-Condon theory, in our case of coherent vibrons steps in the current-voltage characteristics are completely non-regular. Moreover, for the vibrons being in coherent state, the current saturates at much lower bias voltages. This can be effective in experiments which require working in a regime out of the polaronic blockade, i.e., maximal currents.

In the **section 2.5** a quite simple analytical formula for the electric current is found. The approximation gives high-precision agreement with the main results.

The **chapter 3** is devoted to the obtaining and analysis of entanglement between electronic and mechanical degrees of freedom in a superconducting nanoelectromechanical device.

In the **section 3.1** a model of the nanoelectromechanical device under consideration is introduced. The system consists of a superconducting nanowire suspended over two superconducting leads. The nanowire which is treated as a charge qubit (Cooper pair box), undergoes bending vibrations in the perpendicular to the nanowire axis direction. Furthermore, the nanowire is capacitively coupled to

the gate electrodes which allow one to control the difference between the energy levels of the qubit. Also, the superconducting phase difference between the electrodes can be tuned by the constant bias voltage applied to them as a result of non-stationary (ac) Josephson effect. The Hamiltonian of the system is derived.

In the **section 3.2** time evolution of the pure state of the system is found. It is demonstrated that initial pure state evolves into the state represented by entanglement between the two qubit states and two coherent states of the mechanical resonator.

In the **section 3.3**, which represents the main result of this chapter, we propose and derive a specific bias voltage manipulation protocol which results in the formation of entanglement between two states of the charge qubit and two Schrödinger-cat states (superposition of two coherent states) starting from the initial pure state. The considered protocol due to its simplicity can effectively be implemented in experiments with encoding quantum information from the electronic qubit states to coherent (cat states, in particular) of a nanomechanical resonator. Moreover, the cat states due to its structure are not sensitive to errors. Thus, the proposed scheme does not require additional quantum error correction protocols.

In the **section 3.4** the entanglement (von Neumann) entropy is considered in order to quantitatively analyse the entanglement between charge states of the qubit and coherent states of the nanomechanical resonator. Further, in the **section 3.5** time evolution of the mechanical subsystem is discussed. A clear justification of presence of the entanglement is presented by analysing corresponding Wigner functions.

In the **section 3.6** an experimentally feasible method for the detection of signatures of the entanglement by measuring average current is discussed.

The **chapter 4** is devoted to the derivation and analysis of nanomechanical phenomena which arise due to proximity effect in the following hybrid nanoelectromechanical device. The system under consideration involves a carbon nanotube suspended above a trench in a normal metal electrode and positioned in a gap between two superconducting leads. Moreover, the nanotube undergoes bending vibrations in between two superconducting electrodes in such a way that the bending of the nanotube moves it closer to one electrode and further away from the other. It results in the position-dependent tunneling amplitudes. In addition,

due to the presence of superconducting phase difference between the leads, the off-diagonal order parameter of the quantum dot emerges as a result of superconducting proximity effect. Lastly, the bias voltage applied to the normal electrode induces directed electron dynamics in the system.

In the **section 4.1** the semi-classical approach within the density matrix approximation is used to obtain and analyse the regime of mechanically *unstable* states.

In the **subsection 4.1.1** the model of the considered nanoelectromechanical device and Hamiltonian are introduced. In the **subsection 4.1.2** the density matrix approximation is considered. The system of equation for the density matrix elements together with the second-order nonlinear differential equation for the quantum dot displacement is derived. Additionally, in the **subsection 4.1.3** the Green function formalism is used to find the quantum dot order parameter induced by superconducting proximity effect.

In the **subsection 4.1.4** the consideration within an adiabatic limit allow one to simplify the problem to one strongly nonlinear differential equation (which is the central one in this chapter) for the displacement and analytically analyse it by using a simple linearization method as in **subsection 4.1.5**. Furthermore, in the **subsection 4.1.6** the Krylov-Bogoliubov method of averaging is used to find an approximate solution and analyse regimes in which the nanoelectromechanical system under consideration can operate. Two states of mechanical subsystem are discussed. In particular, it is demonstrated that in the mechanically *unstable* regime the limit cycles of self-sustained oscillations occur. Moreover, the self-saturation effect takes place. In the **subsection 4.1.7** the main results are generalized to the case of asymmetric tunnel contacts and the influence of a thermodynamic environment.

In the **subsection 4.1.8** a possibility to experimentally detect the mechanical instability in the system due to electric current measurements is discussed. It is demonstrated that the device can operate in transistor and diode regimes.

In the **subsection 4.1.9** we discuss numerically calculated time evolution of the considered system in the diabatic limit which cannot be done analytically.

In the **section 4.2** quantum-mechanical fluctuations are taken into account. It is demonstrated that we can achieve ground-state cooling regime as a result of the superconducting proximity effect.

In the **subsection 4.2.1** Hamiltonian of the nanoelectromechanical under consideration is introduced. In the **subsection 4.2.2** the system of equations that describes dynamics in the stationary regime is derived and analysed by using the Wigner function representation.

In the **subsection 4.2.3** the regime of cooling of nanomechanical vibrations is discussed.

In the **subsection 4.2.4** the electric current through the system is discussed. It is demonstrated that the cooling of the mechanical vibrations and ground-state cooling, particularly, can be experimentally explored via electric current measurements.

Keywords: Quantum dot (QD), nanoelectromechanical system (NEMS), molecular transistor, coherent state, proximity effect, qubit.

АНОТАЦІЯ

Багрова О.М. ЕЛЕКТРОМЕХАНІЧНІ ЯВИЩА В НОРМАЛЬНИХ ТА НАДПРОВІДНИХ НАНОСТРУКТУРАХ НА ОСНОВІ РУХОМОЇ КВАНТОВОЇ ТОЧКИ. — Рукопис.

Дисертація на здобуття наукового ступеня доктора філософії за спеціальністю 104 – фізика та астрономія. – Фізико-технічний інститут низьких температур імені Б.І. Веркіна НАН України, Харків, 2023.

Дисертація присвячена вивченню нових фундаментальних явищ, які виникають внаслідок електромеханічного зв'язку в мезоскопічних системах на основі рухомої квантової точки.

У **вступі** коротко обґрунтовано актуальність теми дисертації, визначено мету та основні завдання дослідження, а також об'єкт, предмет і методи дослідження. Сформульовано наукову новизну та практичне значення отриманих результатів. Наведено відомості про публікації, особистий внесок здобувача та апробацію результатів дисертації. Також приведено відомості про структуру та обсяг дисертаційної роботи.

Розділ 1 присвячено огляду та аналізу літератури за темою дисертації. Розглянуто основні явища, які виникають при транспортуванні електронів через одноелектронний транзистор. Зокрема, введено підхід Ландауера-Бюттікера та поняття кулонівської блокади тунелювання електронів. **Пункт 1.1.2** присвячено розгляду поляронних ефектів у транспорті електронів у молекулярних транзисторах. Зокрема, обговорюється походження блокади Франка-Кондона (поляронної) і поляронного звуження ширини енергетичного рівня, а також немонотонна температурна залежність диференціальної провідності. Окрім того, в останній частині **пункту 1.1.2** коротко розглянуто окремий випадок нерівноважної вібронної підсистеми.

На відміну від першої частини **розділу 1**, де обговорюється вплив механічних коливань квантової точки на транспорт електронів, на противагу цьому в подальших частинах розглядається еволюція механічної підсистеми під впливом тунелювання електронів. Так, у **підрозділі 1.2** введено поняття керованого кубіта та формулу Ландау-Зенера-Штукельберга-Майорани для ймовірності переходу. Крім того, обговорено деякі протоколи для квантових

кодів корекції помилок та їх важливість для подальшого розгляду. У **підрозділі 1.3** розглянуто природу явища механічної нестійкості.

Розділ 2 присвячено розгляду та аналізу поляронних ефектів, які виникають завдяки *нерівноважній* когерентній вібронній підсистемі.

У **підрозділі 2.1** представлено модель системи, що розглядається. Одномолекулярний транзистор складається з макромолекули, яку розміщено між двома об'ємними електродами, до яких прикладено постійну тягнучу напругу. Квантова точка, яка моделює молекулу, зазнає квантових коливань у напрямку, перпендикулярному до напрямку переносу електронів. За допомогою напруги на затворі виникає можливість керування енергією одноелектронного рівня квантової точки.

У **підрозділі 2.2** представлено гамільтоніан досліджуваної системи та отримано рівняння для матриці густини електронної підсистеми.

У **підрозділі 2.3** отримано аналітичний вираз для електричного струму через одномолекулярний транзистор. У **підрозділі 2.4** наведено та проаналізовано результати чисельних розрахунків вольт-амперних ($I-V$) характеристик (ВАХ). Встановлено відповідність між ВАХ, отриманими в припущенні, що вібронна підсистема перебуває в когерентному (*нерівноважному*) стані, та франк-кондонівськими сходами для вібронів у рівноважному стані. Показано, що на відміну від теорії Франка-Кондона, у випадку когерентних вібронів сходи на вольт-амперних характеристиках є нерегулярними. Більш того, для когерентного стану вібронів струм насичення виникає при значно менших тягнучих напругах. Останній факт може бути вирішальним в експериментах, які вимагають роботи в режимі зняття поляронної блокади, тобто максимальних струмів.

У **підрозділі 2.5** знайдено аналітичну формулу для електричного струму. Наближення дає гарне узгодження з основними чисельними результатами.

Розділ 3 присвячено отриманню та аналізу заплутаності, яка виникає між електронними та механічними ступенями свободи в надпровідному наноелектромеханічному пристрої.

У **підрозділі 3.1** представлено модель наноелектромеханічного пристрою, що розглядається. Система складається з надпровідного нанодроту, що підвішений між двома надпровідними електродами. Нанодріт,

який розглядається як зарядовий кубіт (сховище куперівських пар), зазнає згинальних коливань у напрямку, перпендикулярному до осі нанодоту. Окрім того, нанодріт з'єднаний з електродами затвора за допомогою ємнісного зв'язку, що дозволяє керувати відстанню між енергетичними рівнями кубіта. До того ж, різниця фаз між надпровідними електродами може бути підлаштована постійною тягнучою напругою, що прикладена до них, як результат нестационарного ефекту Джозефсона. Також представлено гамільтоніан системи.

У **підрозділі 3.2** знайдено часову еволюцію чистого стану системи. Показано, що початковий чистий стан еволюціонує до стану, представленого заплутаністю між двома станами кубіта та двома когерентними станами механічного резонатора.

У **підрозділі 3.3**, який представляє основний результат цього розділу, запропоновано і виведено специфічний протокол маніпуляції тягнучою напругою, який призводить до утворення заплутаності між двома станами зарядового кубіта і двома станами типу "Schrödinger cat" (суперпозиція двох когерентних станів), починаючи з чистого стану. Розглянутий протокол завдяки своїй простоті може бути ефективно реалізований в експериментах з кодуванням квантової інформації з електронних станів кубіта до когерентних (зокрема, так званих "cat states") наномеханічного резонатора. До того ж, "cat states" завдяки своїй структурі не чутливі до виникнення помилок. Таким чином, запропонована схема не потребує додаткових протоколів корекції квантових помилок.

У **підрозділі 3.4** розглянуто ентропію заплутаності (фон Неймана) з метою кількісного аналізу заплутаності між зарядовими станами кубіта і когерентними станами наномеханічного резонатора. Далі в **підрозділі 3.5** обговорено часову еволюцію механічної підсистеми. Чітке обґрунтування наявності заплутаності представлено шляхом аналізу відповідних функцій Вігнера.

У **підрозділі 3.6** описано чіткий метод для експериментального виявлення заплутаності шляхом вимірювання середнього струму.

Розділ 4 присвячено розгляду та аналізу наномеханічних явищ, які виникають завдяки ефекту близькості в наступному гібридному наноелектромеханічному пристрої. Система, що розглядається, включає

вуглецеву нанотрубку, підвішену над канавкою в звичайному металевому електроді і розміщену в проміжку між двома надпровідними електродами. Крім того, нанотрубка зазнає згинальних коливань між двома надпровідними електродами таким чином, що згинання нанотрубки переміщує її ближче до одного електрода і далі від іншого. Це призводить до залежних від положення амплітуд тунелювання. До того ж, завдяки наявності різниці фаз між надпровідними електродами, недіагональний параметр порядку квантової точки виникає в результаті надпровідного ефекту близькості. На додаток, тягнуча напруга, що прикладена до нормального електрода, спричиняє направлену динаміку електронів у системі.

У **підрозділі 4.1** напівкласичний підхід в рамках наближення матриці густини використано для отримання та аналізу режиму *нестійких* станів механічної підсистеми.

У **пункті 4.1.1** вводиться модель досліджуваного наноелектромеханічного пристрою та його гамільтоніан. У **пункті 4.1.2** розглянуто наближення матриці густини. Виведено систему рівнянь для елементів матриці густини разом з нелінійним диференціальним рівнянням другого порядку для координати квантової точки. Крім того, в **пункті 4.1.3** формалізм функцій Гріна використано для знаходження параметра порядку квантової точки, який виникає за рахунок надпровідного ефекту близькості.

У **пункті 4.1.4** розгляд в рамках адіабатичного режиму дозволяє спростити задачу до одного нелінійного диференціального рівняння (яке є центральним у цьому розділі) для координати квантової точки і аналітично проаналізувати його за допомогою методу лінеаризації, як у **пункті 4.1.5**. Крім того, в **пункті 4.1.6** використано метод усереднення Крилова-Боголюбова для знаходження наближеного розв'язку та аналізу режимів, в яких може працювати наноелектромеханічна система, що розглядається. Розглянуто два стани механічної підсистеми. Зокрема, показано, що в механічно *нестійкому* режимі виникають граничні цикли самопідтримних коливань. До того ж, має місце ефект самонасичення. У **пункті 4.1.7** основні результати узагальнено на випадок несиметричних тунельних контактів і впливу термодинамічного оточення.

У пункті 4.1.8 обговорюється можливість експериментального виявлення механічної нестійкості в системі за допомогою вимірювання електричного струму. Продемонстровано, що дана система може працювати в транзисторному та діодному режимах.

У пункті 4.1.9 обговорюється чисельно розрахована еволюція розглянутої системи в діабатичній границі, що не може бути зроблено аналітично.

У підрозділі 4.2 враховано вплив квантово-механічних флуктуацій. Продемонстровано, що можна досягти режиму охолодження до основного стану в результаті ефекту близькості.

У пункті 4.2.1 введено гамільтоніан наноелектромеханічної системи, що розглядається. У пункті 4.2.2 виведено систему рівнянь, яка описує динаміку в стаціонарному режимі, і проаналізовано її за допомогою представлення функцій Вігнера.

У пункті 4.2.3 розглянуто режим охолодження наномеханічних коливань.

У пункті 4.2.4 розглянуто електричний струм через систему. Показано, що охолодження механічних коливань і, зокрема, охолодження до основного стану можна експериментально дослідити за допомогою вимірювання електричного струму.

Ключові слова: квантова точка, наноелектромеханічна система, молекулярний транзистор, когерентний стан, ефект близькості, кубіт.

List of the candidate's publications related to the dissertation

The main results of the dissertation are published in 10 scientific works, 4 research papers in leading special scientific journals among them [1-4]:

1. **O.M. Bahrova**, S.I. Kulinich, I.V. Krive, Polaronic effects induced by non-equilibrium vibrons in a single-molecule transistor, *Low Temp. Phys.* **46**, No. 7, 671, (2020) [*Fiz. Nizk. Temp.*, **46**, 799 (2020)], DOI: 10.1063/10.0001362
2. **O.M. Bahrova**, L.Y. Gorelik, S.I. Kulinich, Entanglement between charge qubit states and coherent states of nanomechanical resonator generated by ac Josephson effect, *Low Temp. Phys.*, **47**, No. 4, 287, (2021) [*Fiz. Nizk. Temp.*, **47**, 315 (2021)], DOI: 10.1063/10.0003739
3. **O.M. Bahrova**, L.Y. Gorelik, S.I. Kulinich, R.I. Shekhter, H.C. Park, Nanomechanics driven by the superconducting proximity effect, *New J. Phys.*, **24**, 033008 (2022), DOI: 10.1088/1367-2630/ac5758
4. **O.M. Bahrova**, L.Y. Gorelik, S.I. Kulinich, R.I. Shekhter, H.C. Park, Cooling of nanomechanical vibrations by Andreev injection, *Low Temp. Phys.*, **48**, No. 6, 476 (2022) [*Fiz. Nizk. Temp.*, **48**, 535 (2022)], DOI: 10.1063/10.0010443
5. **O.M. Bahrova**, I.V. Krive, How to control transport of spin-polarized electrons via magnetic field in a molecular transistor, Physics and Scientific&Technological progress: student scientific conference, p.3, (2018).
6. **O. M. Bahrova**, S. I. Kulinich, I. V. Krive, Polaronic effects induced by coherent vibrons in a single-molecule transistor, I International Advanced Study Conference Condensed matter & Low Temperature Physics, June 8-14, 2020, Ukraine, Kharkiv, Abstracts, p. 183, (2020).
7. A.D. Shkop, **O.M. Bahrova**, Coulomb and vibration effects in spin-polarized current through a single-molecule transistor, XI Conference of Young Scientists "Problems of Theoretical Physics", December 21-23, 2020, Ukraine, Kyiv, Abstracts, p.15-16, (2020).
8. **O.M. Bahrova**, L.Y. Gorelik, S.I. Kulinich, Schrödinger-cat states generation via mechanical vibrations entangled with a charge qubit, II International Advanced Study Conference Condensed matter & Low Temperature Physics, June 6–12, 2021, Ukraine, Kharkiv, Abstracts, p.201, (2021).

9. **O.M. Bahrova**, L.Y. Gorelik, S.I. Kulinich, H.C. Park, R.I. Shekhter, Self-sustained mechanical oscillations promoted by superconducting proximity effect, The International Symposium on Novel maTerials and quantum Technologies, December 14–17, 2021, Abstracts, p.134, (2021).
10. **O.M. Bahrova**, L.Y. Gorelik, S.I. Kulinich, H.C. Park, R.I. Shekhter, Nanomechanics provoked by Andreev injection, 29th International Conference on Low Temperature Physics, August 18-24, 2022, Abstracts, p.1554 & 1771, (2022).

CONTENTS

	P.
INTRODUCTION	16
CHAPTER 1 EFFECTS OF ELECTROMECHANICAL COUPLING IN NANOSCALE SYSTEMS	21
1.1. Electron transport in single-electron transistors.	21
1.1.1. Coulomb blockade regime of electron tunneling.	23
1.1.2. Transport properties of molecular transistors.	26
1.2. Coherence effects in electron transport through a nanoelectromechanical system.	34
1.3. Mechanical instability in nanoelectromechanical devices.	36
CHAPTER 2 POLARONIC EFFECTS INDUCED BY NON-EQUILIBRIUM VIBRONS IN A SINGLE-MOLECULE TRANSISTOR	42
2.1. Model of a single-electron transistor.	42
2.2. Hamiltonian of the system and equations for density matrix.	42
2.3. Electric current.	48
2.4. Results of numerical calculations of I - V characteristics.	49
2.5. Estimation of the probability and current in steady-state regime . .	51
Conclusions	53
CHAPTER 3 ENTANGLEMENT BETWEEN CHARGE QUBIT STATES AND COHERENT STATES OF NANOMECHANICAL RESONATOR GENERATED BY AC JOSEPHSON EFFECT . .	54
3.1. Model and Hamiltonian of the nanoelectromechanical device.	54
3.2. Time evolution of the system.	57
3.3. Generation of "Schrödinger-cat states".	60
3.4. Entanglement entropy.	62
3.5. Time evolution of the mechanical subsystem.	64
3.6. Time-averaged electric current.	65
Conclusions	67

CHAPTER 4	NANOMECHANICS DRIVEN BY	
	SUPERCONDUCTING PROXIMITY EFFECT	69
4.1.	Self-sustained nanomechanical oscillations.	69
4.1.1.	Model of nanoelectromechanical device. Hamiltonian and dynamics.	69
4.1.2.	Density matrix approximation.	72
4.1.3.	Equation of motion method for Green functions.	75
4.1.4.	Dynamics of the system in adiabatic regime.	78
4.1.5.	Stability of a static solution. Linearization.	80
4.1.6.	Self-saturation effect.	81
4.1.7.	Influence of the asymmetry and friction generated by a thermodynamic environment.	86
4.1.8.	Transistor- and diode-like behaviour in electric current.	88
4.1.9.	Numerical results.	92
4.2.	Ground-state cooling of nanomechanical vibrations by Andreev tunneling.	95
4.2.1.	Quantum-mechanical description of the mechanical subsystem.	95
4.2.2.	Equations for Wigner distribution functions.	96
4.2.3.	Ground-state cooling of nanomechanical vibrations.	106
4.2.4.	Non-monotonic behaviour of electric current.	109
	Conclusions	111
CONCLUSIONS		113
BIBLIOGRAPHY		115
Appendix A	List of the candidate's publications related to the dissertation	136
Appendix B	Information on the approbation of the dissertation results	138

INTRODUCTION

Justification of the relevance of the research topic. Nanotechnology is in the front of modern science nowadays. State-of-the-art technology allows one to manipulate with molecular orbitals of a single molecule and to molecule-based transistors of a high quality. Single-molecule transistors (SMTs) mostly studied in experiments are a macromolecule (fullerenes or carbon nanotubes)-based device, where a molecule is tunnel coupled to source and drain electrodes and capacitively coupled to a gate electrode. As a result of coupling of the mechanical (vibronic) and electronic degrees of freedom, the transport properties of such a nano-scale transistor are drastically changed. The main new effect caused by vibrons is the appearance of inelastic channels of electron tunneling in single-electron transistor. For strong electron-vibron interaction the current at low voltages is strongly suppressed (Franck-Condon or polaronic blockade) and the lifting of this blockade by bias voltage or by temperature leads to step-like I - V characteristics and nonmonotonic temperature dependence of conductance. If the vibration excitations (vibrons) of the central part of the transistor are coupled to a heat bath and the vibron relaxation time is much smaller than the characteristic time of electron tunneling, the vibron subsystem is in equilibrium. The electron transport through molecular transistors with equilibrated vibrons is usually considered. However, it is not the case when the coupling of vibron subsystem to the environment is weak.

On the other hand, nanoelectromechanical systems (NEMS) provide a promising platform for investigations into the quantum mechanical interplay between mechanical and electronic subsystems. One of the most important phenomena providing the foundation of NEMS functionality is the generation of self-sustained mechanical oscillations by a constant value current flow. Nevertheless, nanoelectromechanical systems promise to manipulate the mechanical motion of a nano-object using electronic dynamics. There are many approaches to control nanomechanical performance providing a number of new functionalities of nano-device operations, in particular, pumping or cooling of the mechanical subsystem. One of the main approaches exploits the electronic flow through a nanosystem induced by either the bias voltage or temperature drop between two electronic reservoirs connected by a quantum dot (QD).

In general, there are several types of interaction between the electronic and mechanical subsystems. The most common cause of this interaction is due to localization of the electron charge or spin. However, incorporating of superconducting elements into NEMS allows one to use the coupling based on delocalization of Cooper pairs, as a foundation for the electro-mechanical performance.

The above range of unresolved issues related to the study of nanoelectromechanical systems and polaronic effects in single-electron transistors determines the **relevance** of the topic of this dissertation.

Relation to research programs, plans, topics.

The dissertation was performed at the B. Verkin Institute for Low Temperatures Physics and Engineering of the National Academy of Sciences of Ukraine within the framework of the thematic plan of the B. Verkin ILTPE of NASU on department topics: "Theoretical studies of collective phenomena in quantum condensed structures and nanomaterials" (registration number 0117U002292, code 1.4.10.26.4, the period of execution is 2017-2021), "Theoretical studies of quantum phenomena in complex low-dimensional condensed matter" (registration number 0122U001505, code 1.4.10.26.5, the period of execution is 2022-2026). Part of the dissertation work was carried out at the Center for Theoretical Physics of Complex Systems, Institute for Basic Science, Daejeon, Republic of Korea, as part of the projects "Condensed matter theory at nanoscale" (IBS-R024-D1) and "Disorder and chaos in low-dimensional systems" (IBS Young Scientist Fellowship (IBS-R024-Y3-2021)).

Goal and tasks of the research.

The goal of the dissertation work is a theoretical description of quantum effects in electron transport in nanoelectromechanical systems and molecular transistors.

To achieve this goal, it was necessary to solve the following *tasks*:

- to study the electron transport through a single-molecule transistor for the case when the mechanical subsystem is in a non-equilibrium state, in particular, the coherent state;
- to obtain the time evolution of a superconducting nanoelectromechanical system based on a carbon nanotube;
- to study the nature of entanglement between the charge states of the qubit and coherent states of the nanomechanical oscillator;

- to study the dynamics of a hybrid nanoelectromechanical device which arise due to the superconducting proximity effect;
- to obtain regions of the mechanical instability of such a system;
- to study the influence of quantum fluctuations on the steady state of the hybrid nanomechanical system based on a carbon nanotube.

Object of research of the dissertation is quantum transport of electrons in nanostructures based on a movable quantum dot.

Subjects of research are mechanical instability and tunneling processes in nanoelectromechanical systems, in particular, molecular transistors.

Research methods. The results of the dissertation were obtained using the methods of theoretical condensed matter physics. The density matrix method and perturbation theory were used to analytically find the regions of mechanical instability and study polaron effects in nanoelectromechanical systems. Also, to find the effects associated with coherent oscillations in a molecular transistor, numerical calculations were performed (solving the system of differential equations by the Runge-Kutta method).

Scientific novelty of the obtained results.

1. *For the first time*, electron transport through a single-molecule transistor was studied for the case when the mechanical subsystem is in a non-equilibrium coherent state, in particular, the current-voltage characteristics of such a transistor were obtained;
2. *For the first time*, possibility of generating quantum entanglement between the charge states of the qubit and coherent states of the nanomechanical resonator using the protocol of bias voltage manipulation was shown;
3. Quantum dynamics of a hybrid nanoelectromechanical system based on a carbon nanotube which emerge due to the superconducting proximity effect was studied *for the first time*;
4. *For the first time*, regions of instability for the nanoelectromechanical system based on a carbon nanotube were found and the self-saturation phenomenon was obtained, which arise as a result of delocalization of Cooper pairs due to the proximity effect;
5. *For the first time*, the effect of ground-state cooling of nanomechanical vibrations for a nanoelectromechanical system where the electromechan-

ical coupling is of quantum origin — arising from the proximity effect — was theoretically obtained.

Practical significance of the results.

The results of the research presented in this dissertation are of fundamental importance, as they deepen and extend the knowledge of electron transport in nanoelectromechanical systems. The effects predicted in the work, such as self-sustained nanomechanical oscillations and cooling to the ground state of ones, can be detected in experiments. The obtained protocols for bias voltage manipulation can be used to encode quantum information between qubit and nano-resonator states within a single system. Based on the study of electron transport in a single-electron transistor, the basic element of which is a movable quantum dot, more efficient molecular transistors can be created.

The candidate’s contribution. In all works that were co-authored and included in the dissertation, the author performed all analytical calculations, participated in the discussion of the results and wrote the articles. Thus, the personal contribution of the candidate to the solution of the theoretical problems discussed in the dissertation is decisive.

Approbation of results of the dissertation. The main results which this dissertation includes were presented on the following 7 international scientific conferences:

- Physics and Scientific&Technological progress: student scientific conference (Kharkiv, Ukraine, April 10-12, 2018);
- I International Advanced Study Conference Condensed matter & Low Temperature Physics (Kharkiv, Ukraine, June 8-14, 2020);
- XI Conference of Young Scientists “Problems of Theoretical Physics” (Kyiv, Ukraine (online), December 21-23, 2020);
- II International Advanced Study Conference Condensed matter & Low Temperature Physics (Kharkiv, Ukraine, June 6–12, 2021);
- The International Symposium on Novel maTerials and quantum Technologies, (Kanagawa, Japan (online), December 14–17, 2021);
- Quantum Thermodynamics Conference 2022, (Belfast, United Kingdom (online), June 27-July 1, 2022);
- 29th International Conference on Low Temperature Physics, (Sapporo, Japan (online), August 18-24, 2022);

Publications. Results which this dissertation based on have been published in 4 research papers [1–4] and 6 conference abstracts [5–10].

Structure of the dissertation. The dissertation consists of abstracts, introduction, review chapter, three original chapters with figures, conclusions, and bibliography. The total length of the dissertation is 138 pages. It contains 26 figures and bibliography with 210 sources in 21 pages.

CHAPTER 1

EFFECTS OF ELECTROMECHANICAL COUPLING IN NANOSCALE SYSTEMS

In this chapter we briefly review main effects emerged in the electron tunneling in mesoscopic devices.

1.1. Electron transport in single-electron transistors.

In contrast to a conventional transistor, a single-electron transistor (SET) exhibits some non-trivial features due to relevance of quantum effects. Main phenomena that arise in the electron transport in nanoelectrical and nonelectromechanical devices are Coulomb blockade, vibration and shuttle effects, Kondo and Luttinger liquid effects. In this section we start with a simple model of a SET and proceed to more complex through the consideration, so that we leave behind vibration effects in the first subsection, 1.1.1.

A single-electron transistor can be viewed in a simplest model as a quantum dot (QD) placed between two bulk source and drain electrodes and gated by a third electrode, see Fig. 1.1. The central part of the system, i.e., quantum dot, is a zero-dimensional mesoscopic structure with a discrete energy spectrum. It can be represented by a metallic grain (island), quantum nanowire (including a carbon nanotube (CNT)) or a big molecule (like fullerene one). In the latter case they are usually called by molecular transistors, see subsection 1.1.2. There are enough comprehend reviews and textbooks on the topic, see, e.g., Refs. [11–15]. The QD is coupled to bulk (with non-interacting electrons) electrodes by quantum tunneling processes (tunnel). It means that this system can be considered as one-dimensional double-barrier one (with ballistic transport inside) which is connected to the reservoirs of electrons. The case when the energy of tunneling electrons is within the energy window of the tunneling width of the resonant energy level inside the structure, is referred to the resonant tunneling. The completely coherent tunneling process is usually called by resonant quantum tunneling (RQT). However, when electrons tunnel incoherently to and from intermediate state (on the QD), such a process is called by sequential tunneling (ST) [11]. The later is exactly the case we are interested in below. Thus, the electron transport through such a double-barrier system can be described within

the Landauer-Büttiker approach [16, 17]. Within this method the average current I determined by tunneling events through the system is related to the transmission coefficient $T(\varepsilon)$,

$$I(V) = \frac{2e}{h} \int d\varepsilon T(\varepsilon) [f_L(\varepsilon) - f_R(\varepsilon)], \quad (1.1)$$

where $f_{L,R}$ is the Fermi-Dirac distribution function in the Left (source) or Right (drain) electrode, $f_{L,R}(\varepsilon) = 1/[\exp\{(\varepsilon - \mu_{L,R})/T\} + 1]$, $\mu_{L,R}$ is the chemical potential, T stands for temperature and e is the electron charge. For weak tunneling barriers the transmission coefficient is determined by the Breit-Wigner formula,

$$T_{BW}(\varepsilon) = \frac{\Gamma^2}{(\varepsilon - \varepsilon_i)^2 + \Gamma^2}, \quad (1.2)$$

where ε_i corresponds to the resonant level energies of the QD (inside the double-barrier structure), and $\Gamma \propto |t_0|^2$ is the energy level width which is associated with the decay rate of the resonant state, Γ/\hbar , (t_0 is the tunneling amplitude). It is useful also to note that for the linear conductance $G = I/V$ one can obtain the following expression from Eq. (1.1) (in the linear response regime, $V \rightarrow 0$), which is the well-known Landauer formula for conductance,

$$G = G_0 \int_0^\infty d\varepsilon T(\varepsilon) \left(-\frac{\partial f}{\partial \varepsilon} \right), \quad (1.3)$$

where $G_0 = 2e^2/h$ is the so-called conductance quantum. From this equation, Eq. (1.3), one can obtain the high-temperature ($T \gg \Gamma$) $1/T$ scaling of the linear conductance for sequential electron tunneling, $G \propto \Gamma/T$. Also, Eq. (1.3) can serve as a ground of the note "conductance is transmission" [18].

The partial derivative in the integrand of Eq. (1.3) gives the temperature dependence of the conductance, while from transmission coefficient, Eq. (1.2), it is seen that the conductance has the maxima at $\varepsilon = \varepsilon_i$. Here positions of the peaks defined by the quantum dot energy levels (intrinsic effect) and the chemical potential in the electrodes (leads). But it is not only the situation. Modern experimental techniques allow one change parameters of the central part of the transistor (QD). In particular, using an additional electrode (gate) contact which create a capacitor with the island, one can change potential of the quantum dot with respect to leads, so that the energy of the each level in the dot will be shifted

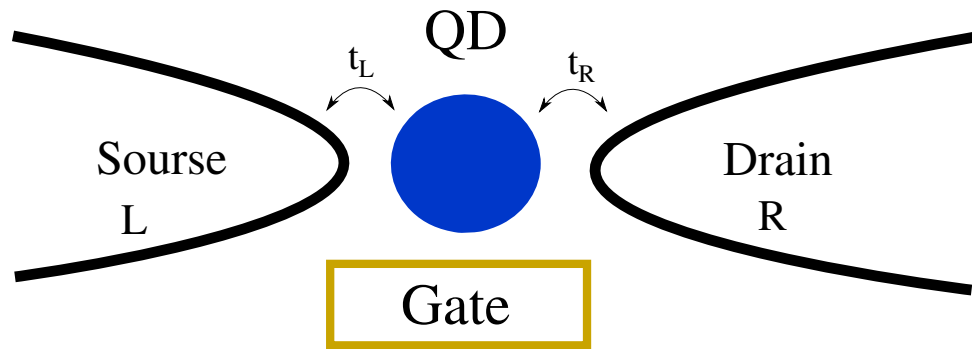


Fig. 1.1 Schematic representation of a single-electron transistor. A quantum dot is placed between two bulk electrodes (source and drain) and tunnel couples ($t_{L,R}$) to them. The gate voltage is set to manipulate the energy of the QD.

on the value determined by the voltage applied to the gate electrode, eV_G [19]. As a consequence, the linear differential conductance has a resonant dependence on the gate voltage. This, for example, brings a possibility to identify a quantum dot energy spectrum via electric current measurements.

Transport properties of single-electron transistors based on one or several quantum dots, quantum wires are belong to the hot topic in theoretical as well as experimental studies, see, e.g., Refs. [20–27].

1.1.1. Coulomb blockade regime of electron tunneling.

In the above consideration we treated the electrons as non-interacting ones. This assumption can work very well for the macroscopic leads (and we will maintain it for the electrodes in what follows). However, it is not so for the quantum dot where one electron can affect its state due to the discreteness of the electron charge.

The important energy parameter scale is an energy associated with adding one electron to a neutral quantum dot, i.e., the charging energy, which is an electrostatic one caused by own capacity C of the dot,

$$\varepsilon_C = \frac{e^2}{2C}. \quad (1.4)$$

It means that at low temperatures, $T \ll \varepsilon_C$, and if the bias voltage applied to the electrodes is small, $V < V_C = e/2C$, the transport of electrons through the system is completely blocked. This corresponds to the Coulomb blockade effect. There are a lot of literature on the Coulomb blockade phenomena, see, e.g.,

Refs. [12, 13, 15, 19, 28]. It is important to note that the Coulomb blockade can be lifted by adjusting the gate voltage V_G (now in the condition for the resonant tunneling we need to include the charging energy because when an electron come to the island, it shifts the energy levels by the value of the charging energy), in contrast, for example, to the Franck-Condon blockade which we will consider in details in the next subsection, 1.1.2. This leads to the Coulomb blockade oscillations, i.e., resonant behaviour of the differential conductance with the oscillation period equals e/C (in gate voltage). Also, we should say that if the size of a QD become very small (the capacity increases), the charging energy start to be negligible in comparison to the energy spacing between quantized energy levels on the island. This results in the fact that the Coulomb blockade oscillations are linear conductance oscillations (as a function of the gate voltage) with the period determined by the energy level spacing.

The suppression of the electric current through a SET in the Coulomb blockade regime can be understood in the following ostensive picture. The chemical potentials of the source and drain electrodes define the so-called "conducting window", so that when we increase the bias voltage, the width of the "window" became bigger. The resonant transport of electron is possible when (resonant) energy levels of the QD are within the "conducting window". The gate voltage allows one to shift the levels with respect to the Fermi energy of the electrodes and thus bring them to the "conducting window" (or vice versa).

One of the features of the Coulomb blockade phenomenon in single-electron transistors is the Coulomb staircase of current-voltage characteristics which is more pronounced in the case of asymmetric tunneling barriers, see, e.g., Ref. [15]. The effect takes place due to the contribution (to the electron transport) of states with the higher energy at higher bias voltages. It may be clear within the above-mentioned picture of the "conducting window". For example, for a given value of the gate voltage, the electric current is suppressed at low bias voltages up to the critical value V_C , and electrons start to tunnel after that through the first state on the dot. At higher voltages next electron states became available which results in a jump of the current. As a consequence, in general case for n th step for the the current one finds [15],

$$V_C^n = \frac{2(2n - 1)\epsilon_C}{e}. \quad (1.5)$$

The heights of the steps drastically decrease withal and a current-voltage dependence becomes linear at big values of the bias voltage. Also, the temperature smooths and eventually smears out the steps, i.e., one can estimate a relevant temperature to observe the effects as $T \approx 1K$ [22].

A very informative and usually used to present experimental results are stability diagrams. They are contour plots of electric current $I(V, V_G)$ and differential conductance $dI/dV(V, V_G)$ dependencies on the bias and gate voltages. In such plots effects of the Coulomb blockade are clearly seen via the so-called Coulomb diamonds (the regime of Coulomb blockade corresponds to regions of a diamond (rhombus) form). It is worth to mention that additional lines (peaks) can be seen on stability diagrams due to presence of several energy level on a QD ($\Delta\varepsilon \approx \varepsilon_C$, where $\Delta\varepsilon$ stands for an energy level difference) or due to the influence of vibration effects (in molecular transistors, see subsection 1.1.2) [22, 29].

As a next point, let us note about a generalization of the Landauer formula for the electric current, Eq. (1.1). In case of interacting electrons, one usually uses approaches based on the Green function formalism in order to calculate the transport properties of such a system. The generalized Landauer-like expression for the electric current is the following:

$$I(V) = \frac{ie}{2e} \int d\varepsilon \text{Tr}\{[f_L(\varepsilon)\Gamma_L - f_R(\varepsilon)\Gamma_R] (G^r - G^a) + (\Gamma_L - \Gamma_R) G^<, \quad (1.6)$$

which is called by the Meir-Wingreen formula obtained using the Keldysh technique (non-equilibrium Green function approach) [30]. In particular, for the case when partial level width are proportional [30], it has a form:

$$I(V) = -\frac{2e}{h} \int d\varepsilon [f_L(\varepsilon) - f_R(\varepsilon)] \text{Tr}\{T \text{Im}G^r\}. \quad (1.7)$$

Moreover, this formula was enlarged to the time-dependent electron transport in Refs. [31, 32]. Here Tr denotes the trace operation, transmission coefficient T now is a matrix, and $G^{r,a,<}$ is a retarded, advanced, or Keldysh Green function, respectively, which is a correlation function with QD operators. For time-independent case and single-level quantum dot, the retarded Green function has the following form [11, 31] in the energy representation,

$$G^r(\varepsilon) = [\varepsilon - \varepsilon_0 - \Lambda(\varepsilon) + i\Gamma(\varepsilon)]^{-1}, \quad (1.8)$$

where $\Lambda(\varepsilon)$ and $\Gamma(\varepsilon)$ are the shift and broadening of the energy level (linewidth) of the quantum dot, ε_0 [11, 32]. For the non-interacting electrons in the wide band approximation [33, 34] (the level width is energy-independent) one gets from Eq. (1.6) the Landauer formula, Eq. (1.1).

1.1.2. Transport properties of molecular transistors.

A single-molecular transistor (SMT) can be meant as a SET where the central part of the system is movable. It can be a macromolecule (like fullerene one) or a quantum nanowire (particularly, a carbon nanotube) placed between two massive electrodes. Quantitatively new effects arise in transport properties of such devices (as well as in molecular junctions) due to the electron-vibron coupling and new phenomena as polaronic effects and the phonon-assisted electron tunneling, mechanical instability and the electron shuttling come to pass. There are comprehend reviews on the topic of polaronic effects, see, e.g., Refs. [11, 35, 36]. Thus, in this subsection we only introduce the basic concepts and review recent achievement in this field, where the vibrons (quants of the QD oscillations) are associated with a mode unrelated to the direction of the electron tunneling [11]. However, the electron shuttling will be considered in the section 1.3.

Tunneling spectroscopy is a well-known method to study of electron-phonon interaction in bulk metals (see, e.g., Ref. [37]). Electron transport spectroscopy can be used for studying of vibration properties of molecules in single-molecule-based transistors [20, 38]. Current-voltage characteristics of single-electron transistors, where fullerene molecule [20], suspended single-wall carbon nanotube [22, 39, 40] or carbon nano-peapod [38] are used as a base element, demonstrate at low temperatures additional sharp features (steps) at bias voltages $eV_n \simeq n\hbar\omega$ (ω is the angular frequency of vibrational degree of freedom). The simplest models (see, e.g., review Ref. [11]) that describe step-like behavior of $I - V$ curves are based, as a rule, on a theory where phonon excitations are dispersion-less (vibrons with a single frequency) and they are assumed to be in equilibrium with the heat bath at temperature T (bulk metallic electrodes can play the role of this heat bath). Steps in current-voltage dependencies (equidistant peaks in differential conductance) are associated with the opening of inelastic channels of electron tunneling through vibrating quantum dot. For strong electron-vibron interaction these models predict:

- (i) Franck-Condon blockade [41] (exponential suppression) of conductance at low temperatures $T \ll \hbar\omega$,
- (ii) non-monotonous temperature dependence of the differential linear conductance.

All these effects were observed in experiments with molecular transistors based on a single fullerene molecule [20] or carbon nanopeapods [38].

The minimal model that describes the effects consists of a vibrating single-level quantum dot placed between two bulk normal metal electrodes biased by a constant voltage. The position of the QD energy level is tuned by a gate voltage (usually, in a way to obtain the maximal current, $\varepsilon_0(V_G) = \varepsilon_F$). For simplicity let us firstly consider spinless electrons (non-interacting). The Hamiltonian of such a system (tunnel model or Anderson-Holstein Hamiltonian) includes the following parts,

$$H = H_l + H_d + H_v + H_{int} + H_t. \quad (1.9)$$

Here H_l is the Hamiltonian of non-interacting electrons in the leads $\kappa = L, R$,

$$H_l = \sum_{k\kappa} \varepsilon_{k\kappa} a_{k\kappa}^\dagger a_{k\kappa}, \quad (1.10)$$

where $a_{k\kappa}^\dagger$ ($a_{k\kappa}$) is the creation (annihilation) electron operator with the standard anti-commutation relation. In the Hamiltonian of the single-level quantum dot,

$$H_d = \varepsilon_0 c^\dagger c, \quad (1.11)$$

c^\dagger (c) is the creation (annihilation) operator of the electron state in the QD with the energy ε_d . The vibrational subsystem is described by the harmonic oscillator Hamiltonian,

$$H_v = \frac{p^2}{2m} + \frac{m\omega^2 x^2}{2}, \quad (1.12)$$

with the canonically conjugate operators of coordinate and momentum, $[x, p] = i\hbar$. The electron-vibron interaction Hamiltonian reads as follows

$$H_{int} = \Delta x c^\dagger c. \quad (1.13)$$

The tunnel Hamiltonian is the following,

$$H_t = \sum_{k\kappa} t_\kappa a_{k\kappa}^\dagger c + \text{H.c.}, \quad (1.14)$$

where t_κ is the tunneling amplitude which we consider in the symmetric case, $t_L = t_R = t_0$, for simplicity in what follows. The case of position-dependent tunneling amplitude will be taken into account in the section 1.3.

In order to diagonalize the Hamiltonian, Eq. (1.9), one can perform the unitary Lang-Firsov [42] or "small polaron" [11] transformation,

$$\hat{V} = \exp [i\lambda p c^\dagger c], \quad (1.15)$$

with $\lambda = \Delta/\hbar m\omega^2$ is the electron-vibron coupling constant. After this transformation we get the re-normalization of the tunneling amplitude as follows

$$H_t \rightarrow H_t = \sum_{k\kappa} t_0 e^{-i\lambda p} a_{k\kappa}^\dagger c + \text{H.c.}, \quad (1.16)$$

and shift (decrease) of the electron energy in a vibrating QD is known as the polaronic shift, $\varepsilon_p = \varepsilon_d - \lambda^2 \hbar\omega$, see, e.g., Refs. [11, 36, 41, 43], and the electron-vibron bound state is called by the *polaron* one.

There are several approaches to calculate transport through a single-molecular transistor, such as, equation of motion (EOM) method [44], master equation [11] using the Fermi Golden rule, Keldysh technique [30, 41], or density matrix approximation [45]. However, in all these methods one of the crucial point is how to treat electron-vibron correlations in the averaging procedure. The usual approach which is valid in the perturbation theory over the small parameter of the electron level width (small junction transparency), is to disregard correlations between electrons and vibrons and evaluate the averages with the Hamiltonian of the non-interacting vibrons or with fermion part of the Hamiltonian for the fermionic averages [11]. Even so, one needs to be accurate in the considering of regimes of the transport within the validity of the perturbation theory because some of the results can become questionable [46]. Also, it is a usual assumption to take into account the case of the strong coupling of the vibrons to bosonic environment (heat bath with a temperature T) so that the process of the equilibration of their

distribution function is sufficiently fast (faster than the time corresponding to a tunneling event) [11]. The main average one needs to calculate is a correlation function with exponential function of the vibron operators. It can be done via several methods, see, e.g., Ref. [47], where the Feynman disentangling of operators technique is well explained. Moreover, it is convenient to use the well-known Campbell-Baker-Hausdorff-Dynkin formula. The result of the calculations of the correlation functions is the following [11, 41, 43, 47, 48],

$$\langle e^{\mp i\lambda\hat{p}(t)} e^{\pm i\lambda\hat{p}(t')} \rangle_0 = \sum_{n=-\infty}^{+\infty} A_n e^{-i\omega n(t-t')}, \quad (1.17)$$

where $\langle \dots \rangle_0$ indicates averaging with the vibron equilibrium distribution function (density matrix which has the Gibbs form), and

$$A_n = e^{-\lambda^2(1+n_B)} I_n(z) e^{-n\omega/(2T)}, \quad (1.18)$$

with the normalization condition $\sum_n A_n = 1$. In this equation $I_n(z)$ is the modified Bessel function of the first kind [49], $z = 2\lambda^2 \sqrt{n_B(1+n_B)}$, where n_B is the Bose-Einstein distribution function,

$$n_B = 1 / \left[e^{\hbar\omega/T} - 1 \right]. \quad (1.19)$$

Then for the electric current, using, for example, the Meir-Wingreen formula, Eq. (1.7), we get the following expression [46],

$$I(V) = -\frac{e}{h} e^{-\lambda^2(1+2n_B)} \sum_{n=-\infty}^{+\infty} I_n e^{-n\omega/(2T)} \int d\varepsilon T_{BW}^n(\varepsilon) [f_L(\varepsilon) - f_R(\varepsilon)], \quad (1.20)$$

which is presented in the form of the sum over the inelastic vibron channels, and now the Breit-Wigner transmission coefficient reads as

$$T_{BW}^n = \frac{\Gamma^2}{(\varepsilon - \varepsilon_p + n\hbar\omega)^2 + \Gamma^2}. \quad (1.21)$$

By analyzing Eq. (1.20), one can conclude several features in the electron transport due to the electron-vibron coupling. Firstly, the appearance of inelastic resonant channels for electron tunneling with emission ($n < 0$) or absorption

($n > 0$) of vibrons. This is associated with the so-called *phonon-assisted tunneling*. As a consequence, the current-voltage characteristics of a molecular transistor at low temperatures are step-like functions (see, e.g., Fig. 2.2). Hence, each step (Franck-Condon step) corresponds to the opening of new inelastic channel for electron tunneling when the bias voltage increase (more inelastic channels enter the "conducting window"). Secondly, for sufficiently ($\lambda \gtrsim 1$) strong electron-vibron interaction, the electric current is extremely suppressed at low temperatures and low bias voltages (see, e.g., Fig. 2.2). This effect is referred to the Franck-Condon [41] or polaronic blockade [11]. And the important point here that this blockade cannot be lifted via tuning the gate voltage as it is for the Coulomb blockade. Also, the electron-vibron coupling results in the non-monotonic temperature dependence of the linear conductance due to the polaronic narrowing of the QD energy level width Γ ,

$$G_\lambda(T) \propto G_0(T)e^{-\lambda^2}, \quad (1.22)$$

for the low temperatures, $\Gamma \ll T \ll \hbar\omega$. In Equation (1.22), $G_0 = \Gamma/T$ is the high-temperature conductance through a unmovable single-level quantum dot.

As a next step let us take into account the electron spin. It is easy to include in the Hamiltonian, Eq. (1.9), spin $\sigma = \uparrow, \downarrow$, degree of freedom, and add the term corresponding to the Coulomb interaction (with the strength U) on the QD,

$$H_U = U c_\uparrow^\dagger c_\uparrow c_\downarrow^\dagger c_\downarrow. \quad (1.23)$$

Thus, the unitary transformation, Eq. (1.15), results in the re-normalization of the Coulomb interaction strength, $U_p = U - 2\lambda^2\hbar\omega$. We can see, that this may lead to the Coulomb attraction case for strong electron-vibron interaction, $U < 2\lambda^2\hbar\omega$. However, this case needs special consideration [50]. All the features we have been discussed for spinless electron remain in presence of the electron-electron interaction.

In Ref. [51] in molecular transistors made from C_{140} fullerene molecules, the vibration-assisted tunneling associated with an internal stretching mode of the molecule was observed, see also Refs. [20, 22]. The strong coupling of this mode to tunneling electrons, relative to the other molecular modes, is consistent with

molecular modeling. Variations in the measured strength of vibration-assisted tunneling between different devices are presented [51].

In a recent paper, Ref. [43], the transport properties of a single-molecular transistor with the spin-polarized leads was considered in the presence of not only the electron-vibron and Coulomb interaction but the influence of the magnetic field directed perpendicular to the current flow was taken into account. The case of fully spin-polarized leads allows to emphasize the effect emerged due to the interplay between the above-mentioned phenomena. The magnetic field, which induces the spin-flip processes on the quantum dot, leads to the lifting of spin blockade in the spintronic device. The term in the Hamiltonian emerged due to the Zeeman effect (splitting) in the magnetic field H reads as

$$H_H = -\frac{g\mu_B H}{2} \left(c_{\uparrow}^{\dagger} c_{\downarrow} + c_{\downarrow}^{\dagger} c_{\uparrow} \right), \quad (1.24)$$

where g and μ_B stand for the gyromagnetic ratio and the Bohr magneton, respectively. This non-diagonal term in the Hamiltonian can be vanished out by the performing the canonical transformation of the dot fermionic operators [5, 43, 52–55] which results in the re-normalization of the dot energy level (splitting) $\varepsilon_{1,2} = \varepsilon_d \pm g\mu_B H/2$, and tunneling amplitude,

$$H_t \rightarrow H_t = \frac{t_0}{\sqrt{2}} e^{-i\lambda\hat{p}} \sum_{k\kappa} a_{k\kappa}^{\dagger} (j_{\kappa} d_1 + d_2) + \text{H.c.}, \quad (1.25)$$

where $j_{L,R} = \pm 1$ and $d_{1,2}$ is the new dot operator. The reduced density matrix technique and the perturbation theory over the QD level width was used in Ref. [43], see also Ref. [7], in order to calculate the transport properties of the system. It has been obtained that the current-voltage dependencies have doubled number of Franck-Condon steps compared to a conventional molecular transistor. Every voltage interval $eV = 2\hbar\omega$ has two steps. The doubling is explained by the fact that the system with the Zeeman splitting has doubled number of elastic channels, with the inelastic channels associated with each of them [43]. The doubling of the steps can also be observed in the presence of the Coulomb interaction. Moreover, it is found that the lifting of the Coulomb blockade by the bias voltage proceeds in stages, so that there are two elastic channels for tunneling of the second electron to the quantum dot, and one of these channels opens earlier

than the other in energy. The steps are separated by the voltage interval equal to energy splitting in the external magnetic field [43]. In addition, it is obtained that for strong electron-vibron interaction, $\lambda \gtrsim 1$, the temperature dependence of the linear conductance is non-monotonic and anomalous growth of a conductance maximum depends on the Coulomb interaction strength as well as on the external magnetic field [43]. Also, thermoelectric properties of the device under consideration in Ref. [43] and with the temperature drop through the system are studied in Ref. [56].

In addition, transport properties of the following spintronic device are investigated in Ref. [52]. (Let us omit the electron-vibron interaction for a moment.) Within the model under consideration, a unmovable QD is placed between magnetic fully spin-polarized (for simplicity) leads (half-metals) which are held at different temperatures and chemical potentials (tuned by a bias voltage). In such a setup the effect of spin blockade occurs: an electron with the spin \uparrow cannot tunnel to the lead with the spin polarization \downarrow and vice versa. However, an external magnetic field applied perpendicular to the lead magnetization, induces spin-flip processes of an electron in the quantum dot. An arbitrary direction of the magnetic field was considered in Ref. [57], where the case of non-interacting as well as interacting electron was taken into account and the dependence of the conductance was found using the Green function approach. The equation of motion method was used in Ref. [52] to calculate the electric and heat currents in case of non-interacting electrons explicitly. It was shown that in an optimal regime the figure of merit (ZT) of the proposed spintronic device is essentially enhanced [52] in comparison with the analogous device with unpolarized electrons [58]. In particular, it was shown [52] that (in the simplest case) the electric current (transmission coefficient) has the following dependence of the magnetic field, see also Refs. [5],

$$I = I_0 \frac{\hbar^2/2}{\hbar^2 + \Gamma^2} [f_L^+ - f_R^+], \quad (1.26)$$

where $I_0 = e\Gamma$ is the maximal current through the SET with an unmovable dot and $\hbar = g\mu_B H$ and $2f_{L,R}^+ = f_{L,R}(\varepsilon_1) + f_{L,R}(\varepsilon_2)$. Also, the influence of the Coulomb interaction on thermoelectric properties was calculated using the density matrix approximation. It has been obtained that in the Coulomb blockade regime the figure of merit is not suppressed due to electron-electron interaction [52].

Nevertheless, when coupling of vibron subsystem to the heat bath is weak and vibrons are not in equilibrium during the time of electron tunneling through the system, their density matrix can not be in the Gibbs form and it has to be evaluated from the solution of kinetic equations. This problem can be solved only numerically (see, e.g., Ref. [59]). There are only few papers [60–64], where vibrons in electron transport through a SET were considered as non-equilibrated. In Ref. [62] it was assumed that vibron subsystem is in a coherent state. In the approach used in the cited paper, the density matrix of coherent state was time-independent, that contradicts Liouville-von Neumann equation for density matrix of *non-interacting* vibrons. Therefore the results of this approach are questionable and the problem of electron transport through a vibrating quantum dot with coherent vibrons has to be re-examined.

It is worth to mention about one case of non-interacting vibrons, particularly, when the vibron subsystem is in a Fock state with the vibron number n or in a superposition of ones. In Ref. [65] it is reported about an experimental generation of the multi-phonon Fock states in a bulk acoustic-wave resonator with a sufficient fidelity (up to $n = 8$). A Wigner tomography and state reconstruction to highlight the quantum nature of the prepared states was also performed [65]. Thus, in the case when the density matrix of mechanical subsystem describes the one being in a Fock state, the correlation function, Eq. (1.17), has the following form [47, 61],

$$\begin{aligned} \langle n | e^{\mp i\lambda\hat{p}(t)} e^{\pm i\lambda\hat{p}(t')} | n \rangle &= e^{-\lambda^2[1-e^{i\omega(t-t')}] L_n [2\lambda^2(1 - \cos\{\omega(t-t')\}]} = \\ &= \sum_{m=0}^n \sum_{k=0}^{\infty} A_{mk}^n e^{i\omega[m-k](t-t')}, \end{aligned} \quad (1.27)$$

with

$$A_{mk}^n = e^{-\lambda^2} \frac{(-1)^{m+k} n!}{(m!)^2 (n-m)!} (2\lambda)^{2m} L_k^{2m-k}(\lambda^2), \quad (1.28)$$

where $L_i^j(z)$ is a generalized (associated) Laguerre polynomial [49]. Note that Eq. (1.17) can be obtained from Eq. (1.27) by the summation over n with corresponding coefficients [47, 66].

In contrast, in the next chapter 2 we will consider single-electron transistor with vibrating quantum dot, where vibronic subsystem is described by *time-dependent* density matrix. Physically this approach corresponds to coherent oscil-

lations of quantum dot treated as harmonic quantum oscillator. Coherent states of harmonic oscillators are well known in physics (see, e.g., Refs. [67, 68]). In tunnel electron transport they appear, for instance, in weak superconductivity (Josephson current through a vibrating quantum dot, see Ref. [69] and references therein). Last years coherent states of photons ("Schroedinger-cat" states) coupled to qubits and qubits formed by the coherent photon states became a hot topic of studies in quantum computing science, see, e.g., review Ref. [70].

1.2. Coherence effects in electron transport through a nanoelectromechanical system.

Electro-mechanical phenomena on the nanometer scale attract significant attention during the last two decades [71]. Recent advantages in nanotechnologies acquire a promising platform for studying the fundamental phenomena generated by the interplay between quasi-classical and pure quantum subsystems. A charge qubit formed by a tiny superconducting island (Cooper-pair box (CPB)) whose basis states are charge states (e.g. states which represent the presence or absence of excess Cooper pairs on the island), is one of a large group of pure quantum systems [72]. There are many types of solid-state systems which qubit based on, such as quantum superconducting circuits (including biased Josephson junctions, SQUIDs and CPBs), see, e.g., review Refs. [73, 74]; quantum dots [75, 76] and atomic ones [77].

In general, a qubit is one of the physical realizations of a two-level system [78], including ultracold atoms, classical nanomechanical resonators and semiconductor microcavities, where extremely controllable qubits can be realized on the exciton-polariton condensates [79, 80]. One of the main features related to a two-level system is the fact that it usually exhibits an avoided level crossing (anticrossing) of its energy levels as an external parameter is varied [81]. A driven two-level system is described by a standard Hamiltonian,

$$H = -\frac{\Delta}{2}\sigma_x - \frac{\varepsilon(t)}{2}\sigma_z, \quad (1.29)$$

where $\varepsilon(t)$ is a bias energy and Δ stands for an energy gap [82]. By solving the time-dependent Schrödinger equation for linearly driven system, $\varepsilon(t) = vt$, one gets the following expression for the transition probability that is

the probability to find the system in the excited state known as Landau-Zener-Stückelberg-Majorana (LZSM) formula,

$$P_{LZSM} = e^{-2\pi\delta}, \quad (1.30)$$

with $\delta = \Delta^2/(2\hbar v)$ being the adiabaticity parameter, see review Ref. [78]. The non-linear driving is considered in Ref. [83]. Additionally, the LZSM transitions in a periodically driven Cooper-pair box system was investigated [84]. At the same time modern nanomechanical resonators which dynamics according to Ehrenfest theorem to great extent is described by classical equations, are ideal representatives of quasiclassical subsystem [85]. Systems, which dynamics is determined by the mutual influence between a superconducting qubit and a nanomechanical resonator, are a subject of cutting-edge research in quantum physics, especially, in quantum communication, see, e.g., Refs. [86–91]

There are two main questions that arise related to an interplay between quasi-classical dynamics of the mechanical resonator and quantum dynamics of the charge qubit. The first one is: how quasi-classical motion may affect pure quantum phenomena? Considering this question, it was shown that the superconducting current between two remote superconductors can be established by mechanical transportation of Cooper pairs performed by an oscillating CPB [92]. Even more, it was demonstrated that such transportation could generate correlations between the phases of space-separated superconductors [93]. Another question is how coherent Josephson dynamics of a charge qubit will affect the dynamics of the quasi-classical resonator, in particular, whether or not the quantum entanglement between a superconducting qubit and mechanical vibrations can be achieved? Recently it was demonstrated that individual phonons can be controlled and detected by a superconducting qubit enabling coherent generation and registration of quantum superposition of zero and one-phonon Fock states [86, 87]. At the same time nanomechanical resonators provide the possibility to store quantum information in the complex multi-phonon coherent states. Such states, in contrast to single-phonon states, where mechanical losses irreversibly delete the quantum information, allow their detection and correction [70, 94].

A huge challenge in the realisation of full-scale quantum computer systems is controlling qubits in an error-free way. Quantum error correction (QEC) protocols offer a solution to this problem, in principle allowing for arbitrary suppression of

the logical error rate provided certain threshold conditions on the physical qubits are met [95]. For now several quantum error correction methods are proposed. QEC codes [96] based on cat states are widely used [70]. Because of phases are more robust against photon loss errors, information is typically encoded in the phase of a coherent state. In analogy to classical phase-shift keying, quantum information can also be encoded to the phase of a coherent state. The simplest code (two-component cat code) is thus to use two coherent states with opposite phases that is, the cat states [97]. Another QEC protocols are GKP codes. They are quantum error-correcting codes that protect a state of a finite-dimensional quantum system (qudit) that is encoded in an infinite-dimensional system (harmonic oscillator) [98]. For a typical two-level logical qubit, the GKP code is defined as coherent superposition of infinitely squeezed states or the eigenstates of the position operator \hat{x} with a spacing of $2/\sqrt{\pi}$ [97]. Besides, recently binomial codes for QEC were proposed [99, 100]. These “binomial quantum codes” are formed from a finite superposition of Fock states weighted with binomial coefficients. It was shown that the binomial codes are protected to given order in the time step against continuous dissipative evolution under loss, gain, and dephasing errors [99].

Motivated by such a challenge, in the chapter 3 we will discuss the possibility to generate quantum entanglement between the charge qubit states and mechanical coherent ones in a particular nanoelectromechanical system (NEMS) where mechanical vibrations are highly affected due to the weak coupling with movable a Cooper-pair box. Moreover, a protocol of bias voltage manipulation which results in the formation of entangled states incorporating so-called cat-states (the quantum superposition of the coherent states) which are robust in manipulation, is proposed.

1.3. Mechanical instability in nanoelectromechanical devices.

In contrast to the previous sections 1.1, 1.2, where we have considered the influence of electron-vibron interaction on transport properties of single-molecule transistors within the approach when this coupling is associated with mechanical modes unrelated to the direction of the electron flow, in this section we pay attention to the case when the position of a QD between the toward the leads exponentially modifies the tunneling probability [11]. This can result in the fact

that an equilibrium position of the QD is no more stable, that is, mechanical instability and electron shuttling regime [101] can take place. This is usually the case of weak electromechanical coupling, the influence of polaronic effect on electron shuttling phenomenon was studied in Ref. [102, 103]. There are several comprehend reviews on the topic, see Refs. [103–107]. Thus, we will briefly introduce effects of mechanical instability in such a system and review some recent results.

The simplest model that can catch the electric shuttle and mechanical instability effects, is described by the Hamiltonian Eq. (1.9), where now the tunneling amplitude is position-dependent and the term Eq. (1.13) can be presented as $H_{int} = (\varepsilon_d - e\mathcal{E}x)c^\dagger c$, where \mathcal{E} is an electric field due to presence an electron on the quantum dot,

$$H_t = \sum_{k\kappa} t_\kappa(\hat{x}) a_{k\kappa}^\dagger c + \text{H.c.}, \quad (1.31)$$

with $t_\kappa = t_0 e^{\pm \hat{x}/\lambda}$, where λ is the tunneling length. In order to solve the problem, the Liouville-von Neumann equation (or, the Lindblad equation, more generally) is used as well as Green function approach in the perturbation theory over the parameter of the electromechanical coupling. In this case if we neglect the effects of zero-point fluctuations of a quantum dot, we can use the semi-classical treatment within which $\langle \hat{x} \rangle = x$ and we are interested in the big values of the dot oscillation amplitude. Hence, the dot coordinate is governed by the Newton equation,

$$\ddot{x} + \omega^2 x = \mathcal{F}(t)/m, \quad (1.32)$$

where the average force has a form:

$$\mathcal{F}(t) = -\text{Tr} \left[\hat{\rho} \frac{\partial H}{\partial x} \right]. \quad (1.33)$$

It was shown analytically [108] that the mechanical (or shuttle) instability can occur, that is, the amplitude of the QD oscillations which being small after an initial fluctuation from an equilibrium position, start to grow exponentially with the increment $r_s \sim \lambda\Gamma$ if the bias voltage is bigger than the threshold one, $eV > 2(\varepsilon_d + \hbar\omega)$. In this case it can develop into a limit cycle in presence of small but finite mechanical friction (term $\gamma\dot{x}$ in the l.h.s. of Eq. (1.32)) [44, 108]. In addition, the fully quantum-mechanical approach (treatment of a QD coordinate quantum-mechanically with the help of the Wigner function representation) can

be used in order to investigate the mechanical instability. It was obtained that the Wigner function in the regime of developed self-oscillations has a circle-like form (not Gaussian shape), see Refs. [45, 109]. A sharp increase in current with the transition to the stationary regime was also obtained. Hence, in the limit cycle regime $I \sim e\omega$ [109].

The internal friction caused by the temperature drop T (not a bias voltage) across the system in case of spinless electrons is considered in Ref. [110]. The following temperature dependence of it was found,

$$\gamma(T) \sim T^{-1} [\cosh^2 \{\varepsilon_d/(2T)\}]^{-1}. \quad (1.34)$$

The next step in generalization is to take into account the electron spin. A spintronic nanoelectromechanical single-electron transistor with spin-polarized leads is considered in Ref. [109]. The density matrix approximation and the high bias voltage limit was used to find a steady-state solution. It was found that there are two types of transitions between steady states when the electric or magnetic field is varied [109]. In addition, the hysteresis behavior of a steady-state amplitude and electric current in the hard transition regime was obtained. The so-called spin-mechanical coupling was considered in Refs. [111, 112]. The semi-classical approach was used to derive the increment of the dot oscillation growth in the mechanically unstable regime in the system under periodic magnetic field [111]. An opposite regime of the mechanical ground-state cooling was proposed in Ref. [112].

Another type of electromechanical coupling in the magnetic shuttle structures is based on the ferromagnetic exchange coupling between a QD and magnetic leads. The region of the mechanical instability for such a nanoelectromechanical device with the spin-polarized leads and for interacting electrons was obtained in Ref. [113], see also Refs. [114–116]. It has been found that a shuttle regime of the electron transport occurs at sufficiently low magnetic field strength ($\hbar \ll \Gamma$) in contrast to the electric one. This setup under the temperature drop across the system was investigated in Refs. [117–120]. The region of the mechanical instability was obtained analytically in the adiabatic limit within the semi-classical approach. It is shown that the shuttle instability occurs in the region of external magnetic fields between a lower, which depends only on the phenomenological friction, and upper (which is temperature-dependent and saturates at the value $\hbar_{c2}/\hbar\omega = \sqrt{7/2}$ at high temperatures) critical values [120]. The regime of the

instability does not emerge at high values of the magnetic field strength because in this case the spin-flip time exceeds the characteristic time scales determined by mechanical (ω^{-1}) and electronic (\hbar/Γ) time scales [120]. Moreover, temperature dependence of the friction coefficient remains the same as for the case of spinless electrons, Eq. (1.34). The effects of Coulomb interaction on the mechanical instability of the magnetic shuttle device are described in Refs. [118, 119]. It was shown that such a spintro-mechanical shuttle instability can be triggered by the electron-electron repulsion. The critical value of the strength of this interaction crucially depends on the temperature and the strength of the magnetic field [119]. Also, the self-saturation effect was predicted for a magnetic shuttle device [113, 119]. This effect comes out in the fact of the presence of the stationary regime of mechanical self-oscillations even without the influence of an external friction determined by the quality factor of a nanomechanical system bath as it is for an electrical one. In addition, Coulomb correlation effects in a thermally driven and voltage-biased magnetic devices were investigated numerically in Ref. [118]. It has been obtained that thermally induced magnetic shuttling of spin-polarized electrons is a threshold phenomenon [118] as it is for electric shuttle device. Eventually, in Ref. [117] electric and magnetic exchange forces were taken into account at the same time. It leads to the several non-trivial effects which can be seen in an experiments with electric current measurements as such a possibility has been demonstrated in Ref. [117] by obtaining numerically I - V curves of the considered spintro-mechanical transistor. The non-monotonic dependence of the differential conductance in the stable (vibronic) regime was obtained, on the one hand. On the other hand, the effect of negative differential conductance in the stationary regime of mechanical self-oscillation was shown [117].

There are a number of the experiments where the regime of the mechanical instability in nanoelectromechanical systems was observed, see, e.g., Refs. [121–129]. A coherent spin shuttle processes in a GaAs/AlGaAs quantum dot array was considered in Ref. [130].

The effect of self-sustained oscillations is itself an interesting problem from a fundamental point of view, opening new possibilities for mass and force sensing [131, 132], while its underlying physical processes show potential applications for mechanical cooling [133]. Self-sustained mechanical oscillations were first observed in a carbon nanotube (CNT)-based transistor [128], with further studies

later verifying their transport signatures [134–136]. Recently, the experimental observation of self-driven oscillations of a CNT-based quantum dot in the Coulomb blockade regime has been reported [137].

Nevertheless, superconducting (SC) elements incorporated into nanoelectromechanical systems extend the horizon of this phenomenon, namely through the effects of superconducting phase coherence; see, e.g., the following reviews [103, 138]. A SC electrode located near a quantum dot can affect its electronic state via the tunneling exchange of Cooper pairs due to SC proximity effect. In Ref. [92] (see also [93]) it was demonstrated that a movable Cooper-pair box oscillating periodically between two remote superconducting electrodes can serve as a mediator of Josephson coupling leading to coherent transfer of Cooper pairs between the SC leads. The polaronic effects influence on the Josephson current in a S-QD-S system was considered in Ref. [139]. Also, analogously to a system in a normal state where the lifting of the Franck-Condon blockade leads to the non-monotonic temperature dependence of the differential conductance [38, 140], for the SC one is accompanied by non-monotonic temperature dependence of the critical Josephson current [139, 141, 142]. The polaronic narrowing of the Josephson critical current was considered in Refs. [69, 143, 144].

Furthermore, if the tunneling amplitude depends on the distance between the QD and the SC leads, such exchange also provides a connection between the electronic and mechanical degrees of freedom. Additional injection of electrons from a biased normal metal electrode into the QD generates peculiar dynamics of Cooper pairs on it. Interplay between electromechanical effects and phase coherence gives new and unusual properties to a number of normal metal/superconducting hybrid junctions [145–148]. In particular, it has recently been shown that in a normal metal–suspended CNT–superconductor transistor, Andreev reflection [149, 150] may give rise to a cooling of the mechanical subsystem [26, 151, 152] or generate a single-atom lasing effect [26] if certain conditions are fulfilled. The resonant Andreev tunneling in a N-QD-S system was observed in Ref. [153].

The mechanical functionality of NEMS is to a large extent determined by the physical principles underlying the interaction between the electronic and mechanical subsystems. In all studies mentioned above, this interaction was due to the *localization* of the charge [108, 145] or spin [113, 119] carried by electrons in the movable part of the system. In the chapter 4, we will consider a fundamentally

new type of electromechanical coupling based on the *quantum delocalization* of Cooper pairs (see also Ref. [154]). We demonstrate that such coupling can promote a self-saturated mechanical instability resulting in the generation of *self-sustained* mechanical oscillations. The effect of the *ground-state cooling* of nanomechanical vibrations in the considered system is also proposed. It is also shown that regime of pumping or either cooling significantly affect the average current through the system, making it possible to carry out direct experimental detection.

CHAPTER 2

POLARONIC EFFECTS INDUCED BY NON-EQUILIBRIUM VIBRONS IN A SINGLE-MOLECULE TRANSISTOR

In this chapter electron transport in a molecule transistor is considered in the assumption that the mechanical subsystem is in a non-equilibrium, namely, coherent state. The current-voltage characteristic of such a transistor based on a vibrating quantum dot are calculated. Also, the obtained electric current dependencies on the oscillation amplitude of the QD are analyzed.

2.1. Model of a single-electron transistor.

The model device we are interesting in is depicted in Fig. 2.1. It consist of two bulk electrodes, source (Left) and drain (Right) leads, with chemical potential biased by voltage, $\mu_L - \mu_R = eV$, and a single-level quantum dot, which oscillates in the direction x perpendicular to the direction of electron current flow. The gate voltage V_G is adjusted to obtain maximal tunnel current, $\varepsilon_0(V_G) = \varepsilon_F$, where $\varepsilon_0(V_G)$ is the dot level energy and ε_F is the Fermi energy of the leads. For simplicity we consider tunneling of spinless electrons in a symmetric junction and it is assumed that the vibration of QD does not change tunneling matrix elements $t_L = t_R = t_0$. Here we consider the process of sequential electron tunneling, when $\max(eV, T) \gg \Gamma$, where $\Gamma \propto |t_0|^2$ is the QD level width which is a characteristic energy of dot-leads tunnel coupling. This model device can simulate, for instance, a single-electron transistor based on a suspended single-wall carbon nanotube.

2.2. Hamiltonian of the system and equations for density matrix.

The Hamiltonian of the system, which is schematically illustrated in Fig. 2.1, consists of four terms,

$$H = H_l + H_{dot} + H_{v-d} + H_{tun}, \quad (2.1)$$

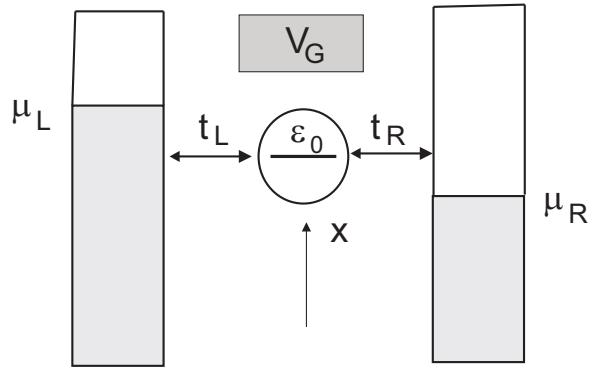


Fig. 2.1 Sketch of the single-electron transistor. A vibrating one-level (ε_0 is the level energy) quantum dot (macromolecule) is placed between two bulk electrodes biased by the voltage V . The dot tunnel couples ($t_L = t_R = t_0$ is the tunneling amplitude) to the leads with the chemical potentials $\mu_{L,R}$, $\mu_L - \mu_R = eV$ and the temperature T . The gate voltage V_G is set $\varepsilon_0(V_G) = \varepsilon_F$, where ε_F is the Fermi energy, to get maximal current. The dot oscillates in x direction perpendicular to the electric current flow. QD oscillations are modelled by the coherent state of one-dimensional harmonic oscillator.

where H_l, H_{dot} are the Hamiltonians of the non-interacting electrons in the leads and the dot, respectively,

$$H_l = \sum_{k,\kappa} \varepsilon_{k,\kappa} a_{k,\kappa}^\dagger a_{k,\kappa}, \quad H_{dot} = \varepsilon_0 c^\dagger c, \quad (2.2)$$

$a_{k,\kappa}^\dagger$ ($a_{k,\kappa}$) is the creation (annihilation) operator of an electron in the lead $\kappa = L, R$ with momentum k and energy $\varepsilon_{k,\kappa}$, c^\dagger (c) is the creation (annihilation) operator of electron state in the dot with the energy ε_0 . These operators in the occupation-number representation (second quantization) obey the standard anti-commutation relations $\{a_{k,\kappa}^\dagger, a_{k',\kappa'}\} = \delta_{kk',\kappa\kappa'}$, where $\delta_{k,\kappa}$ is the Kronecker delta.

Hamiltonian H_{v-d} describes the vibronic (mechanical) subsystem and the interaction between electrons and vibrons,

$$\hat{H}_{v-d} = \frac{p^2}{2m} + \frac{m\omega^2 x^2}{2} + \Delta x c^\dagger c. \quad (2.3)$$

In Equation (2.3) x, p are the canonical conjugating operators of coordinate and momentum, $[x, p] = i\hbar$. Here ω, m are the frequency of dot oscillations and the mass of the dot, Δ is the electron-vibron coupling constant.

Hamiltonian H_{tun} describes the tunnelling of electrons between the dot and the leads and it takes the standard form,

$$H_{tun} = \sum_{k,\kappa} t_\kappa a_{k,\kappa}^\dagger c + \text{H.c.}, \quad (2.4)$$

where t_κ is the tunnelling amplitude. In what follows we restrict ourselves to the symmetric case, $t_L = t_R = t_0$, which does not affect the obtained results qualitatively.

In order to diagonalize the Hamiltonian (2.1), it is convenient to perform the unitary transformation, $UHU^\dagger \rightarrow H$, where $U = \exp[i\lambda pc^\dagger c]$, so-called Lang-Firsov canonical transformation or polaronic transformation [47]. By equating coefficients of bosonic operators of the same power, one can obtain the re-normalized constant of the electron-vibron interaction, $\lambda = \Delta/\hbar m\omega^2$. Then Eq. (2.3) takes the diagonal form,

$$H_{v-d} \rightarrow H_v = \frac{p^2}{2m} + \frac{m\omega^2 x^2}{2}, \quad (2.5)$$

while the tunnelling Hamiltonian H_{tun} is transformed to the following one,

$$H_{tun} \rightarrow H_{tun} = t_0 \sum_{k,\kappa} e^{-i\lambda p} a_{k,\kappa}^\dagger c + \text{H.c.}. \quad (2.6)$$

The quantum consideration of electron-vibron interacting system is based in what follows on the approximation that the density matrix of the system is factorized [45] to direct product of the leads equilibrium density matrix, the vibron density matrix and the density matrix of the dot,

$$\rho \approx \rho_l \otimes \rho_v \otimes \rho_{dot}. \quad (2.7)$$

This approximation corresponds to the case of sequential electron tunneling, which holds when $\max\{eV, T\} \gg \Gamma$, where Γ is the electron level width, T is the temperature and V is the bias voltage. Here we assume that vibrons are described by a time-dependent coherent state $|z(t)\rangle$. Note, that in Ref. [61] current-voltage characteristics of a single-electron transistor were calculated for time-independent coherent state of vibrons. This assumption contradicts the equation of motion of

non-interacting vibrons in our model,

$$|z(t)\rangle = \exp(-\imath H_v t) |z\rangle, \quad (2.8)$$

($\hbar = 1$). Here $|z\rangle$ is the eigenfunction of vibron annihilation operator b , $b|z\rangle = z|z\rangle$ (z is the complex number). The corresponding density matrix takes the standard form,

$$\rho_v(t) = |z(t)\rangle\langle z(t)|. \quad (2.9)$$

Time evolution of the system is described by the Liouville-von Neumann equation for the density matrix,

$$\frac{\partial \rho}{\partial t} + \imath[H_0 + H_{tun}, \rho] = 0, \quad (2.10)$$

where $H_0 = H_l + H_v + H_{dot}$. It has the following formal solution,

$$\rho(t) = \rho(-\infty) - \imath \int_{-\infty}^t dt' e^{-\imath H_0(t-t')} [H_{tun}, \rho(t')] e^{\imath H_0(t-t')}. \quad (2.11)$$

Then by substituting Eqs. (2.7), (2.11) into Eq. (2.10) and tracing out both the electronic degrees of freedom of the leads and vibronic degrees of freedom of the dot, one gets the following equation for the reduced density matrix of the QD, $\rho_{dot} = \text{Tr}_{leads, v} \rho$,

$$\frac{\partial \rho_{dot}}{\partial t} + \imath[H_{dot}, \rho_{dot}] = -\text{Tr} \int_{-\infty}^t dt' [H_{tun}, e^{-\imath H_0(t-t')} [H_{tun}, \rho(t')] e^{\imath H_0(t-t')}. \quad (2.12)$$

Now we can explicitly calculate averages of electronic and vibronic operators in the approximation of the factorized density matrix, Eq. (2.7). For equilibrium density matrix of electrons in the leads we use the standard expression,

$$\langle a_{k, \kappa}^\dagger a_{k', \kappa'} \rangle = f_\kappa(\varepsilon_{k, \kappa}) \delta_{k, k'} \delta_{\kappa, \kappa'}, \quad (2.13)$$

where $f_\kappa(\varepsilon) = (\exp((\varepsilon - \mu_\kappa)/T) + 1)^{-1}$ is the Fermi-Dirac distribution function, $\mu_{L,R} = \mu_0 \pm (eV/2)$ is the electrochemical potential in the lead κ . Calculations of the vibronic correlation function

$$F(t, t_1; \lambda) = \langle \exp[-\imath \lambda p(t)] \exp[\imath \lambda p(t_1)] \rangle, \quad (2.14)$$

in coherent state representation result in the equation,

$$F(t, t_1; \lambda) = \text{Tr} [e^{-i\lambda p(t)} |z\rangle \langle z| e^{i\lambda p(t_1)}] = \exp \left\{ -\lambda^2 \left[1 - e^{i\omega(t-t_1)} \right] - \lambda z \left[e^{-i\omega t} - e^{-i\omega t_1} \right] + \lambda z^* \left[e^{i\omega t} - e^{i\omega t_1} \right] \right\}. \quad (2.15)$$

Here we introduce the dimensionless constant of the electron-vibron interaction $\lambda \hbar \sqrt{2}/l_0 \rightarrow \lambda$, where $l_0 = \sqrt{\hbar/m\omega}$ is the amplitude of zero-point oscillations. The parameter λ can be rewritten in the form $\lambda = \sqrt{2}l/l_0$, where $l = \Delta/m\omega^2$ is the characteristic displacement length of classical oscillator. Note that in the case of averaging with a nonequilibrium vibronic density matrix, the using of a well-known formula, which still $\langle e^{\hat{A}} \rangle = e^{\frac{1}{2}\langle \hat{A}^2 \rangle}$ [155] leads to a wrong result.

With the help of Eqs. (2.13), (2.15), Eq. (2.12) for the reduced density matrix of the QD can be represented as follows,

$$\begin{aligned} \frac{\partial \rho_{dot}}{\partial t} + i[H_{dot}, \rho_{dot}] &= \frac{\Gamma}{4\pi} \sum_{\kappa} \int d\tau \int d\varepsilon \times \\ &\left\{ F(t, t - \tau; \lambda) e^{i\varepsilon\tau} [1 - f_{\kappa}(\varepsilon)] c e^{-iH_{dot}\tau} \rho_{dot}(t - \tau) c^{\dagger} e^{iH_{dot}\tau} + \right. \\ &+ F(t, t - \tau; -\lambda) e^{-i\varepsilon\tau} f_{\kappa}(\varepsilon) c^{\dagger} e^{-iH_{dot}\tau} \rho_{dot}(t - \tau) c e^{iH_{dot}\tau} - \\ &- F^*(t, t - \tau; -\lambda) e^{i\varepsilon\tau} f_{\kappa}(\varepsilon) c e^{-iH_{dot}\tau} c^{\dagger} \rho_{dot}(t - \tau) e^{iH_{dot}\tau} - \\ &\left. - F^*(t, t - \tau; \lambda) e^{-i\varepsilon\tau} [1 - f_{\kappa}(\varepsilon)] c^{\dagger} e^{-iH_{dot}\tau} c \rho_{dot}(t - \tau) e^{iH_{dot}\tau} + \text{H.c.} \right\} \quad (2.16) \end{aligned}$$

where $\Gamma = 2\pi\nu t_0^2$ is the level width of electron state in the dot, ν is the density of states of the leads, which we assume to be energy independent (wide-band approximation, see, e.g., Ref. [33]). It should be noted that unlike the case of equilibrated vibrons (see, e.g., Ref. [43]), the vibronic correlation function, Eq. (2.15), depends on two times independently. This means that time-invariance in our system is explicitly broken. The vibrons in coherent state $|z(t)\rangle$, (which physically describes oscillations of a quantum pendulum) violates time-invariance.

The reduced density matrix (operator) ρ_{dot} acts in Fock space which in our case is a two dimensional space of a spinless electron level in a dot. The matrix elements of the density operator are: $\rho_0(t) = \langle 0 | \rho_{dot}(t) | 0 \rangle$, $\rho_1(t) = 1 - \rho_0(t) = \langle 1 | \rho_{dot}(t) | 1 \rangle$, where $|1\rangle = c^{\dagger} |0\rangle$, a $|0\rangle$ is a vacuum (ground) state. From Eq. (2.16)

it follows that the probability $\rho_0(t)$ satisfies the integro-differential equation,

$$\begin{aligned} \frac{\partial \rho_0}{\partial t} = \frac{\Gamma}{4\pi} \sum_{\kappa} \int d\tau \int d\varepsilon \left\{ F(t, t - \tau; \lambda) e^{i(\varepsilon - \varepsilon_0)\tau} [1 - f_{\kappa}(\varepsilon)] [1 - \rho_0(t - \tau)] - \right. \\ \left. - F^*(t, t - \tau; -\lambda) e^{i(\varepsilon - \varepsilon_0)\tau} f_{\kappa}(\varepsilon) \rho_0(t - \tau) \right\}. \end{aligned} \quad (2.17)$$

This equation is strongly simplified after integration over ε . This integration can be done by using the Sokhotski–Plemelj theorem, see, e.g., [156],

$$\int d\varepsilon e^{-i\varepsilon\tau} f_{\kappa}(\varepsilon) = -i\pi\delta(\tau) + \text{p.v.} \frac{i\pi T e^{-i\mu_{\kappa}\tau}}{\sinh \pi T \tau}, \quad (2.18)$$

where the symbol p.v. denotes the principal value of an integral (Cauchy principal value). In the limit $T \gg \Gamma$ one can neglect the retardation effects and Eq. (2.18) takes a simple local form,

$$-\frac{\partial \rho_0}{\partial t} = M_1(t)\rho_0 - M_2(t), \quad (2.19)$$

where

$$M_i(t) = 1 - \frac{1}{2} \sum_n A_n^{(i)}(t) [f_L(\varepsilon_0 - n\omega) + f_R(\varepsilon_0 - n\omega)]. \quad (2.20)$$

The coefficients $A_n^{(i)}(t)$ are periodic functions of time (with the period $2\pi/\omega$) and they can be presented as the Fourier series,

$$A_n^{(i)}(t) = \sum_p a_{n,p}^{(i)} e^{i\omega p t}, \quad (2.21)$$

$$\begin{aligned} a_{n,p}^{(1)} = \frac{1}{\pi} \int_{-\pi}^{\pi} d\vartheta e^{-\lambda^2(1-\cos\vartheta)} \sin\left(n\vartheta - \frac{\pi p}{2}\right) \times \\ \times \sin(\lambda^2 \sin\vartheta) \cos\left(\frac{p\vartheta}{2}\right) J_p\left(4\lambda|z| \sin\frac{\vartheta}{2}\right), \end{aligned} \quad (2.22)$$

$$\begin{aligned} a_{n,p}^{(2)} = \frac{1}{2\pi} \int_{-\pi}^{\pi} d\vartheta e^{-\lambda^2(1-\cos\vartheta)} \cos\left(\frac{p\vartheta}{2}\right) \times \\ \times \cos\left(\frac{\pi p}{2} - n\vartheta + \lambda^2 \sin\vartheta\right) J_p\left(4\lambda|z| \sin\frac{\vartheta}{2}\right). \end{aligned} \quad (2.23)$$

In Equations (2.22), (2.23) $J_p(x)$ is the Bessel function of the first kind and we parameterized the coherent state eigenvalue z in the form $z = |z| \exp(i\varphi)$, where the parameter $|z|$ determines the amplitude of the dot oscillations.

In the asymptotic ($t \gg 1/\Gamma$) steady state regime of oscillations the probability $\rho_0(t)$ is a periodic function of time, $\rho_0(t + T_0) = \rho_0(t)$, and therefore it can be presented as the Fourier series,

$$\rho_0(t) = \sum_n \rho_n e^{i\omega n t}, \rho_{-n} = \rho_n^*. \quad (2.24)$$

Then the equation for the Fourier harmonics takes the following form,

$$ip\rho_p = \delta_{p,0} - \rho_p - \frac{1}{2} \sum_n \left[a_{n,p}^{(2)} - \sum_k a_{n,p+k}^{(1)} \rho_k \right] \times [f_L(\varepsilon_0 - n\omega) + f_R(\varepsilon_0 - n\omega)], \quad (2.25)$$

and is a basic equation of this chapter. Its solutions are discussed in the subsection 2.4.

2.3. Electric current.

We are interested in current-voltage ($I - V$) characteristics of the single-electron transistor. Therefore we need to calculate time-averaged current through the system in the stationary regime,

$$I = \frac{1}{T_0} \int_{T_0} J(t) dt, \quad (2.26)$$

where $J(t) = (J_L + J_R)/2$, with left (L) and right (R) electric currents are defined as change of electrons in the corresponded lead,

$$J_\kappa = \eta_\kappa e \text{Tr} \left(\rho \frac{\partial N_\kappa}{\partial t} \right), \quad N_\kappa = \sum_k a_{k,\kappa}^\dagger a_{k,\kappa}, \quad (2.27)$$

where $\eta_{L/R} = \pm 1$, a N_κ is the electron number operator in the lead κ . With the help of Eq. (2.11) the averaged current takes the form,

$$J_\kappa = \eta_\kappa \text{Tr} \int_{-\infty}^t dt' e^{iH_0(t-t')} I_\kappa e^{-iH_0(t-t')} [H_{tun}, \rho] + \text{c.c.},$$

$$I_\kappa = et_0 e^{-i\lambda p} \sum_k c a_{k,\kappa}^\dagger. \quad (2.28)$$

The straightforward calculation of Eq.(2.28) yields the following equation analogous to Eq.(2.19),

$$\frac{J(t)}{I_0} = -\rho_0(t)P_1(t) + P_2(t), \quad (2.29)$$

where $I_0 = e\Gamma/2$ is the saturation current through a single-level symmetric junction,

$$P_i(t) = \sum_n A_n^{(i)}(t) [f_L(\varepsilon_0 - n\omega) - f_R(\varepsilon_0 - n\omega)], \quad (2.30)$$

and coefficients $A_n^{(i)}$ are determined by Eqs. (2.21)-(2.23). From Equations (2.24),(2.26) and (2.29) one gets the following expression for the averaged current,

$$I = I_0 \sum_{n,k} \left[a_{n,k}^{(2)} \delta_{k,0} - a_{n,k}^{(1)} \rho_k \right] [f_L(\varepsilon_0 - n\omega) - f_R(\varepsilon_0 - n\omega)]. \quad (2.31)$$

Note that the average current does not depend on the phase φ of the coherent state.

2.4. Results of numerical calculations of I - V characteristics.

Equation (2.25) is the system of infinite number of equations for the Fourier harmonics. However, in this case the series for the coefficients of the harmonics converge quickly enough to allow one to consider only first several terms. Meanwhile, the sufficient number of the terms depends on parameters of the system, especially on the coherent state parameter $|z|$. Results of numerical calculations of Eq. (2.31) and (2.25) are presented in Figs. 2.2,2.3.

As one can see, the plots for coherent vibrons (black dotted curves) demonstrate step-like behavior of current versus bias voltage at low temperatures, $T \ll \hbar\omega$. This behavior is similar (however, in general case not identical) to Franck-Condon steps in $I - V$ curves known for equilibrated vibrons (see e.g. review paper Ref. [11] and references therein). The curves for equilibrated and coherent vibrons coincide (see Fig. 2.2) when the amplitude of oscillations of QD is less or of the order of the amplitude of zero-point oscillations l_0 , $|z| \leq 1$.

It is physically clear that in this case both systems are close to their ground state (the average number of vibrons $\langle n \rangle \ll 1$) and there is no difference in the behavior of coherent and non-coherent vibrons. The strong differences appear

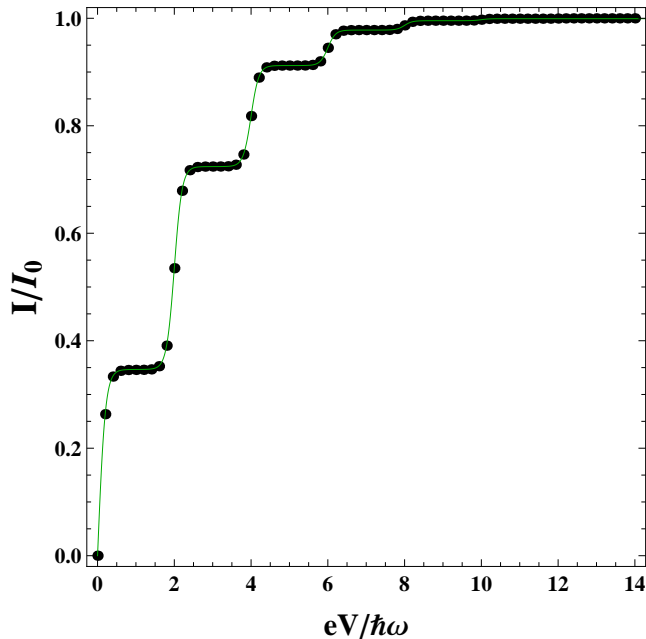


Fig. 2.2 The current-voltage dependencies for small value of coherent state parameter of vibrons $|z| = 0.25$ and for strong electron-vibron interaction $\lambda = 1$. The black dotted curve corresponds to numerical calculation of current when the vibrons are in the coherent state. The thin green curve represents $I - V$ characteristics when the vibrons are in equilibrium and characterized by the effective temperature T^* determined by Eq. (2.32). In calculations the values $T/\hbar\omega = 0.05, \Gamma/\hbar\omega = 0.001$ was used.

for large amplitudes of oscillations when $|z| \gg 1$ (see Fig. 2.3 where the dotted curve corresponds to vibrons in the coherent state with parameter $|z| = 10$). It is useful to introduce effective temperature of vibrons T^* by equating the average number of vibrons in coherent and equilibrium state,

$$|z|^2 = (\exp(\hbar\omega/T^*) - 1)^{-1}. \quad (2.32)$$

Then for large amplitudes of oscillations ($|z| \gg 1$) and moderately strong electron-vibron interaction ($\lambda \sim 1$) $T^* \simeq |z|^2 \hbar\omega \gg \lambda^2 \hbar\omega$. It is clear that at these high temperatures of the leads the Franck-Condon steps in $I - V$ characteristics will be smeared out. It means that coherent vibrons for large amplitudes of QD oscillations lead to strong suppression of current at low biases and to pronounced step-like behavior of $I - V$ curves. It is interesting to compare this behavior with the Franck-Condon theory by assuming that the vibronic subsystem is hot (it is described by Bose-Einstein distribution with the temperature T^*), while the leads

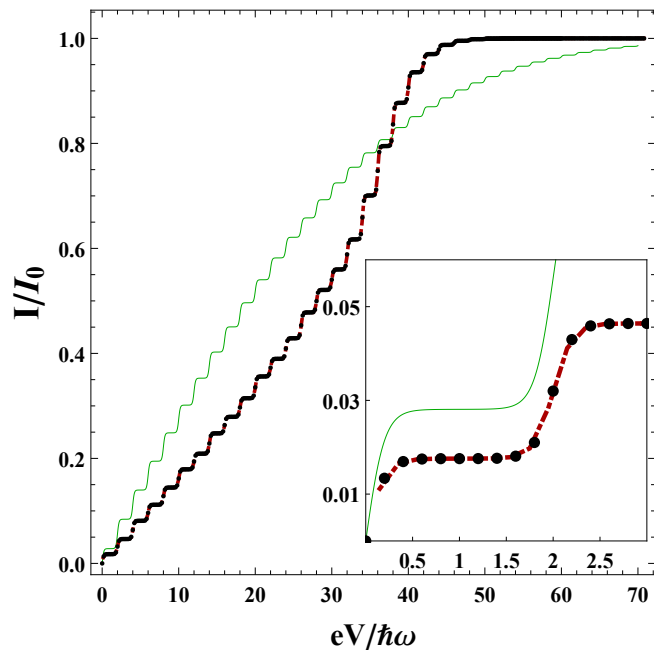


Fig. 2.3 $I - V$ plots for the large value of the parameter $|z| = 10$. All other parameters are the same as in Fig. 2.2. The thin green curve corresponds to the case of equilibrated vibrons with the effective temperature determined by the parameter $|z| = 10$. The red dash-dotted curve represents calculation of current in the approximation when $\rho_0 = 0.5$ (see subsection 2.5). Inset shows the region of low voltages.

are kept at low temperatures $T \ll \hbar\omega$. The thin green curve in Fig. 2.3 demonstrates this case. We see rather strong differences in current-voltage dependencies: (i) the height of the steps for coherent vibrons are not regular, and (ii) the current in the case of coherent vibrons saturates at lower voltages ($eV_s \simeq |z|\hbar\omega$) than for equilibrated vibrons.

2.5. Estimation of the probability and current in steady-state regime

While computing of Eqs. (2.31) and (2.25), one can note that the coefficient ρ_0 (zeroth harmonic) of the Fourier series (2.24) in the stationary regime is equal to $\rho_0 = 0.5$ with very high accuracy, $\sim 10^{-5}$. It means that the probability (matrix elements of the reduced density matrix) does not depend on time, $\rho_0 = \rho_1 = 1/2$. Then, by substituting $\rho_0 = 1/2$ and $\rho_p = 0$ for $p \geq 1$ in Eq. (2.31), we obtain a simple *analytic* formula for the time-averaged electric current,

$$I = I_0 \sum_n a_n [f_L(\varepsilon_0 - n\omega) - f_R(\varepsilon_0 - n\omega)], \quad (2.33)$$

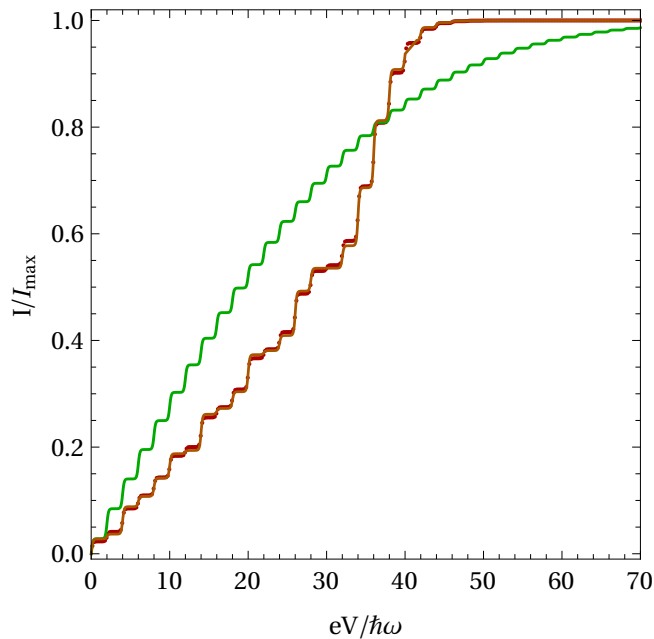


Fig. 2.4 $I - V$ plots for the large value of the parameter $|z| = 20$ and $\lambda = 0.5$.

All other parameters are the same as in Fig. 2.2. The thin green curve corresponds to the case of equilibrated vibrons with the effective temperature determined by the parameter $|z| = 20$. The red dash-dotted curve represents calculation of current in the approximation when $\rho_0 = 0.5$ (using Eqs. (2.31) and (2.25)) and almost matches the solid orange curve obtained with the help of Eq. (2.35).

where

$$a_n = \frac{1}{\pi} \int_0^\pi d\vartheta e^{-\lambda^2(1-\cos\vartheta)} \times \\ \times \cos n\vartheta \cos(\lambda^2 \sin\vartheta) J_0\left(4\lambda|z| \sin\frac{\vartheta}{2}\right). \quad (2.34)$$

Furthermore, for the case $\lambda \leq 1$ we can proceed with estimation of the integral in Eq. (2.34),

$$a_n \simeq J_n^2(2\lambda|z|). \quad (2.35)$$

This allows us to strongly simplify numerical calculations. Figures 2.3 and 2.4 represent obtained current-voltage characteristics. The red dash-dotted curve corresponds to calculations using Eqs. (2.33) та (2.34). This approximate analytical calculations coincide with the numerical ones with a sufficiently high accuracy ($\sim 10^{-5}$).

It needs to be noted that Eq. (2.33) has the same form as a well-known equation (see, e.g., Ref.[11]) for the current of spinless electrons through a vibrating QD with equilibrated vibrons (when the mechanical subsystem is described by equilibrium density matrix ρ_{eq}),

$$I_{eq} = I_0 \sum_n A_n [f_L(\varepsilon_0 - n\omega) - f_R(\varepsilon_0 - n\omega)], \quad (2.36)$$

where now spectral densities A_n are defined by the expression $\text{Tr} [e^{-i\lambda p(t)} e^{i\lambda p(0)} \rho_{eq}] = \sum_n A_n e^{i\omega n t}$, see subsection 1.1.2.

Conclusions

In this chapter the electron transport in a molecular transistor has been considered, assuming vibrations of quantum dot oscillations to be in a coherent state. It was shown that $I - V$ curves at low temperatures have a step-like form which is similar to the steps that accompany the lifting of the Franck-Condon blockade by bias voltage. However, for large amplitudes of oscillations there are strong differences in the predictions of the Franck-Condon theory and the model considered in this chapter. By using numerical calculations we found strong suppression of conductance even for a weak or moderately strong electron-vibron coupling. The lifting of this coherent oscillations-induced blockade by a bias voltage occurs at voltages much lower than the ones predicted by the Franck-Condon theory. In addition, $I - V$ characteristics of a single-electron transistor with coherent vibrons do not depend on the phase of coherent state parameter.

The main statements of this chapter are based on the publications [1, 5, 6].

CHAPTER 3

ENTANGLEMENT BETWEEN CHARGE QUBIT STATES AND COHERENT STATES OF NANOMECHANICAL RESONATOR GENERATED BY AC JOSEPHSON EFFECT

In this chapter a superconducting nanoelectromechanical system based on a nanowire is considered. An experimentally simple protocol for bias voltage manipulation is discussed. This protocol results in the formation of the entanglement, which can be controlled by parameters of the device, between the charge qubit and the nanomechanical resonator. An experimentally feasible detection of the effects by measuring average current is also considered.

3.1. Model and Hamiltonian of the nanoelectromechanical device.

A schematic representation of the nanoelectromechanical system (NEMS) prototype, which is under the consideration, is presented in Fig. 3.1. It consists of the superconducting nanowire (SCNW) [157, 158], which is suspended between two bulk superconductors and is capacitively coupled to two side gate electrodes. In what follows we consider the case when SCNW represents a superconducting island that can be treated as a charge qubit (Cooper-pair box) whose basis states are charge states — states which represent the presence or absence of excess Cooper pairs on the island. Usually these states are referred to as charge and neutral states correspondingly. As this takes place, the gate voltage V_G and the voltage applied between the gates $V_{\mathcal{E}}$ are chosen in the way that the difference in the electrostatic energies of the charged and neutral states equals to zero at the straight configuration of the nanowire, while nanowire bending removes this degeneracy. We also reduce the bending dynamics of the SCNW to the dynamics of the fundamental flexural mode described by the harmonic oscillator.

Joint Cooper pairs dynamics and mechanical one of this system is described by the Hamiltonian which can be presented in the form,

$$H = H_q + H_m + H_{int}. \quad (3.1)$$

Here

$$H_{q,int} = \frac{[\hat{Q} + Q_G(\hat{x})]^2}{2C(\hat{x})} - \sum_{\sigma} [E_{J,\sigma} \cos(\phi_{\sigma} - \hat{\phi})], \quad (3.2)$$

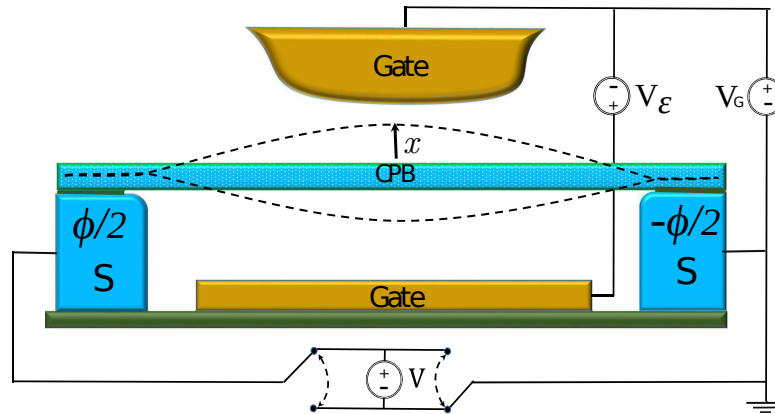


Fig. 3.1 Schematic illustration of the NEMS under consideration. The superconducting nanowire, treated as a charge qubit, is tunnel coupled to two bulk superconductors (S) with the superconducting phase difference ϕ and capacitively coupled to the two gate electrodes. The bending oscillations in the x direction are described by the harmonic oscillator.

where $\hat{Q} = 2e\hat{n}$ is discrete charge operator on the dot (\hat{n} is Cooper pair number operator on the dot), $Q_G(\hat{x}) = V_G C_G(\hat{x})$ is continuous charge generated by the gate voltage V_G , $C(\hat{x}) = 2C_J + C_G(\hat{x})$ is the mutual capacitance that includes gate and Josephson junctions ones. The constant $E_J = E_{J,L} = E_{J,R}$ is the Josephson coupling energy (we consider only the case of symmetric coupling), $\hat{\phi}$ is the phase operator on the dot that satisfies commutation relation $[\hat{\phi}, \hat{n}] = i$. Thus, Eq. (3.2) can be rewritten as:

$$H_{q,int} = E_c(\hat{x}) \left(\hat{n} + \frac{C_G(\hat{x})V_G}{2e} \right)^2 - 2E_J \cos \phi \cos \hat{\phi}. \quad (3.3)$$

Here $E_c(\hat{x}) = (2e)^2/(2C(\hat{x}))$ is the charging energy. The coordinate-dependent gate capacitance $C_G(\hat{x})$ is tuned in such a way that the difference of the electrostatic energies between the charge (with one exceed Cooper pair) and neutral state is proportional to the CPB dimensionless displacement \hat{x} and is equal to zero at an equilibrium point of oscillations. Then in Coulomb blockade regime ($E_C(0) \gg E_J$) in a charge basis with determined number of Cooper pairs on the

island the operator function $\exp[\imath\hat{\phi}]$ is:

$$e^{\imath\hat{\phi}}|n\rangle = \frac{1}{\sqrt{2\pi}} \int_0^{2\pi} d\phi e^{\imath(n+1)\phi} |\phi\rangle = |n+1\rangle. \quad (3.4)$$

Therefore, in the basis netted on the neutral $|0\rangle = (0; 1)^T$ and charged $|1\rangle = (1; 0)^T$ state and in the particle number representation for mechanical variables one gets:

$$\begin{aligned} H_q &= -E_J \sigma_1 \cos \phi, \\ H_m &= \frac{\hbar\omega}{2} (\hat{x}^2 + \hat{p}^2), \\ H_{int} &= \varepsilon \hat{x} \sigma_3. \end{aligned}$$

where $\sigma_i, i = 1, 2, 3$, are the Pauli matrices, E_Q is actually the energy associated with the electrostatic field generated by gate voltage V_G . It implies that only the first order of the gate capacitance matters and the case of toward the degeneracy point in an equilibrium point is considered. Note that one can diagonalize the non-perturbation part of the Hamiltonian, Eq. (3.5), by the unitary transformation:

$$\hat{U} = (I + \imath\sigma_2) / \sqrt{2}, \quad (3.5)$$

which turns $\sigma_1 \rightarrow \sigma_3, \sigma_3 \rightarrow -\sigma_1$. Then,

$$H = \varepsilon \hat{x} \sigma_1 + E_J \cos \phi(t) \sigma_3 + \frac{\hbar\omega}{2} (\hat{x}^2 + \hat{p}^2). \quad (3.6)$$

Here Hamiltonian H_q represents Josephson coupling between the Cooper Pair Box (CPB) and bulk superconductors with $\phi = \phi(t)$ is the superconducting phase difference between electrodes, $\sigma_i (i = 1, 2, 3)$ are the Pauli matrices acting in the qubit Hilbert space in a basis where vectors $(1, 0)^T$ and $(0, 1)^T$ represent charged and neutral states, respectively. Hamiltonian H_m in Eq. (3.1) represents dynamics of the fundamental bending mode described by the harmonic oscillator with frequency ω (here momentum and coordinate operators, \hat{p} and \hat{x} , are normalized on the amplitude of zero-point oscillations $x_0 = \sqrt{\hbar/M\omega}$, M is an effective mass of the island, $[\hat{x}, \hat{p}] = \imath$). The third term, H_{int} , describes the electromechanical coupling between the charge qubit and the mechanical oscillator induced by the electrostatic force acting on the charged state of the qubit, $\varepsilon = e\mathcal{E}x_0$. In the

last equality, \mathcal{E} is an effective electrostatic field that is controlled by the difference of the applied voltages V_G and V_ε . Below we assume $\varepsilon \ll \hbar\omega, E_J$ that corresponds to a typical experimental situation [86, 91, 159].

The states of the system described by the Hamiltonian, Eq. (3.1), are a superposition of direct products of qubit states, \mathbf{e}_i^\pm , and eigenstates of the oscillator $|n\rangle$. Here and below \mathbf{e}_i^ν denotes the eigenvectors of the Pauli matrices σ_i with eigenvalues $\nu = \pm 1$.

If $\varepsilon = 0$, the interaction between the qubit and the mechanical subsystem is switched off and stationary states of the Hamiltonian, Eq. (3.1), are pure states. The entropy of entanglement is an integral of motion, i.e. if the system is initially in a pure state, it will be in a pure state at any moment of time. If we apply a constant bias voltage between superconducting leads, an oscillatory ($\propto \sin \phi(t)$) current emerges due to ac Josephson effect, $\dot{\phi}(t) = 2eV/\hbar$, where V is a bias voltage. The synchronous switching on the electrical field \mathcal{E} and the bias voltage between the superconducting leads results in the evolution of such pure states in the states represented by entanglement between the qubit and oscillator states.

3.2. Time evolution of the system.

To carry out an analysis of time evolution of the system, we introduce the dimensionless time and energies, $\omega t \rightarrow t, E_J/\hbar\omega \rightarrow E_J, \varepsilon/\hbar\omega \rightarrow \varepsilon$ and assume that at the moment of switching on the interaction between the subsystems ($t = 0$), the difference between the superconducting phases is $\phi = \phi_0$ and the system has been in a pure state,

$$|\Psi(0)\rangle = \mathbf{e}_{in} \otimes |0\rangle. \quad (3.7)$$

At $t > 0$, according to the (second) Josephson relation,

$$\dot{\phi}(t) = 2eVt/\hbar\omega + \phi_0. \quad (3.8)$$

The Hamiltonian, Eq. (3.1), and, as a consequence, the time evolution operator $\hat{U}(t, t')$, which is defining evolution of the arbitrarily initial state, have the following properties,

$$\hat{H}(t + T_V) = \hat{H}(t), \quad \hat{U}(t, t') = \hat{U}(t + T_V, t' + T_V), \quad (3.9)$$

that is they are periodic in time with the period

$$T_V = 2\pi/\Omega_V = \pi\hbar\omega/e|V|. \quad (3.10)$$

To analyze the evolution operator, one can use the interaction picture (with respect to the interaction Hamiltonian H_{int}) taking,

$$\hat{U}(t,t') = \hat{U}_\kappa(t)\hat{U}_\kappa(t,t')\hat{U}_\kappa^\dagger(t'), \quad (3.11)$$

where

$$\hat{U}_\kappa(t) = \exp \left[\frac{iE_J}{\Omega_V} \sigma_1 \sin(\Omega_V t + \kappa\phi_0) - ia^\dagger a t \right], \quad (3.12)$$

is the unitary evolution operator corresponded to the non-perturbed Hamiltonian and describes free evolution of mechanical and electronic subsystem independently. The parameter $\kappa = \text{sgn}(V/|V|) = \pm$ characterizes the direction of the bias voltage drop. The operator $\hat{U}_\kappa(t,t')$ obeys the following equations,

$$\begin{aligned} i \frac{\partial \hat{U}_\kappa(t,t')}{\partial t} &= \hat{\mathcal{H}}_\kappa(t) \hat{U}_\kappa(t,t'), \\ \hat{\mathcal{H}}_\kappa(t) &= \varepsilon \hat{x}(t) \sigma_3(t), \quad \hat{U}_\kappa(t,t) = \hat{I}. \end{aligned} \quad (3.13)$$

Here

$$\begin{aligned} \hat{x}(t) &= \frac{1}{\sqrt{2}}(\hat{a}e^{-it} + \hat{a}^\dagger e^{it}), \\ \sigma_3(t) &= \sigma_3 \cos \left(\frac{E_J}{\Omega_V} \sin(\Omega_V t + \kappa\phi_0) \right) - \\ &\quad - \sigma_2 \sin \left(\frac{E_J}{\Omega_V} \sin(\Omega_V t + \kappa\phi_0) \right). \end{aligned} \quad (3.14)$$

If the frequencies ω and Ω_V are incommensurable, the operator $\hat{\mathcal{H}}_\kappa(t)$ is a quasiperiodic function of time. In such a case one can expect that the mechanical subsystem, being initially in the ground state, does not significantly deviate from this state in the process of evolution. A rigorous consideration of this case is done numerically [160]. Here let us consider the resonant case when $\Omega_V = \omega$ and assume that $\varepsilon \ll 1$. The first condition stipulates the following properties of the evolution operator,

$$\hat{\mathcal{U}}_{\kappa}(2\pi N, 2\pi N') = \left(\hat{\mathcal{U}}_{\kappa}(2\pi, 0) \right)^{N-N'}, \quad (3.15)$$

where N, N' are natural numbers. The second assumption allows us to make the following substitution in a leading approximation regarding small ε ,

$$\hat{\mathcal{U}}_{\kappa}(t, t') = \hat{\mathcal{U}}_{\kappa}(2\pi N, 2\pi N'), \quad (3.16)$$

where $N(N') = [t(t')/2\pi]$ ($[x]$ is an integer part of x), and obtain an expression for $\hat{\mathcal{U}}_{\kappa}(2\pi, 0)$ which can be written as,

$$\begin{aligned} \hat{\mathcal{U}}_{\kappa}(2\pi, 0) &= \exp \left[i\tilde{\varepsilon}\sigma_2\hat{p}(\kappa\phi_0) + \varepsilon^2\mathcal{O}(\hat{I}) \right], \\ \hat{p}(\phi) &= \hat{p}\cos\phi + \hat{x}\sin\phi. \end{aligned} \quad (3.17)$$

Here $\tilde{\varepsilon} = 2\pi\varepsilon J_1(2E_J)$ and $J_1(x)$ is the Bessel function of the first kind. Using the above relations one can obtain an expression for the evolution operator $\hat{U}(t, t')$, which in the main approximation regarding ε has a form,

$$\hat{U}(t, t') = \hat{\mathcal{U}}_{\kappa}(t) \exp [i\tilde{\varepsilon}\sigma_2\hat{p}(\kappa\phi_0)(t - t')] \hat{\mathcal{U}}_{\kappa}^{\dagger}(t'). \quad (3.18)$$

Using Eqs. (3.7),(3.18), one gets that at the time t , with the accuracy to small parameter $\tilde{\varepsilon} \ll 1$, the state of the system $|\Psi(t)\rangle$ is given by an expression,

$$|\Psi(t)\rangle = \sum_{\nu} A_{\nu}^{\kappa} \mathbf{e}_2^{\nu}(t, \kappa\phi_0) \otimes |-\nu z(t, \kappa)/\sqrt{2}\rangle. \quad (3.19)$$

Here

$$\mathbf{e}_2^{\nu}(t, \kappa\phi_0) = \mathbf{e}_2^{\nu} \exp [iE_J\sigma_1 \sin(t + \kappa\phi_0)],$$

and $\mathbf{e}_2^{\nu} = \sigma_1 \mathbf{e}_2^{-\nu}$ are the eigenvectors of the Pauli matrix σ_2 with eigenvalues $\nu = \pm 1$,

$$A_{\nu}^{\kappa} \equiv (\mathbf{e}_2^{\nu}(0, \kappa\phi_0), \mathbf{e}_{in}) = \cos(\kappa E_J \sin\phi_0) c_2^{\nu} - i \sin(\kappa E_J \sin\phi_0) c_2^{-\nu}, \quad (3.20)$$

where an initial state can be presented in a basis of eigenvectors of the matrix σ_2 as:

$$\mathbf{e}_{in} = \sum_{\nu=\pm 1} c_2^{\nu} \mathbf{e}_2^{\nu}. \quad (3.21)$$

The symbol $|\alpha\rangle$ (where α is a complex number) denotes the coherent states of the harmonic oscillator, $\hat{a}|\alpha\rangle = \alpha|\alpha\rangle$, while a complex function $z(t, \kappa)$ is defined as:

$$z(t, \kappa) = \tilde{\epsilon}t \exp[-\imath(t + \kappa\phi_0)]. \quad (3.22)$$

It should be stressed that Eq. (3.19) is valid only for restricted time interval $t \leq \tilde{\epsilon}^{-2}$. Time t should be also shorter than any dephasing and relaxation times. From Eq. (3.19) one can see that initially pure state $|\Psi(t = 0)\rangle = \mathbf{e}_{in} \otimes |0\rangle$ evolves into the state represented by the entanglement between the two qubit states and two coherent states of the mechanical resonator. Moreover, the details of this entanglement depend on switching time (parameter ϕ_0) and direction of the bias voltage (parameter κ). These circumstances allow one to manipulate the described above entanglement by changing the bias voltage direction.

3.3. Generation of "Schrödinger-cat states".

To demonstrate the effect of the entanglement between the charge qubit and mechanical vibrations that comprehends the formation of so-called Schrödinger-cat states of nanomechanical resonator, we consider the following time protocol for $V(t)$:

$$2eV(t) = -\hbar\omega\theta(t) [1 - 2\theta(t - t_s)].$$

Namely, during the time interval $0 < t < t_s$ the bias voltage $V(t) = -\hbar\omega/2e$ and then it switches its sign. Using Eqs. (3.11), (3.15), (3.17), one gets that at $t > t_s$ the evolution operator has the form:

$$\hat{U}(t, 0) = \hat{U}_+(t) e^{i\sigma_2 \tilde{\epsilon}(t-t_s) \hat{p}(\phi_0)} \hat{S} e^{i\sigma_2 \tilde{\epsilon} t_s \hat{p}(-\phi_0)} \hat{U}_-(0), \quad (3.23)$$

where

$$\begin{aligned} \hat{S} &= \hat{U}_+^\dagger(t_s) \hat{U}_-(t_s) \equiv \rho(t_s, \phi_0) + i\tau(t_s, \phi_0) \sigma_1, \\ \rho(t_s, \phi_0) &= \cos(2E_J \cos t_s \sin \phi_0), \\ \tau(t_s, \phi_0) &= -\sin(2E_J \cos t_s \sin \phi_0). \end{aligned} \quad (3.24)$$

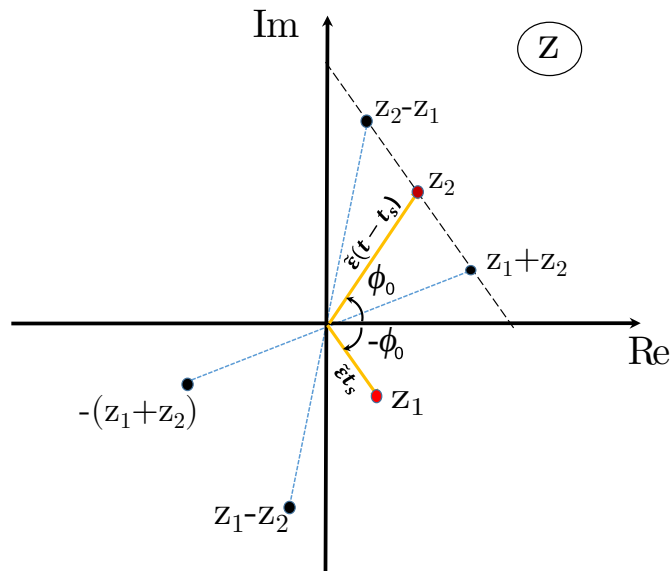


Fig. 3.2 Schematic illustration of the positions of the coherent states described by the complex numbers $z_{1,2}$ and their combinations z_{\pm} in the complex plane. It denotes the time evolution of the coherent states, on the one hand, and the dependence on the initial phase difference ϕ_0 , on the other one.

As a result, the state of the system after changing the direction of the bias voltage takes the following form:

$$|\Psi(t)\rangle = \sum_{\nu} \mathbf{e}_2^{\nu}(t, \phi_0) \otimes \left(\rho A_{\nu}^{-} | -\nu z_{+} / \sqrt{2} \rangle + \nu \tau A_{-\nu}^{-} | \nu z_{-} / \sqrt{2} \rangle \right), \quad (3.25)$$

where $z_{\pm} = z_1 \pm z_2$ and

$$\begin{aligned} z_1 &= e^{-i(t-\phi_0)} \tilde{\epsilon} t_s, \\ z_2 &= e^{-i(t+\phi_0)} \tilde{\epsilon} (t - t_s). \end{aligned} \quad (3.26)$$

A schematic representation of evolution of the coherent states can be seen in Fig. 3.2. Equation (3.25) demonstrates that the state of the system is represented by the entanglement of two qubit state with two so-called "cat states" (superposition of coherent states) whose structure is controlled by the parameters E_J (ρ) and ϕ_0 . As it follows from Eqs. (3.25), (3.26), the bias voltage switching does not affect the dynamics of the system if $\phi_0 = \pi n$ with n standing for an integer number.

3.4. Entanglement entropy.

Let us limit ourselves for simplicity to considering a most interesting case when $\phi_0 = \pi/2$ and put $\mathbf{e}_{in} = (\mathbf{e}_2^+ + \mathbf{e}_2^-)/\sqrt{2}$, that is, we suppose that immediately before the interaction was switched on, the qubit was in the eigenstate of the operator $\hat{H}_q(t = 0 - \delta)$. With these assumptions Eq. (3.20) transforms to:

$$A_+^- = A_-^- = \exp(iE_J)/\sqrt{2}. \quad (3.27)$$

To characterize the entanglement between the qubit states and the states of the mechanical oscillator, we introduce the reduced density matrices, $\hat{\rho}_{q(m)}(t) = \text{Tr}_{m(q)}\hat{\rho}$, where

$$\hat{\rho} = |\Psi(t)\rangle\langle\Psi(t)| \quad (3.28)$$

is a complete density matrix of the system and $\text{Tr}_{m(q)}$ denotes the trace over mechanical (qubit) degrees of freedom. Using Eqs. (3.19),(3.25), one can get the following expression for the reduced qubit density matrix $\hat{\rho}_q$,

$$\hat{\rho}_q(t) = \frac{I + \lambda(t,t_s)\sigma_1}{2}, \quad (3.29)$$

where

$$\lambda(t,t_s) = \exp(-\tilde{\varepsilon}^2 t^2), \quad 0 < t \leq t_s, \quad (3.30)$$

$$\lambda(t,t_s) = \rho^2 \exp[-\tilde{\varepsilon}^2(t - 2t_s)^2] + \tau^2 \exp(-\tilde{\varepsilon}^2 t^2), \quad t > t_s. \quad (3.31)$$

Note that $\lambda(t,t_s) \geq 0$. When deriving Eq. (3.29), we took into account relation $\mathbf{e}_2^+(\mathbf{e}_2^-)^\dagger + \mathbf{e}_2^-(\mathbf{e}_2^+)^\dagger = \sigma_1$. The entropy of entanglement (also called the von Neumann entropy) is defined as:

$$S_{en}(t) \equiv -\text{Tr} \hat{\rho}_q(t) \log \hat{\rho}_q(t) = -\text{Tr} \hat{\rho}_m(t) \log \hat{\rho}_m(t). \quad (3.32)$$

Since the basis of the coherent state is not orthonormal (quasiorthogonal, in fact) and overcomplete, it is suitable to use Eq. (3.29). In order to calculate the entanglement entropy, it is convenient to present the matrix in a diagonal form. The reason is if $\lambda_i, i = 1,2$ is an eigenvalue of the matrix $\hat{\rho}_q$, then Eq. (3.32) can be

rewritten as:

$$S_{en}(t) = - \sum_{i=1,2} \lambda_i \log \lambda_i. \quad (3.33)$$

One can easily find the eigenvalues of the reduced qubit density matrix $\hat{\rho}_q$, Eq. (3.29),

$$\lambda_{1,2} = \frac{1}{2} [1 - \lambda(t, t_s)]. \quad (3.34)$$

From these equations one can see that the maximal value of the entanglement is $S_{en}^{(max)} = \log 2$ (when $\lambda_{1,2} = 1/2$), meaning that correlations between the electronic and mechanical subsystems are maximal. In the calculations such a usual way of treating the uncertainty $0 \log 0 = 0$ is accepted. In general, entropy of entanglement is a limited function, $0 \leq S_{en} \leq \log N$, where N stands for the number of subsystems (degrees of freedom) which a whole system consists of.

A plot of $S_{en}(t)$ for $\tilde{\varepsilon}t_s = 1$ and different values of ρ (equally, for $\tau^2 = 1 - \rho^2$) is presented in Fig. 3.3. The entanglement entropy monotonically increases in time within intervals $0 < t < t_s$ and $2t_s < t < \infty$ saturating to the maximal value $S_{en}^{(max)}$ at $t \rightarrow \infty$. Within interval $t_s < t \leq 2t_s$ behavior of the entanglement entropy depends on the relation between ρ and τ . In particular, for $\rho^2 > \tau^2$ the entanglement entropy $S_{en}(t)$ starts to decrease after switching, reaching some minimal value (equals zero for the $\rho^2 = 1$, i. e., our system is separable) within interval $t_s < t \leq 2t_s$. If $\rho^2 < \tau^2$, the entropy continues to grow just after the switching. However, its derivative might be also negative within some time interval whose existence is controlled by the parameters $\tilde{\varepsilon}t_s$ and τ^2/ρ^2 .

In addition let us also briefly consider a more general case of an arbitrary value of initial superconducting phase difference ϕ_0 . For the time interval $0 < t \leq t_s$, the qubit density matrix is given by Eqs. (3.29), (3.30). However, for the time after the bias voltage switching, $t > t_s$, one can find the following expression for the density operator of the qubit,

$$\begin{aligned} \rho_q(t) = & \frac{1}{2}I + I\rho\tau e^{-\tilde{\varepsilon}^2 t_s^2} \sin \{ \tilde{\varepsilon}^2 t_s (t - t_s) \sin (2\phi_0) \} + \\ & + \frac{1}{2}\sigma_1 e^{-\tilde{\varepsilon}^2 (t_s^2 + (t-t_s)^2)} \left[\rho^2 e^{-2\tilde{\varepsilon}^2 t_s (t-t_s) \cos (2\phi_0)} + \tau^2 e^{2\tilde{\varepsilon}^2 t_s (t-t_s) \cos (2\phi_0)} \right] - \\ & - \sigma_1 \rho \tau e^{-\tilde{\varepsilon}^2 (t-t_s)^2} \sin \{ \tilde{\varepsilon}^2 t_s (t - t_s) \sin (2\phi_0) \}. \end{aligned} \quad (3.35)$$

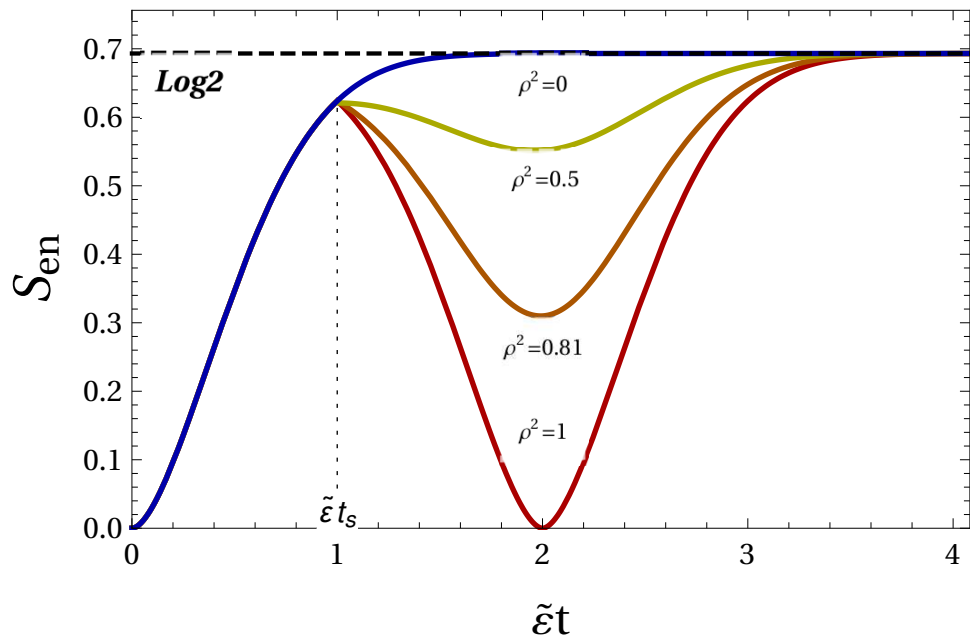


Fig. 3.3 The entanglement entropy dependent on time for different values of $\rho = 0, 1/\sqrt{2}, 0.9, 1$ (blue, yellow, orange and red curves). The thin dotted line indicates the bias voltage switching time. The dashed curve corresponds to the maximal value of the entanglement, $\log 2$.

From this equation one can find, in particular, following the above-mentioned procedure, that the maximal effect is achieved at $\phi_0 = \pi/2$ and one get Eq. (3.29).

3.5. Time evolution of the mechanical subsystem.

To describe the evolution of the mechanical subsystem, we consider the reduced density matrix $\hat{\varrho}_m(t)$. From Eq. (3.25) one gets that at $t > t_s$ the reduced density matrix of the mechanical subsystem takes a form,

$$\hat{\varrho}_m(t) = \frac{1}{2} \sum_{\nu} \left[\rho^2 |\nu z_+ / \sqrt{2}\rangle \langle \nu z_+ / \sqrt{2}| + \tau^2 |\nu z_- / \sqrt{2}\rangle \langle \nu z_- / \sqrt{2}| - \right. \\ \left. - i\rho\tau \left(| - \nu z_+ / \sqrt{2}\rangle \langle \nu z_- / \sqrt{2}| - \text{H.c.} \right) \right]. \quad (3.36)$$

To visualize the state of the mechanical subsystem, it is convenient to use the Wigner function representation for the density matrix $\hat{\varrho}_m(t)$,

$$W(x, p, t) = \frac{1}{\pi} \int \varrho_m(x + y, x - y, t) \exp(2ipy) dy,$$

where $\varrho_m(x, x', t) = \langle x | \hat{\varrho}_m(t) | x' \rangle$. Using Eq. (3.36), one gets

$$W(x, p, t) = W_t(x \cos t - p \sin t, p \cos t + x \sin t), \quad (3.37)$$

where the function $W_t(x, p)$ is defined according to the relation,

$$W_t(x, p) = \frac{1}{2} \sum_{\nu} [\rho^2 W_0(x, p + \nu |z_+|) + \tau^2 W_0(x, p - \nu |z_-|) + 2\rho\tau \sin(2\nu Z_- x) W_0(x, p + \nu Z_+)]. \quad (3.38)$$

In Eq. (3.38) $Z_{\pm} = (|z_-| \pm |z_+|) / 2$ and

$$W_0(x, p) = \frac{1}{\pi} \exp[-(x^2 + p^2)] \quad (3.39)$$

is the Wigner function corresponding to the ground state of a harmonic oscillator. Plots of $W(x, p, t)$ for $t = 2\pi N$, $\rho = 0$, $\rho = 1$ and $\rho = \tau = 1/\sqrt{2}$ at $|z_+| = 3$ and $|z_-| = 9$ are presented in Figs. 3.5 and 3.5.

From Equations (3.36), (3.38) one can see that in the case when ρ is equal to zero or one (in particular, when $t_s = 0$) the Wigner function is positive and has two maxima, demonstrating the entanglement between two states of the qubit and two coherent states (see Fig. 3.5). In general case $\rho\tau \neq 0$, and the Wigner function takes both positive and negative values at $t > t_s$, demonstrating the entanglement of two states of the qubit with the superposition of two quasi-orthogonal coherent states of the nanomechanical resonator (see Fig. 3.5).

3.6. Time-averaged electric current.

As it follows from the above consideration, the amplitude of mechanical fluctuations, and therefore the energy stored in the mechanical subsystem, changes over time. This energy comes from the electronic subsystem causing a rectification of ac current. To analyze this phenomenon, we calculate the dimensionless (normalized to $I_0 = 2e/\hbar$) ac Josephson current averaged over the N -th period of the Josephson oscillations,

$$I_N = \frac{1}{2\pi} \int_{2\pi(N-1)}^{2\pi N} dt \text{Tr} \left(\frac{\partial \hat{H}_q(t)}{\partial \phi} \hat{\varrho}(t) \right).$$

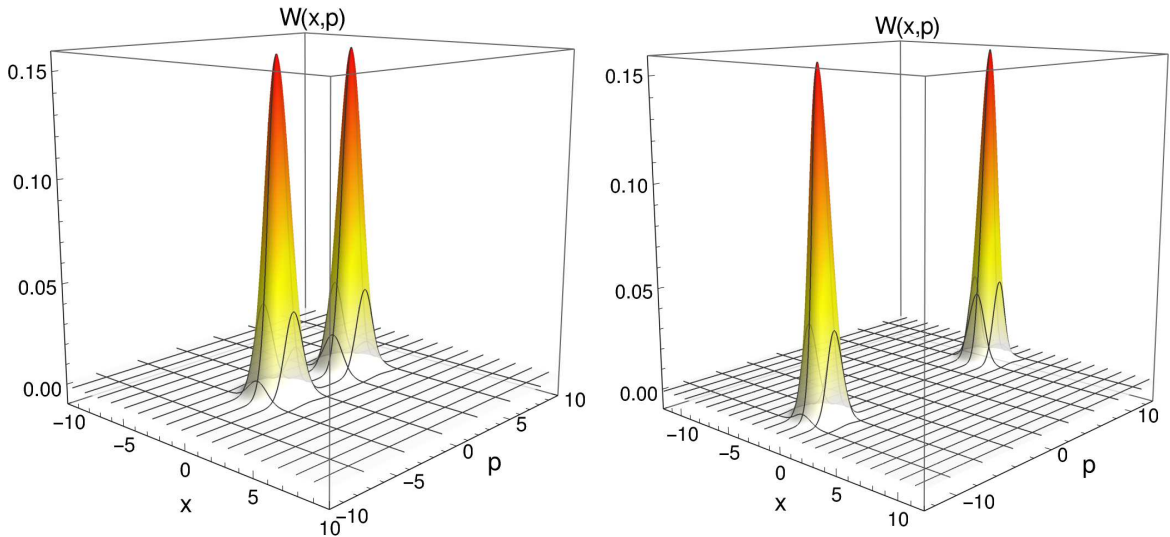


Fig. 3.4 The Wigner functions $W(x,p,t = 2\pi N)$ for $\rho = 1$ (a) and $\rho = 0$ (b). It takes only positive values and has two maxima demonstrating the entanglement between two qubit states and two coherent states of the nanomechanical resonator.

Taking into account that $\partial \hat{H}_q / \partial \Phi = \eta \partial \hat{H} / \partial t$ and $\hat{H}_q(t = 2\pi N) = 0$, one gets the following expression for I_N ,

$$\begin{aligned} I_N &= \frac{\kappa}{2\pi} \nabla_N \text{Tr} \left(\hat{H}_m + \hat{H}_{int} \right) \hat{\rho}(2\pi N) \\ &= \frac{\kappa}{2\pi} \nabla_N [E_m(N) + E_{int}(N)], \end{aligned} \quad (3.40)$$

where $\nabla_N f(N) \equiv f(N) - f(N - 1)$ is the first difference. From this equation, one can see that the average current is given by the change of the mechanical energy E_m and the energy of interaction E_{int} after N -th period. One can find that at $N > N_s = [t_s/2\pi] + 1$ the functions $E_m(N)$ and $E_{int}(N)$ can be written as follows,

$$\begin{aligned} E_m(N) &= 2\pi^2 \tilde{\varepsilon}^2 \left(\rho^2 (2N_s - N)^2 + \tau^2 N^2 \right), \\ E_{int}(N) &= 2\pi \varepsilon \tilde{\varepsilon} \left[\rho^2 (N - 2N_s) e^{-(2\pi \tilde{\varepsilon})^2 (N - 2N_s)^2} + \tau^2 N e^{-(2\pi \tilde{\varepsilon} N)^2} \right]. \end{aligned} \quad (3.41)$$

The change in the interaction energy contributes to the averaged current as well as the mechanical energy. However, this contribution is of the order of $\tilde{\varepsilon}^2$ and important only for periods for which $I(N)/\tilde{\varepsilon} \simeq \tilde{\varepsilon}^2$. Thus, the average current is determined by the change of mechanical energy mainly, and is defined by the

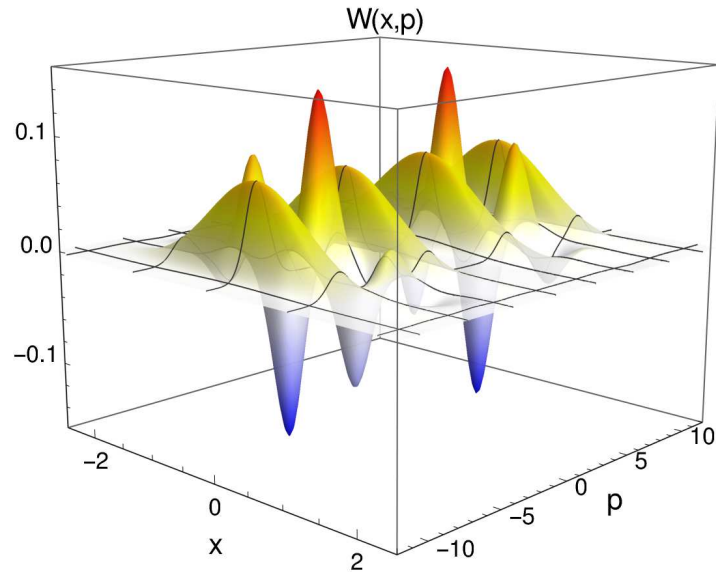


Fig. 3.5 Wigner function $W(x,p,t = 2\pi N)$ for $\rho = 1/\sqrt{2}$. It takes both positive and negative values demonstrating entanglement between the qubit states and "cat states" of the nanomechanical resonator.

following equations,

$$\frac{I(N)}{\tilde{\varepsilon}} \approx I_m(N) = -2\pi\tilde{\varepsilon}N, \quad N \leq N_s - 1 \quad (3.42)$$

$$\frac{I(N)}{\tilde{\varepsilon}} \approx 2\pi\tilde{\varepsilon}(N - 2\rho^2N_s), \quad N > N_s. \quad (3.43)$$

From Fig. 3.6 one can see that the averaged current exhibits a jump equal to $-\rho^2 I(N_s)$ after the period during which the bias voltage is switched. It originates in the fact that when we switch the sign of the bias voltage (at $t = t_s$) the power, pumped into the mechanical subsystem, changes depending on the magnitude of ρ^2 . For $\rho = 1$, the supplied power, $P = IV$, just changes its sign with the bias voltage, and the current continues to flow in the same direction as it did before switching. For $\rho = 0$ supplied power is not changed and consequently the current direction changes after switching.

Conclusions

In this chapter the quantum dynamics of the NEMS comprising the movable CPB qubit, subjected to an electrostatic field and coupled to two bulk superconductors, controlled by the bias voltage, via tunneling processes, is analyzed. It is

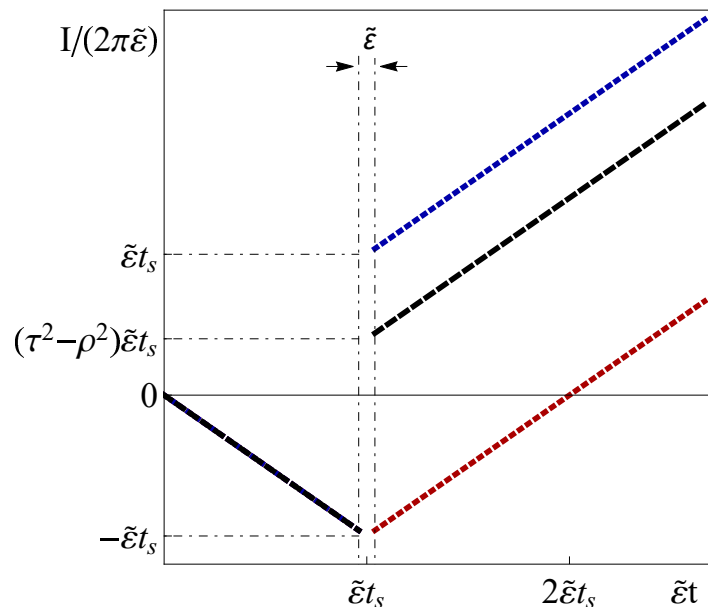


Fig. 3.6 Schematic illustration of the time-averaged Josephson current as a function of time for different values of ρ (black dashed curve). The dotted lines indicate the limiting cases of $\rho = 0$ (top, blue online) and $\rho = 1$ (bottom, red online). The current for $t < t_s$ does not depend on ρ ($\rho = 1$), see Eqs. (3.42), (3.24). The period N_s corresponding to the moment of the bias voltage switching, is out of the consideration.

demonstrated analytically that if the ac Josephson frequency of superconductors, controlled by the bias voltage, is in resonance with the mechanical frequency of the CPB, the initial pure state (direct product of the CPB state and ground state of the oscillator) evolves in time into the coherent states of the mechanical oscillator entangled with the qubit states. Furthermore, we established the protocol of the bias voltage manipulation which results in the formation of entangled states incorporating so-called cat-states (the quantum superposition of the coherent states). The organization of such states is confirmed by the analysis of the corresponding Wigner function taking negative values, while their specific features provide the possibility for their experimental detection by measuring the average current. The discussed phenomena may serve as a foundation for the encoding of quantum information from charge qubits into a superposition of the coherent mechanical states. It may constitute interest for the field of quantum communications due to the robustness of such multiphonon states regarding external perturbation, comparing to a single-phonon Fock state.

The main results of this chapter are published, Refs. [2, 8].

CHAPTER 4

NANOMECHANICS DRIVEN BY SUPERCONDUCTING PROXIMITY EFFECT

In this chapter a hybrid nanoelectromechanical weak link based on a nanotube is considered. More precisely, a carbon nanotube is suspended above a trench in a normal metal electrode and positioned in a gap between two superconducting ones. It is shown that under a constant bias voltage, in such a system the mechanical instability, resulting in self-sustained nanotube oscillations, occurs, on the one hand. On the other hand, the system can also operate in cooling regime. The phenomena emerge due to superconducting proximity effect (the hybrid (normal-superconducting) structure of the device). In the first section (4.1) bending vibrations of the nanotube are treated semi-classically and details of mechanical instability leading to a self-saturation effect is discussed together with an scheme for an possible experimental detection of the considered effects. In the second section (4.2) quantum effects are taken fully into account. It is demonstrated that quantum fluctuations of the nanotube lead to the cooling effect, which can be observed in an experiment due to the electric current measurement discussed in the last subsection.

4.1. Self-sustained nanomechanical oscillations.

In this section the occurrence of the mechanical instability in the hybrid nanoelectromechanical system is discussed. A region and required conditions for it are obtained. Also, a strong enhancement of the electric current through the system in the stationary regime of self-sustained oscillations of the nanotube is found. The latter leads to the possibility for the device to operate as a transistor or a diode.

4.1.1. Model of nanoelectromechanical device. Hamiltonian and dynamics.

A sketch of the NEMS investigated in this paper is presented in Fig. 4.1. A single-walled CNT is suspended above a trench in a bulk normal metal electrode biased by a constant voltage V_b . Two superconducting leads with the superconducting phase difference ϕ are positioned near the middle of the nanotube in such

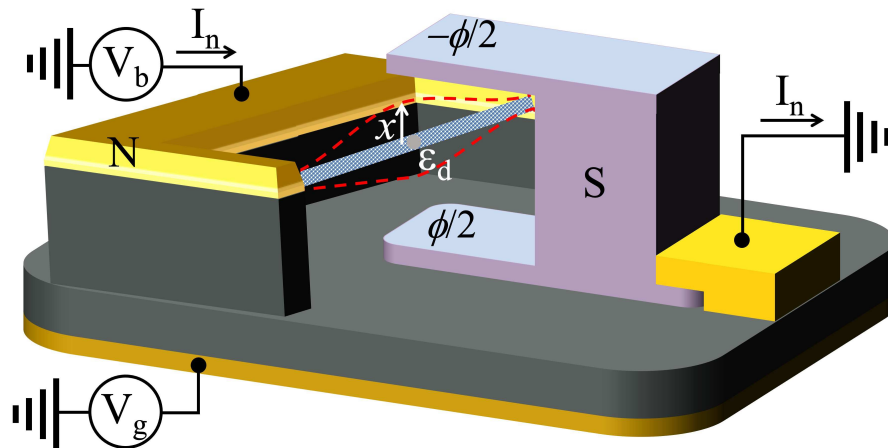


Fig. 4.1 Schematic illustration of the nanoelectromechanical device under consideration. A carbon nanotube (CNT) is suspended in a gap between two edges of a normal electrode (N) and tunnel-coupled to it. The electronic energy levels of the CNT are tuned such that only one energy level with energy ε_d , which is well separated from the other levels, is considered. Bending of the CNT in the x direction between two superconducting leads (S) affects the values of the tunneling barriers between them. The bias voltage V_b is applied to the normal electrode.

a way that the bending of the nanotube moves it closer to one electrode and further away from the other. The distance between the quantized electronic levels inside the nanotube is much greater than the other energy parameters, allowing one to consider the nanotube as a single-level quantum dot (QD). The bending dynamics of the CNT are reduced to the dynamics of the fundamental flexural mode. We suppose that the amplitude of this mode, x , is larger than the amplitude of zero-point oscillations. Thus, we consider it as a classical mechanical oscillator with mass m and frequency ω .

The dynamics of the mechanical subsystem is described by Newton's equation,

$$\ddot{x} + \omega^2 x = -\frac{1}{m} \text{Tr} \left\{ \hat{\rho} \frac{\partial H(x)}{\partial x} \right\}, \quad (4.1)$$

where

$$H = H_d + H_l + H_t \quad (4.2)$$

is the Hamiltonian of the electronic subsystem. The first term H_d represents the single-level QD,

$$H_d = \sum_{\sigma} \varepsilon_d d_{\sigma}^{\dagger} d_{\sigma}, \quad (4.3)$$

where $d_{\sigma}^{\dagger}(d_{\sigma})$ is the creation (annihilation) operator of an electron with spin projection $\sigma = \uparrow, \downarrow$ on the dot. The Hamiltonian $H_l = H_l^n + H_l^s$ describes the normal and superconducting leads, respectively, with

$$H_l^n = \sum_{k\sigma} (\varepsilon_k - eV_b) a_{k\sigma}^{\dagger} a_{k\sigma}, \quad (4.4)$$

$$H_l^s = \sum_{kj\sigma} \left(\varepsilon_k c_{kj\sigma}^{\dagger} c_{kj\sigma} - \Delta_s (e^{i\phi_j} c_{kj\uparrow}^{\dagger} c_{-kj\downarrow}^{\dagger} + \text{H.c.}) \right). \quad (4.5)$$

Here, $a_{k\sigma}^{\dagger}(a_{k\sigma})$, and $c_{kj\sigma}^{\dagger}(c_{kj\sigma})$ are the creation (annihilation) operators of an electron with quantum number k and spin projection σ in the normal and superconducting $j = 1, 2$ leads, respectively, and $\Delta_s e^{i\phi_j}$ is the superconducting order parameter (in the j electrode). Note that the energies $\varepsilon_d, \varepsilon_k$ are counted from the Fermi energy of the superconductors. In what follows, we set $\phi_1 = -\phi_2 = \phi/2$.

The Hamiltonian $H_t = H_t^n + H_t^s$ describes the tunneling of electrons between the dot and the leads, where

$$H_t^n = \sum_{k\sigma} t_0^n (a_{k\sigma}^{\dagger} d_{\sigma} + \text{H.c.}), \quad (4.6)$$

$$H_t^s = \sum_{kj\sigma} t_j^s(x) (c_{kj\sigma}^{\dagger} d_{\sigma} + \text{H.c.}). \quad (4.7)$$

Here is the position-dependent superconducting tunneling amplitude

$$t_{1(2)}^s(x) = t_0^s e^{(-1)^j (x+a)/2\lambda}, \quad (4.8)$$

where 2λ is the characteristic tunneling length and a is a parameter for asymmetry. For a typical CNT-based nanomechanical resonator, $2\lambda \sim 0.5$ nm [161]. We concentrate our attention on the symmetric case $a = 0$ and leave the asymmetric one for a brief discussion in the subsection 4.1.5 because taking into account the asymmetry does not bring any qualitative result, as we will show. Also, the completely asymmetric case (only one SC electrode is present) is discussed in Ref. [154].

4.1.2. Density matrix approximation.

The time evolution of the electronic density matrix $\hat{\rho}$ is described by the Liouville–von Neumann equation ($\hbar = 1$),

$$i\partial_t\hat{\rho} = [H, \hat{\rho}], \quad (4.9)$$

which together with Eq. (4.1) forms a closed system of equations that describe the nanoelectromechanics of our system. We restrict ourselves to the case $\Delta_s \gg |eV_b| \gg \Delta_d \sim \Gamma_n$, where $\Delta_d = (2\pi)\nu_s|t_0^s|^2$ and $\Gamma_n = (2\pi)\nu_n|t_0^n|^2$, with $\nu_{s(n)}$ the density of states in the superconducting (normal) electrode.

To describe the electronic dynamics of the QD, we use the reduced density matrix approximation in which the full density matrix of the system is factorized to the tensor product of the equilibrium density matrices of the normal and superconducting leads and the density matrix of the dot as $\hat{\rho} = \hat{\rho}_n \otimes \hat{\rho}_s \otimes \hat{\rho}_d$. Using the standard procedure, one can trace out the degrees of freedom of the leads and obtain the following equation for the reduced density matrix $\hat{\rho}_d$ [145] (in the deep subgap regime $\Delta_s \rightarrow \infty$),

$$\partial_t\hat{\rho}_d = -i \left[H_d^{eff}, \hat{\rho}_d \right] + \mathcal{L}_n\{\hat{\rho}_d\}, \quad (4.10)$$

where

$$H_d^{eff} = H_d + \Delta_d(x, \phi)d_\downarrow d_\uparrow + \Delta_d^*(x, \phi)d_\uparrow^\dagger d_\downarrow^\dagger, \quad (4.11)$$

$$\begin{aligned} \Delta_d(x, \phi) &= \frac{1}{2}\Delta_d \sum_{j=1,2} e^{(-1)^j(x/\lambda + i\phi/2)} = \Delta'(x, \phi) + i\Delta''(x, \phi) \\ &= \Delta_d \cosh(x/\lambda + i\phi/2). \end{aligned} \quad (4.12)$$

Above, $\Delta_d(x, \phi)$ is the off-diagonal order parameter induced by the superconducting proximity effect [151, 162], and $\Delta', \Delta''(x, \phi)$ are real functions. The Lindbladian term in Eq. (4.10) reflects the incoherent electron exchange between the normal lead and QD. The latter in the high bias voltage regime, $|eV_b| \gg \varepsilon_0, k_B T$,

takes the form:

$$\mathcal{L}_n\{\hat{\rho}_d\} = \Gamma_n \sum_{\sigma} \begin{cases} 2d_{\sigma}^{\dagger}\hat{\rho}_d d_{\sigma} - \{d_{\sigma}d_{\sigma}^{\dagger}, \hat{\rho}_d\}, & \kappa = +1; \\ 2d_{\sigma}\hat{\rho}_d d_{\sigma}^{\dagger} - \{d_{\sigma}^{\dagger}d_{\sigma}, \hat{\rho}_d\}, & \kappa = -1; \end{cases} \quad (4.13)$$

where $\kappa = \text{sgn}(eV_b)$.

Another way to obtain the effective Hamiltonian Eq. (4.11) is to use the equation of motion method within the Green function formalism, see, e.g., Ref. [163] and the appendix in Ref. [151]. The idea of this well-established method is to obtain a series of coupled differential equations for a desired Green function by differentiating it several times.

Figure 4.2 represents the electronic dynamics on the dot for $\kappa = \pm 1$. From Fig. 4.2, one can see that not all electron processes are allowed due to the parameter scales in this work. In the subgap regime, single-electron transitions between the dot and the superconducting leads are prohibited, and thus only an exchange of Cooper pairs occurs. Moreover, because of the high bias voltage, single-electron tunneling between the dot and the normal leads is enabled exclusively in one direction (from the lead to the dot, see Fig. 4.2a, or vice-versa, Fig. 4.2b), establishing that our model is electron-hole symmetric.

As a consequence, the QD density matrix $\hat{\rho}_d$ acts in the Hilbert space \mathcal{H}_4 , which may be presented as a direct sum of two \mathcal{H}_2 spaces via $\mathcal{H}_4 = \mathcal{H}_e \oplus \mathcal{H}_{CP}$ spanned over state vectors $|\uparrow\rangle = d_{\uparrow}^{\dagger}|0\rangle$, $|\downarrow\rangle = d_{\downarrow}^{\dagger}|0\rangle$, and $|0\rangle, |2\rangle = d_{\uparrow}^{\dagger}d_{\downarrow}^{\dagger}|0\rangle$ (with $d_{\uparrow,\downarrow}|0\rangle = 0$). Then, the equations for the dot density matrix are the following:

$$\partial_t \rho_0 = -4\Gamma_n \rho_0 - \imath \Delta_d(x, \phi) \rho_{20} + \imath \Delta_d^*(x, \phi) \rho_{02}, \quad (4.14)$$

$$\partial_t \rho_2 = 2\Gamma_n(1 - \rho_0 - \rho_2) + \imath \Delta_d(x, \phi) \rho_{20} - \imath \Delta_d^*(x, \phi) \rho_{02}, \quad (4.15)$$

$$\partial_t \rho_{02} = -2\Gamma_n \rho_{02} + \imath \Delta_d(x, \phi)(\rho_0 - \rho_2) + 2\imath \varepsilon_d \rho_{02}, \quad (4.16)$$

$$\partial_t \rho_{20} = -2\Gamma_n \rho_{20} - \imath \Delta_d^*(x, \phi)(\rho_0 - \rho_2) - 2\imath \varepsilon_d \rho_{20}. \quad (4.17)$$

Here we use the normalization condition $\rho_0 + \rho_{\uparrow} + \rho_{\downarrow} + \rho_2 = 1$. The equation for the displacement x , Eq.(4.1), has the form,

$$\ddot{x} + \omega x = -\frac{2\Delta_d}{\lambda} \left[\sinh\left(\frac{x}{\lambda} - \imath \frac{\phi}{2}\right) \rho_{02} + \sinh\left(\frac{x}{\lambda} + \imath \frac{\phi}{2}\right) \rho_{20} \right]. \quad (4.18)$$

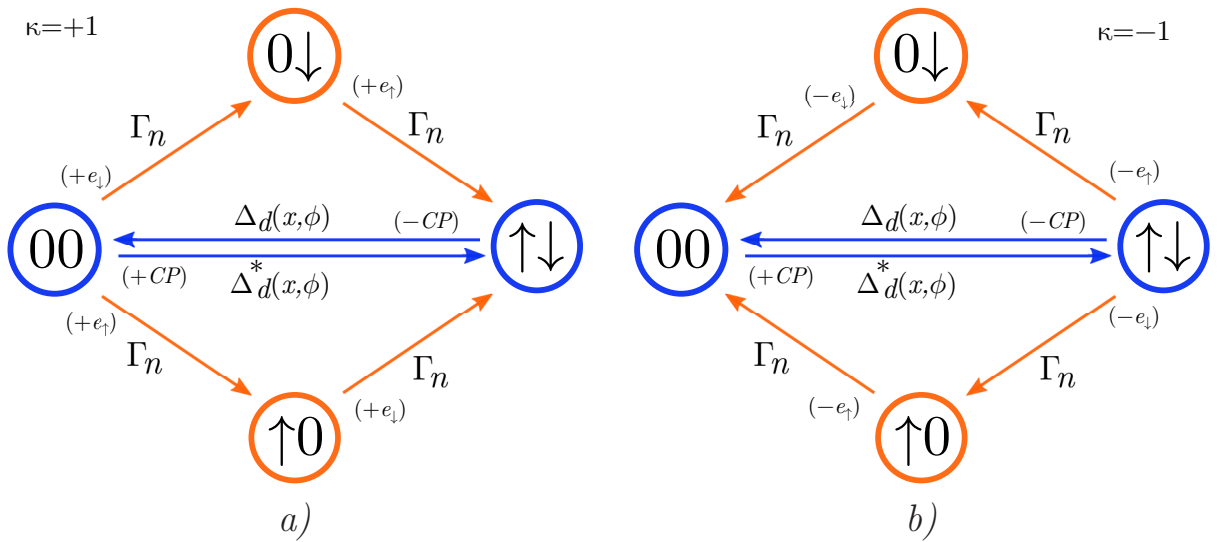


Fig. 4.2 Diagrams representing the transitions between electronic states in the quantum dot. The single-electron states change due to transitions from the empty to the single-occupied QD and then from the single-occupied to the double-occupied one (indicated by orange arrows). In the high bias voltage regime, the tunneling of electrons (a) or holes (b) with spin \downarrow or \uparrow is allowed only from the normal lead to the dot and forbidden in the opposite direction. Transitions between the empty and double-occupied quantum dot are due to coupling with the superconducting leads (indicated by blue arrows).

The superselection rule, which forbids the superposition of states with integer and half-integer spins, allows us to present the density matrix $\hat{\rho}_d$ as a direct sum of two density matrices $\hat{\rho}_d = \hat{\rho}_e \oplus \hat{\rho}_{CP}$ acting in the \mathcal{H}_2 Hilbert space spanned over state vectors $|\uparrow\rangle, |\downarrow\rangle$ and $|0\rangle, |2\rangle$, respectively. Moreover, taking into account spin-rotation symmetry, one can conclude that $\hat{\rho}_e$ should be proportional to the unit matrix, $\hat{\rho}_e = \rho_e \hat{I}$, while $\hat{\rho}_{CP}$ can be written in the form

$$\hat{\rho}_{CP} = \frac{1}{2}R_0\hat{I} + \frac{1}{2}\sum_i R_i\sigma_i, \quad (4.19)$$

where $\sigma_i, (i = 1, 2, 3)$ are the Pauli matrices. Here new variables are $R_i = \text{Sp}(\sigma_i\hat{\rho}_{CP})$, with

$$\hat{\rho}_{CP} = \begin{pmatrix} \rho_0 & \rho_{02} \\ \rho_{20} & \rho_2 \end{pmatrix}, \quad (4.20)$$

(the equation for $R_0 = \frac{1}{2}\text{Sp}\hat{I}\hat{\rho} = (\rho_0 + \rho_2)/2$ is decoupled and is not relevant).

Then by introducing the dimensionless time $\omega t \rightarrow t$ and displacement $x/\lambda \rightarrow x$, and taking into account the normalization condition $\text{Tr}\hat{\rho}_d = 1$, we get the following closed system of equations for $x(t)$ and $R_i(t)$,

$$\ddot{x} + x = -\xi \left[\sinh(x) \cos\left(\frac{\phi}{2}\right) R_1 - \cosh(x) \sin\left(\frac{\phi}{2}\right) R_2 \right], \quad (4.21)$$

$$\alpha \dot{\vec{R}} = \hat{L} \vec{R} - \kappa \vec{e}_3, \quad (4.22)$$

where $\vec{R} = (R_1, R_2, R_3)^T$, $\vec{e}_3 = (0, 0, 1)^T$, $\xi = \Delta_d / (m\lambda^2\omega^2)$ is the nanoelectromechanical coupling parameter, and $\alpha = \omega / (2\Gamma_n)$ is the adiabaticity parameter. For a typical CNT-based NEMS, one can estimate $\xi \sim 10^{-3} \ll 1$ [161, 164]. The matrix \hat{L} is defined as follows,

$$\hat{L}(x) = \begin{pmatrix} -1 & \tilde{\varepsilon}_d & -\tilde{\Delta}''(x, \phi) \\ -\tilde{\varepsilon}_d & -1 & -\tilde{\Delta}'(x, \phi) \\ \tilde{\Delta}''(x, \phi) & \tilde{\Delta}'(x, \phi) & -1 \end{pmatrix}, \quad (4.23)$$

where $\tilde{\varepsilon}_d \equiv \varepsilon_d / \Gamma_n$, $\tilde{\Delta}_d \equiv \Delta_d / \Gamma_n$.

4.1.3. Equation of motion method for Green functions.

In this subsection we present another method to obtain the effective Hamiltonian Eq. (4.11) as it was pointed out in the previous subsection, 4.1.2. It is based on the equation of motion method within the Green function formalism, see, e.g., Ref. [163] and the appendix in Ref. [151]. The idea of this well-established method is to obtain a series of coupled differential equations for a desired Green function by differentiating it several times.

Since in the considered system the dot coupled to superconducting and normal leads independently, in the following derivation we can omit the contribution of the normal lead. Let us define the retarded Green function in the 2x2 Nambu space as [165],

$$\hat{G}^r(t) = -i\theta(t) \begin{pmatrix} \langle \{d_\uparrow(t), d_\uparrow^\dagger(0)\} \rangle & \langle \{d_\uparrow(t), d_\downarrow(0)\} \rangle \\ \langle \{d_\downarrow^\dagger(t), d_\uparrow^\dagger(0)\} \rangle & \langle \{d_\downarrow^\dagger(t), d_\downarrow(0)\} \rangle \end{pmatrix}. \quad (4.24)$$

Then, by differentiating this function two times, we find for the Fourier harmonics

$$\hat{G}^r(\tau) = \int_{-\infty}^{+\infty} \hat{G}^r(t) e^{-i\tau t}, \quad \hat{G}^r(t) = \frac{1}{2\pi} \int_{-\infty}^{+\infty} \hat{G}^r(\tau) e^{i\tau t}, \quad (4.25)$$

the following closed system of equations:

$$\hat{g}_0^{-1}(\tau) \hat{G}^r(\tau) = \hat{I} + \sigma_z \sum_{kj} t_{kj}^s \hat{G}_j^{r,1}(k, \tau), \quad (4.26)$$

$$\hat{g}_{kj}^{s,-1}(\tau) \hat{G}_j^{r,1}(k, \tau) = \sigma_z t_{kj}^s \hat{G}^r(\tau), \quad (4.27)$$

where $\hat{G}_j^{r,1}(\tau)$ is Fourier harmonics of the following correlation function:

$$\hat{G}_j^{r,1}(k, t) = -i\theta(t) \begin{pmatrix} \langle \{c_{kj\uparrow}(t), d_{\uparrow}^{\dagger}(0)\} \rangle & \langle \{c_{kj\uparrow}(t), d_{\downarrow}(0)\} \rangle \\ \langle \{c_{kj\downarrow}^{\dagger}(t), d_{\uparrow}^{\dagger}(0)\} \rangle & \langle \{c_{kj\downarrow}^{\dagger}(t), d_{\downarrow}(0)\} \rangle \end{pmatrix}. \quad (4.28)$$

Here also the Green function of a single-level QD with the level energy ε_d ,

$$\hat{g}_0(\tau) = \begin{pmatrix} \frac{1}{\tau - \varepsilon_d + i0} & 0 \\ 0 & \frac{1}{\tau + \varepsilon_d + i0} \end{pmatrix}, \quad (4.29)$$

with its inverse matrix,

$$\hat{g}_0^{-1}(\tau) = \begin{pmatrix} \tau - \varepsilon_d + i0 & 0 \\ 0 & \tau + \varepsilon_d + i0 \end{pmatrix}, \quad (4.30)$$

and the (standard) Green function of the j superconductor:

$$\hat{g}_{kj}^s(\tau) = \frac{i}{\tau^2 - E_k^2} \begin{pmatrix} \tau + \varepsilon_k & -\Delta_s e^{i\phi_j} \\ -\Delta_s e^{-i\phi_j} & \tau - \varepsilon_k \end{pmatrix}, \quad (4.31)$$

where the eigenvalues of the Hamiltonian H_l^s are $E_k = \pm \sqrt{\varepsilon_k^2 + \Delta_s^2}$ (Andreev level energies).

Then, by substituting Eq. (4.27) into Eq. (4.26), one gets the following Dyson equation for the retarded Green function of the dot $\hat{G}^r(\tau)$:

$$\hat{G}^r(\tau) = \hat{g}_0(\tau) + \hat{g}_0(\tau) \hat{\Sigma}^r(\tau) \hat{G}^r(\tau), \quad (4.32)$$

where the self-energy function is determined as

$$\hat{\Sigma}^r(\tau) = \imath \sum_{kj} (t_{kj}^s)^2 \hat{g}_{kj}^s(-\Delta_s, \tau), \quad (4.33)$$

and after the integrating over the energy variable, we obtain:

$$\hat{\Sigma}^r(\tau) = \frac{1}{2} \sum_j \frac{\Delta_d(x)}{\sqrt{\Delta_s^2 - \tau^2}} \begin{pmatrix} \tau & \Delta_s e^{\imath\phi_j} \\ \Delta_s e^{-\imath\phi_j} & \tau \end{pmatrix}. \quad (4.34)$$

Moreover, in case of symmetric tunneling contacts with the superconducting leads, one can re-write this equation as follows:

$$\hat{\Sigma}^r(\tau) = \frac{\Delta_d}{\sqrt{\Delta_s^2 - \tau^2}} \begin{pmatrix} \tau \cosh(x/\lambda) & \Delta_s \cosh(x/\lambda - \imath\phi/2) \\ \Delta_s \cosh(x/\lambda + \imath\phi/2) & \tau \cosh(x/\lambda) \end{pmatrix}. \quad (4.35)$$

Furthermore, from a formal solution of Eq. (4.32)

$$\hat{G}^r(\tau) = [\hat{g}_0^{-1} + \hat{\Sigma}^r]^{-1}, \quad (4.36)$$

one gets the following expression,

$$\hat{G}^r(\tau) = \frac{1}{\det(\hat{g}_0^{-1} - \hat{\Sigma}^r)} \begin{pmatrix} g_{22}^{-1} - \Sigma_{22}^r & g_{12}^{-1} - (-\Sigma_{12}^r) \\ g_{21}^{-1} - (-\Sigma_{21}^r) & g_{11}^{-1} - \Sigma_{11}^r \end{pmatrix}, \quad (4.37)$$

or, more specifically, see, e.g., Refs. [151, 166],

$$\hat{G}^r(\tau) = \frac{1}{D(\tau)} \begin{pmatrix} g_{22}^{-1} - \Sigma_{22}^r & \Sigma_{12}^r \\ \Sigma_{21}^r & g_{11}^{-1} - \Sigma_{11}^r \end{pmatrix}, \quad (4.38)$$

with

$$D(\tau) = (g_{11}^{-1} - \Sigma_{11}^r) (g_{22}^{-1} - \Sigma_{22}^r) - \Sigma_{12}^r \Sigma_{21}^r, \quad (4.39)$$

by definition. In the deep subgap regime ($\Delta_s \rightarrow \infty$) straightforward calculations leads to:

$$\hat{G}^r(\tau) = \frac{1}{D(\tau)} \begin{pmatrix} \tau + \varepsilon_d & \Delta_d^*(x, \phi) \\ \Delta_d(x, \phi) & \tau - \varepsilon_d \end{pmatrix} \quad (4.40)$$

$$D(\tau) = \tau^2 - \varepsilon_d^2 - |\Delta_d(x, \phi)|^2. \quad (4.41)$$

One the other hand, let us consider an effective QD Hamiltonian of such a type of Eq. (4.11),

$$H' = \sum_{\sigma} \varepsilon_d d_{\sigma}^{\dagger} d_{\sigma} + \mathcal{Y} d_{\downarrow} d_{\uparrow} + \mathcal{Y}^{\dagger} d_{\uparrow}^{\dagger} d_{\downarrow}^{\dagger}, \quad (4.42)$$

where \mathcal{Y} is supposed to be unknown for now function, or an operator-function in more general situation, of the dot position x and superconducting phase difference ϕ . Then, one can find the retarded Green function, Eq. (4.24), of a dot described by the Hamiltonian Eq. (4.42) using the method of equations of motion which was employed above. By differentiating only one time, one gets the following expression for the desired Green function Fourier component:

$$\hat{G}^r(\tau) = \frac{1}{\tau^2 - \varepsilon_d^2 - |\mathcal{Y}|^2} \begin{pmatrix} \tau + \varepsilon_d & \mathcal{Y}^{\dagger} \\ \mathcal{Y} & \tau - \varepsilon_d \end{pmatrix}. \quad (4.43)$$

At this point one can compare Eq. (4.43) with Eq. (4.40) and as a matter of fact justify that $\mathcal{Y} = \Delta_d(x, \phi)$.

4.1.4. Dynamics of the system in adiabatic regime.

The system of Eqs. (4.21) and (4.22) has an obvious static solution $x_{st} = 0 + \mathcal{O}(\xi)$, $\vec{R}_{st} = \kappa L^{-1}(0) \vec{e}_3 + \mathcal{O}(\xi) \vec{R}^{(1)}$, here $\|\vec{R}^{(1)}\| = 1$. The stability of this solution can then be investigated in standard ways, see, for example, Ref. [120] and below. However, to simplify this procedure, we will consider the adiabatic case when $\alpha \ll 1$, which corresponds to a typical experimental situation [137] and reduces the problem to one that allows the use of Poincare analysis. More specifically, this inequality allows one to find a solution of Eq. (4.22) to the accuracy α ,

$$\vec{R}(x, t) = \kappa L^{-1}(x(t)) (1 + \alpha \dot{x} \partial_x L^{-1}(x(t))) + \mathcal{O}(\alpha^2) \vec{e}_3. \quad (4.44)$$

In the zeroth order of the perturbation theory over the adiabaticity parameter α , from Eq. (4.44) one can find:

$$R_1^{(0)}(x,t) = \kappa \frac{\tilde{\Delta}''(x,\phi) + \tilde{\varepsilon}_d \tilde{\Delta}'(x,\phi)}{\tilde{\mathcal{D}}^2(x,\phi)}, \quad (4.45)$$

$$R_2^{(0)}(x,t) = \kappa \frac{\tilde{\Delta}'(x,\phi) - \tilde{\varepsilon}_d \tilde{\Delta}''(x,\phi)}{\tilde{\mathcal{D}}^2(x,\phi)}, \quad (4.46)$$

$$R_3^{(0)}(x,t) = -\kappa \frac{1 + \tilde{\varepsilon}_d^2}{\tilde{\mathcal{D}}^2(x,\phi)}. \quad (4.47)$$

Here $\tilde{\mathcal{D}}^2 \equiv \mathcal{D}^2(x,\phi)/\Gamma_n^2 = \tilde{\Delta}_d^2 [\sinh^2 x + \cos^2(\phi/2)] + \tilde{\varepsilon}_d^2 + 1$.

The equation for the first order correction to the re-normalized matrix elements of the dot density operator, using Eq. (4.44), takes the form:

$$\vec{R}^{(1)}(x,t) = \alpha \dot{x} L^{-1}(x(t)) \partial_x \vec{R}^{(0)}(x,t). \quad (4.48)$$

The coefficients $R_1^{(1)}$ and $R_2^{(1)}$ can be expressed in terms of $R_3^{(1)}$ which has the following form

$$R_3^{(1)}(x,t) = \alpha \kappa \dot{x} \frac{\tilde{\Delta}_d^2}{\tilde{\mathcal{D}}^6} \left[\sinh(2x) \left\{ (1 - \tilde{\varepsilon}_d^2) \tilde{\mathcal{D}}^2 - 4(1 + \tilde{\varepsilon}_d^2) \right\} + 2\tilde{\varepsilon}_d \tilde{\mathcal{D}}^2 \sin \phi \right]. \quad (4.49)$$

Then by substituting these solutions into Eq. (4.21), one gets (to accuracy α) the following nonlinear differential equation for $x(t)$:

$$\ddot{x} - \eta(x,\phi) \dot{x} + x = F(x,\phi), \quad (4.50)$$

the solution of which may be analyzed via Poincaré's theory. Here, the nonlinear force $F(x,\phi)$ and friction coefficient $\eta(x,\phi)$, which in what follows we refer to as a pumping coefficient, are generated by the interaction with the non-equilibrium

electronic environment. In terms of $R_3^{(1)}$, the pumping coefficient takes a form:

$$\begin{aligned} \dot{x}\eta(x, \phi) = & \frac{\tilde{\Delta}_d}{1 + \tilde{\varepsilon}_d^2} \left[- [\sin \phi - \tilde{\varepsilon}_d \sinh(2x)] R_3^{(1)} + \right. \\ & + \frac{\alpha \kappa \dot{x}}{\tilde{\mathcal{D}}^4} \left\{ 2\tilde{\varepsilon}_d \tilde{\mathcal{D}}^2 (\cosh(2x) - \cos \phi) + \right. \\ & \left. \left. + \tilde{\Delta}_d^2 \sinh(2x) [(1 - \tilde{\varepsilon}_d^2) \sin \phi - 2\tilde{\varepsilon}_d \sinh(2x)] \right\} \right]. \end{aligned} \quad (4.51)$$

The straightforward calculations lead to:

$$F(x, \phi) = \kappa \xi \frac{\tilde{\Delta}_d}{2\tilde{\mathcal{D}}^2} [\sin \phi - \tilde{\varepsilon}_d \sinh(2x)], \quad (4.52)$$

$$\begin{aligned} \eta(x, \phi) = & \kappa \alpha \xi \frac{\tilde{\Delta}_d}{2\tilde{\mathcal{D}}^6} \left[\tilde{\Delta}_d^2 \sinh(2x) (\tilde{\mathcal{D}}^2 + 4) \{ \sin \phi - \tilde{\varepsilon}_d \sinh(2x) \} + \right. \\ & \left. + 8\tilde{\varepsilon}_d \tilde{\mathcal{D}}^2 \{ \sin^2(\phi/2) + \sinh^2 x \} \right]. \end{aligned} \quad (4.53)$$

4.1.5. Stability of a static solution. Linearization.

The strongly nonlinear Eq. (4.50) in the adiabatic limit has static solutions determined by the equation:

$$x_{st} = F(x_{st}, \phi), \quad (4.54)$$

which is in the considered limit of small electromechanical coupling, $\xi \ll 1$, has a trivial solution,

$$x_{st} = \kappa \xi \frac{\tilde{\Delta}_d}{2\tilde{\mathcal{D}}^2} \sin \phi \propto \mathcal{O}(\xi). \quad (4.55)$$

It is obvious from Eq. (4.55) that x_{st} is strictly equal to zero when $\phi = \pi n$ (n is an integer number). This corresponds to the straightforward configuration of the nanotube. For the time evolution of a small deviations from the equilibrium position $\delta x(t) = x(t) - x_{st}$ one can obtain the following equation (linearized Eq. (4.50) near the equilibrium point x_{st}),

$$\delta \ddot{x} - \eta(0, \phi) \delta \dot{x} + \delta x = 0. \quad (4.56)$$

Here we ignore a small shift of the mechanical oscillation frequency due to the re-normalization. And,

$$\eta(0,\phi) = +\kappa\alpha\xi \frac{4\tilde{\varepsilon}_d\tilde{\Delta}_d}{\tilde{D}^4(0,\phi)} \sin^2\left(\frac{\phi}{2}\right). \quad (4.57)$$

Thereby, the static solution x_{st} is *unstable*, that is, an initial small spontaneous fluctuation leads to exponential increasing of the QD vibration amplitude, when $\eta(0,\phi) > 0$ and it is stable otherwise. It is clearly seen from Eq. (4.57) that the presence of the *mechanical instability* directly depends on the position of the dot energy level ε_d and the direction of the applied bias voltage κ . In case of positive $\kappa\varepsilon_d$ the equilibrium position x_{st} is *unstable* with respect to the increase of the oscillation amplitude for all values of the superconducting phase difference ϕ (except of $\phi = 0$ which is so only for the symmetric junction as will be discussed in the subsection 4.1.7). The later reveals the reason we have called $\eta(x,\phi)$ as a pumping coefficient. We can also easily note from Eq. (4.57) that the pumping coefficient takes its maximum at $\phi = \pi$ (the force $F(0,\pi) = 0$). One should compare it to the case of $\phi = 0$ when the force and pumping are equal to zero, $F(0,0) = 0$ and $\eta(0,0) = 0$. It is rather an unexpected situation because usually a friction/pumping is generated via the force acting on a QD. However, in our case, the force responsible for the nanomechanical pumping is of electronic nature and is sensitive to the fact that Cooper pairs are delocalized between nanotube and superconducting leads. This force emerges when the Cooper pair is in a state of quantum superposition controlled by phase difference, nanotube bending, and other parameters.

The phase diagram of the mechanical instability occurred in the proposed system is presented in Fig. 4.3. The maximal pumping takes place at $\tilde{\varepsilon}_d = 1/\sqrt{3}$ (and $\phi = \pi$).

4.1.6. Self-saturation effect.

In order to analyse what the mechanical instability leads to, we find the stationary solutions $x_c(t)$ of Eq. (4.50). It is natural to use the smallness of the parameter ξ and, then, Eq.(4.50) can be treated as the one describing an harmonic

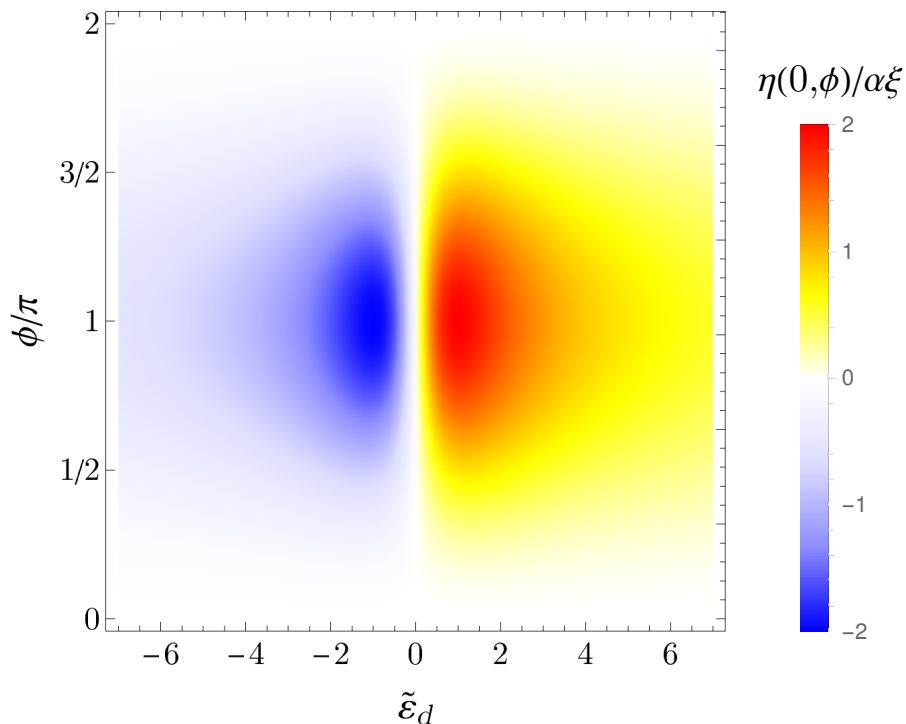


Fig. 4.3 Dependence of the pumping coefficient $\eta(0, \phi)$ (in units of $\alpha\xi$) on the position of the QD energy level $\tilde{\epsilon}_d$ and superconducting phase difference ϕ for the positive direction of the bias voltage $\kappa = 1$ and $\tilde{\Delta}_d = 1$. The red color scheme indicates the regime where the mechanical instability occurs and blue one corresponds to the damping situation.

oscillator slightly perturbed by the interaction with the electronic subsystem,

$$\ddot{x} + x = \xi f(\dot{x}, x). \quad (4.58)$$

In such a case of small electromechanical coupling $\xi \ll 1$, one can use the Krylov-Bogoliubov method of averaging [167] (see also [168]) to find an approximate solution of the Eq.(4.50). In the first order of the perturbation theory this method matches the Van der Pol averaging method. Following it, let us assume that in a stationary regime, the dot displacement x_c takes a form (with the accepted accuracy ξ),

$$x_c(t) = x_{st} + \sqrt{A} \sin(t + \varphi(t)) + \mathcal{O}(\xi), \quad (4.59)$$

where the amplitude $\sqrt{A(t)}$ and the phase $\varphi(t)$ vary slowly in time, $x_{st}, \dot{A}(t), \dot{\varphi}(t) \sim \xi$. Then, by substituting the ansatz (4.59) into Eq.(4.50) and

assuming the same functional form for the derivative \dot{x}_c ,

$$\dot{x}_c(t) = \sqrt{A} \cos(t + \varphi(t)), \quad (4.60)$$

one can find following equations for $A(t)$ and $\varphi(t)$,

$$\dot{A} = 2A \cos^2 \psi \eta \left(\sqrt{A} \sin \psi, \phi \right), \quad (4.61)$$

$$\dot{\varphi} = -A^{-1/2} \sin \psi F \left(\sqrt{A} \sin \psi, \phi \right). \quad (4.62)$$

Since the amplitude and the phase change scarcely during the period of oscillations, the r.h.s. of Eqs.(4.61)-(4.62) can be replaced by their average over the period, and, as a result, one obtain

$$\dot{A} = A \bar{\eta}(A, \phi), \quad (4.63)$$

$$\dot{\varphi} = -A^{-1/2} \bar{F}(A, \phi). \quad (4.64)$$

Here

$$\bar{\eta}(A, \phi) = (\pi)^{-1} \int_0^{2\pi} d\psi \cos^2(\psi) \eta \left(\sqrt{A} \sin \psi, \phi \right) \equiv \kappa \xi \alpha W(A, \phi), \quad (4.65)$$

$$\bar{F}(A, \phi) = (2\pi)^{-1} \int_0^{2\pi} d\psi \sin(\psi) F \left(\sqrt{A} \sin \psi, \phi \right). \quad (4.66)$$

The pumping coefficient $\bar{\eta}(A, \phi)$ has an obvious physical meaning: it gives the ratio between the energy supplied into the mechanical degree of freedom for one period of mechanical oscillations with amplitude \sqrt{A} and the total mechanical energy.

It is evident from Eq. (4.63) that stationary regimes $\dot{A} = 0$ are given by equations $A = 0$ ($x(t) = x_{st}$) and $\bar{\eta}(A, \phi) = 0$. The first one is a static state of the nanotube, and the second one corresponds to periodic oscillations with the amplitude $\sqrt{A_c}$, where $W(A_c, \phi) = 0$. The static regime is stable when $\bar{\eta}(0, \phi) < 0$ and unstable otherwise. The stability of the periodic solution is defined by the sign of the derivative $\partial_A \bar{\eta}(A, \phi)|_{A=A_c}$: if it is negative (positive), then the periodic regime is stable (unstable). Then, analyzing Eqs. (4.50) and (4.65), one can conclude that the pumping coefficient $\bar{\eta}(A, \phi) \propto \kappa$ is an odd function of ε_d (the first term in the r.h.s. of Eq. (4.53) does not give an contribution) and takes the

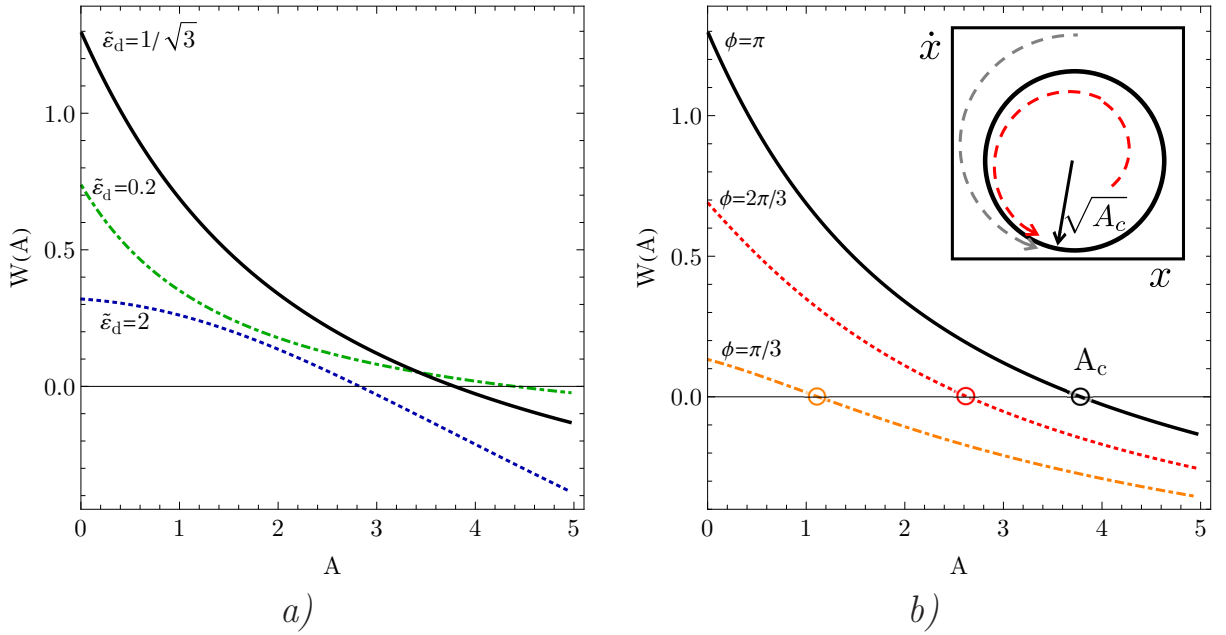


Fig. 4.4 Plots of the function $W(A)$, proportional to the pumping coefficient $\bar{\eta}(A, \phi)$, for different values of (a) the relative position of the dot energy level $\tilde{\varepsilon}_d = 0.2; 1/\sqrt{3}; 2$ for $\phi = \pi$, and (b) the superconducting phase difference $\phi = \pi/3, 2\pi/3, \pi$ for $\tilde{\varepsilon}_d = 1/\sqrt{3}$. The zeroes of the functions correspond to the amplitude of the limiting cycle [see the inset in (b)], which strongly depends on the superconducting phase difference and reaches its maximum at $\phi = \pi$. The other parameters are $\tilde{\Delta}_d = 1, \kappa = +1$.

following limit values,

$$\bar{\eta}(0, \phi) = \kappa \alpha \xi W(0, \phi) = +\kappa \alpha \xi \frac{4\tilde{\varepsilon}_d \tilde{\Delta}_d}{\tilde{D}^4(0, \phi)} \sin^2 \left(\frac{\phi}{2} \right), \quad (4.67)$$

$$\bar{\eta}(A \rightarrow \infty, \phi) = \kappa \alpha \xi W(A \rightarrow \infty, \phi) = -\kappa \alpha \xi \frac{\tilde{\varepsilon}_d}{2\tilde{\Delta}_d}, \quad (4.68)$$

from which follows that at $\phi \neq 0$, the solution of the equation $W(A_c, \phi) = 0$, corresponding to the stationary periodic regime, exists at any values of the other parameters. However, at small $\phi \ll 1$ the pumping coefficient, $\eta(x, \phi)$, determined by interaction with the electronic subsystem, is small and can be equalized by the friction coefficient induced by the thermal environment. The case when $\phi = 0$ is very unstable with respect to the small asymmetry parameter $|a| \ll 1$ and will be discussed in the next section, 4.1.7. The function $W(A)$ and A_c at different $\phi \geq 1$ and $\tilde{\varepsilon}_d > 0$ are presented in Figs. 4.4 and 4.5.

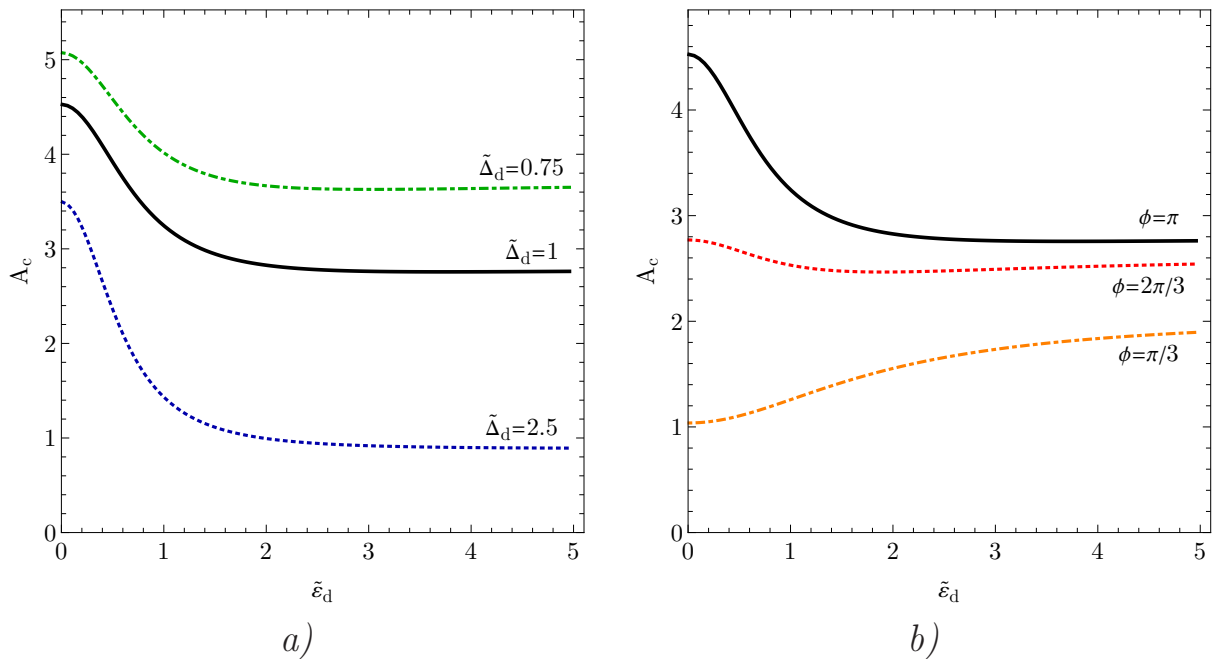


Fig. 4.5 Dependencies of A_c of the limiting cycles on the relative position of the dot energy level $\tilde{\varepsilon}_d$ (counted from the Fermi energy) for different values of (a) $\tilde{\Delta}_d = 0.75; 1; 2.5$ for $\phi = \pi$, and (b) the superconducting phase difference $\phi = \pi/3, 2\pi/3; \pi$ for $\tilde{\Delta}_d = 1$.

It follows from Eq. (4.67) that if $\kappa\varepsilon_d > 0$ and $\phi \neq 0$, the static mechanical state $x = x_{st} \ll 1$ is unstable with respect to the appearance of bending oscillations with amplitudes that exponentially increase in time with the increment

$$\gamma = \kappa\alpha\xi W(0, \phi). \quad (4.69)$$

The latter takes its maximum at $\phi = \pi$ for the fixed values of all other parameters (notice that $x_{st}(\pi) = 0$). However, the increase saturates at the amplitude $\sqrt{A_c}$, resulting in self-sustained oscillations at this amplitude. It should be noted that the amplitude saturation in the system under consideration is a completely internal effect and still takes place when the friction caused by interaction with a thermodynamic environment is zero. A "self-saturation" effect was also reported in [119] where a special magnetic NEM system was considered.

4.1.7. Influence of the asymmetry and friction generated by a thermodynamic environment.

In an experiment the presence of the asymmetry of tunnel contacts naturally arises. Following it, let us take into account the asymmetric superconducting tunnel junctions with a parameter $\Delta_{d1}/\Delta_{d2} = \zeta$, where $\zeta = e^{-a/\lambda}$ (see Eq. (4.8)). Thus, by combining Eqs. (4.8) and (4.12), one gets that the asymmetry in the superconducting tunneling amplitudes results in a relative shift of a dot equilibrium position and we need to do the following replacement in obtained formulae,

$$\Delta_d(x, \phi) \rightarrow \Delta_d(x + a, \phi). \quad (4.70)$$

In what follows it is convenient to introduce the re-normalized parameter of the asymmetry, $a/\lambda \rightarrow a$. Then, for the criterion for the mechanical instability one obtains $\eta(0 + a, \phi) > 0$, where

$$\begin{aligned} \eta(a, \phi) = \kappa \alpha \xi \frac{\tilde{\Delta}_d}{2\tilde{\mathcal{D}}^6} & \left[\tilde{\Delta}_d^2 \sinh(2a) \left(\tilde{\mathcal{D}}^2 + 4 \right) \{ \sin \phi - \tilde{\varepsilon}_d \sinh(2a) \} + \right. \\ & \left. + 8\tilde{\varepsilon}_d \tilde{\mathcal{D}}^2 \{ \sin^2(\phi/2) + \sinh^2 a \} \right]. \end{aligned} \quad (4.71)$$

From this inequality one can get that the mechanical subsystem is *unstable* when

$$\begin{cases} |\tilde{\Delta}_d \sinh a| < \tilde{\Delta}_d^{cr}, & \tilde{\varepsilon}_d > 0; \\ |\tilde{\Delta}_d \sinh a| > \tilde{\Delta}_d^{cr}, & \tilde{\varepsilon}_d < 0; \end{cases} \quad \phi = \pi; \quad (4.72)$$

$$\begin{cases} |\tilde{\Delta}_d \cosh a| < \tilde{\Delta}_d^{cr}, & \tilde{\varepsilon}_d > 0; \\ |\tilde{\Delta}_d \cosh a| > \tilde{\Delta}_d^{cr}, & \tilde{\varepsilon}_d < 0; \end{cases} \quad \phi = 0; \quad (4.73)$$

or,

$$\begin{cases} |\tilde{\Delta}_{d1} \pm \tilde{\Delta}_{d2}| < 2\tilde{\Delta}_d^{cr}, & \tilde{\varepsilon}_d > 0; \\ |\tilde{\Delta}_{d1} \pm \tilde{\Delta}_{d2}| > 2\tilde{\Delta}_d^{cr}, & \tilde{\varepsilon}_d < 0. \end{cases} \quad (4.74)$$

Here "-" corresponds to the case $\phi = \pi$ and "+" - to $\phi = 0$, ($\zeta \neq 1$). The critical value defined as

$$(\tilde{\Delta}_d^{cr})^2 = \frac{1}{2} \left(\sqrt{(3 + \tilde{\varepsilon}_d^2)^2 + 8(1 + \tilde{\varepsilon}_d^2)} - (3 + \tilde{\varepsilon}_d^2) \right), \quad (4.75)$$

is localized around 1, $(\tilde{\Delta}_s^{cr})^2 \in [(\sqrt{17} - 3)/2, 2)$, because of $\lim_{\tilde{\varepsilon}_d \rightarrow \infty} (\tilde{\Delta}_d^{cr})^2 = 2$. Another way to obtain the stability criteria is to present displacement in a form

$$x(t) \sim e^{i\Omega t}, \quad (4.76)$$

substitute into Eq. (4.50) and look for a solution of the inequality $\text{Im}\Omega < 0$ which corresponds to the case of exponential increase of the amplitude of oscillations of the QD. One can conclude from the above-mentioned stability criteria, Eqs. (4.72)-(4.74), that the presence of "self-saturation" effect is not affected by the asymmetry.

Note that an infinitesimal value of the asymmetry can result in the emergence of the mechanical instability even in the case of zero superconducting phase difference. However, in the latter case the strength of the pumping is small and need to be in comparison with the damping generated by the influence of an thermodynamic equilibrium bath. In order to do this, we incorporate the phenomenological friction term $+\gamma\dot{x}$ in the l.h.s. of Eq. (4.1). The friction coefficient γ is determined as $\propto Q^{-1}$, where Q is the quality factor determined by interaction with the thermodynamic environment [128]. Thus, the mechanical instability occurs if

$$\gamma - \eta(a, \phi) < 0. \quad (4.77)$$

It means that for small values of superconducting phase difference, $\phi < 1$, the pumping coefficient $\eta(x + a, \phi)$ determined by interaction with the electronic subsystem, is much smaller than in case of $\phi \approx \pi$ and equalizes a friction coefficient γ associated with the influence of a thermodynamic environment. It results in competition between these two processes because the regime of self-sustained oscillations emerges when the pumping is equal to damping. As a consequence, friction induced by the interaction with a thermal bath leads to a decrease in the amplitude of self-sustained oscillations. Nevertheless, as the pumping caused by electronic non-equilibrium environment strongly depends on the superconducting phase difference ϕ , in the most pronounced case $\phi = \pi$ it dominates over the "thermodynamic" friction for high-quality nanomechanical resonators, $Q \sim 10^5$.

Figures 4.6, 4.7 represent dependencies of function $W(A)$ which is proportional to the pumping coefficient $\bar{\eta}(A, \phi)$ for different values of the asymmetry parameter a . Note that $W(A)$ is an even function of a . One can see

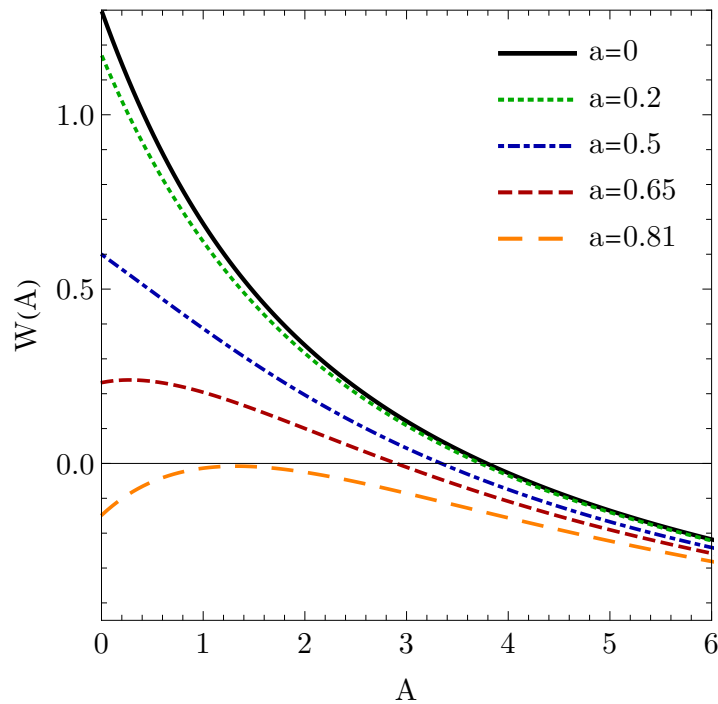


Fig. 4.6 Dependencies of the function $W(A)$, proportional to the pumping coefficient $\bar{\eta}(A, \phi)$, for different values of the asymmetry parameter $|a| = 0$ (black thick curve, symmetric case); 0.2 (green dotted curve); 0.5 (blue dotdashed); 0.65 (red densely dashed); 0.81 (orange loosely dashed curve) for $\phi = \pi$, and $\tilde{\varepsilon}_d = 1/\sqrt{3}$. The zeroes of the functions correspond to the amplitude of the limiting cycle. Other parameters are: $\tilde{\Delta}_d = 1, \kappa = +1$.

from Fig. 4.6, which corresponds to a case of maximal strength of the pumping, $\phi = \pi, \tilde{\varepsilon}_d = 1/\sqrt{3}$, that the value of the amplitude of a limit cycle decreases when the asymmetry increases (shift of the position of a zero of the function to the left). The black curve is associated with the symmetric case ($a = 0$) and is the same one as in Fig. 4.4. The orange curve corresponds to the critical value (with the further increase of the asymmetry parameter the pumping is vanishes) obtained from Eq. (4.75), $(\tilde{\Delta}_d^{cr})^2 = 2/3$ for $\tilde{\varepsilon}_d = 1/\sqrt{3}$. Figure 4.7 demonstrates the case of $\phi = 0$ when the effective pumping is negligibly small and, as a consequence, a limit cycle of self-sustained oscillations does not occurs.

4.1.8. Transistor- and diode-like behaviour in electric current.

The self-sustained oscillations considered above have a very specific transport signature. This raises the possibility of detecting the mechanical instability through an electric current measurement. To explore such a possibility, let us consider the electric current through the system, I_n , determined in a standard

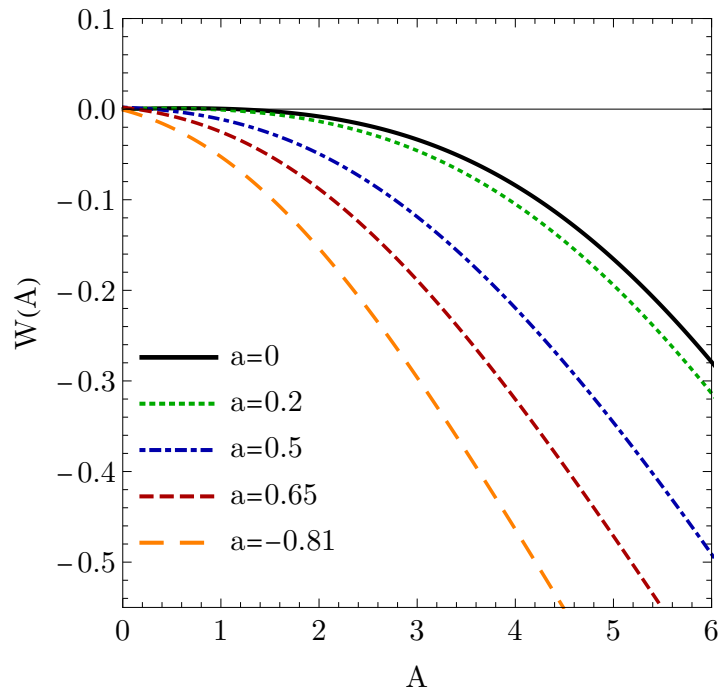


Fig. 4.7 Dependencies of the function $W(A)$, proportional to the pumping coefficient $\bar{\eta}(A, \phi)$, for different values of the asymmetry parameter $|a| = 0$ (black thick curve, symmetric case); 0.2 (green dotted curve); 0.5 (blue dot-dashed); 0.65 (red densely dashed); 0.81 (orange loosely dashed curve) for $\phi = 0$, and $\tilde{\varepsilon}_d = 1/\sqrt{3}$. Other parameters are: $\tilde{\Delta}_d = 1, \kappa = +1, \gamma = 10^{-5}$. The functions take non-positive values which corresponds to the absent of self-sustained oscillations in a limiting cycle.

way,

$$I_n = e\kappa \text{Tr} \left\{ \hat{N} \hat{\rho} \right\}, \quad (4.78)$$

where $\hat{N} = i[\hat{H}, \hat{N}]$ and $\hat{N} = \sum_{k\sigma} a_{k\sigma}^\dagger a_{k\sigma}$ is the operator of the number of electrons in the normal electrode. In the deep subgap regime considered above ($\Delta_s \rightarrow \infty$), one can neglect quasiparticle current since it is exponentially small. As a result, in the high bias voltage regime at $\kappa = +1$, where electron tunneling from the QD to the normal leads is forbidden, an expression for I_n can be easily obtained by analyzing Fig. 4.2. From those diagrams, one can see that a decrease in the number of electrons in the normal electrode is defined by two different processes. The first one is the tunneling of an electron with spin up or down into the empty dot. The rate of this process is $2\Gamma_n \rho_0$, where $\rho_0 = (R_0 + R_3)/2$ is the probability that the dot is empty. The second one is the tunneling of an electron into the dot occupied by a single electron with spin up or down. The rate of this process is

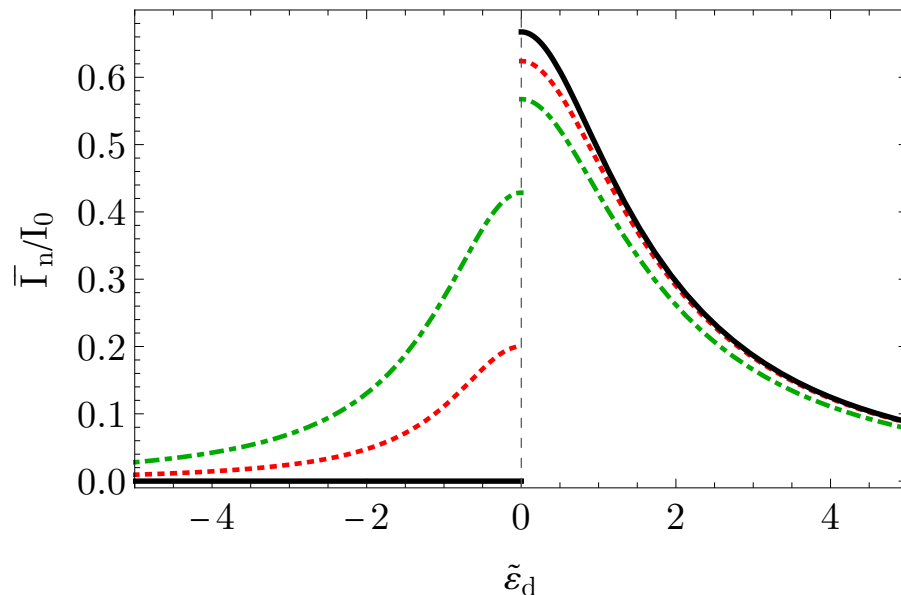


Fig. 4.8 Dependencies of the dc electric current \bar{I}_n (normalized to $I_0 = e\Gamma_n$) on the relative position of the QD energy level $\tilde{\epsilon}_d$ for different values of superconducting phase difference $\phi = \pi/3$ (green dot-dashed curve), $2\pi/3$ (red dotted), and π (black solid) for $\tilde{\Delta}_d = 1$ and $\kappa = +1$. The maximum effect occurs at $\phi = \pi$ when the dc current is absent in the static regime, while it is close to the maximum one in the stable stationary regime of the self-sustained oscillations.

$2\Gamma_n\rho_e$. Taking into account the normalization condition $2\rho_e + R_0 = 1$, and using a similar speculation for $eV_b < 0$, one gets from Eq. (4.44) the following equation for I_n ,

$$I_n(t) = \kappa I_0 (1 + \kappa R_3), \quad (4.79)$$

where $I_0 = e\Gamma_n$. In the adiabatic limit one can use the expansion for \vec{R} in the perturbation theory over the adiabaticity parameter α , Eq. (4.44), and obtain for the current the following equation,

$$I_n(t) = \kappa I_0 \left[\frac{|\Delta_d(x, \phi)|^2}{\mathcal{D}^2(x, \phi)} + \alpha \dot{x} f(x) + \mathcal{O}(\alpha^2) \right]. \quad (4.80)$$

In the stationary regime corresponding to the generation of self-sustained oscillations with amplitude $\sqrt{A_c}$, the averaged over a period of the oscillations electric current \bar{I}_n is defined as

$$\bar{I}_n = \frac{1}{2\pi} \int_0^{2\pi} I_n[x(t)] dt. \quad (4.81)$$

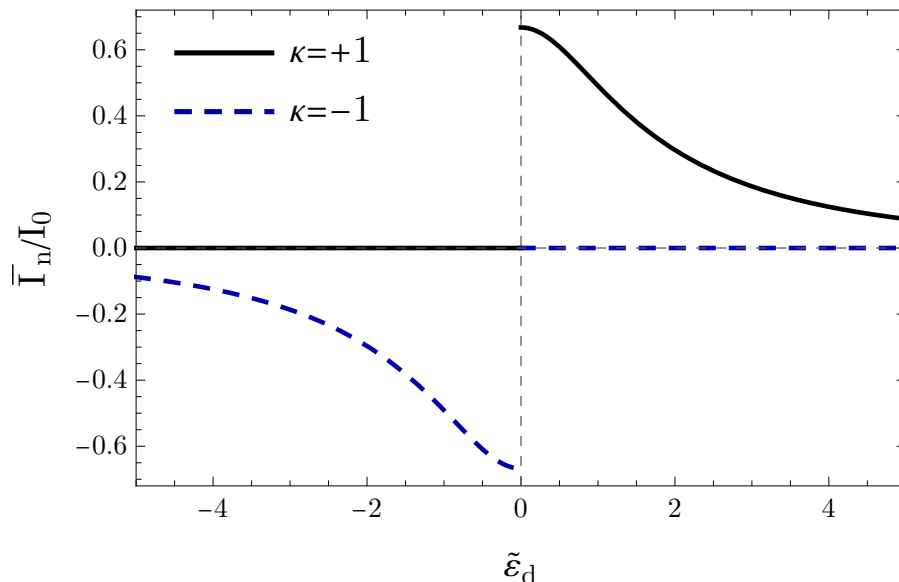


Fig. 4.9 Dependencies of the dc electric current \bar{I}_n (normalized to $I_0 = e\Gamma_n$) on the relative position of the QD energy level $\tilde{\epsilon}_d$ for $\kappa = +1$ (black solid curve, associated with the same one in Fig. 4.8) and for $\kappa = -1$ when the bias voltage is applied in the opposite direction (blue dashed curve), representing a diode-like behaviour of the current. Other parameters: $\phi = \pi$.

After the integrating of Eq. (4.80), the main contribution to the current with an accuracy α^2 (since the first-order term is averaging out) is given as

$$\bar{I}_n(\kappa, \epsilon_d) = \kappa I_0 \left[\frac{\Delta_d^2 \cos^2(\phi/2)}{\Delta_d^2 \cos^2(\phi/2) + \Gamma_n^2 + \epsilon_d^2} + \theta(\kappa \epsilon_d) \delta \bar{I}(A_c) \right]. \quad (4.82)$$

Here the first term corresponds to the static dc current which crucially depends on the superconducting phase difference ϕ . In particular, the first term is equal to zero at $\phi = \pi$, in contrast to the second term,

$$\delta \bar{I}(A_c) = \frac{1}{2\pi} \frac{\Delta_d^2 (\Gamma_n^2 + \epsilon_d^2)}{\mathcal{D}^2(0, \phi)} \int_0^{2\pi} d\psi \frac{\sinh^2(\sqrt{A_c} \sin \psi)}{\mathcal{D}^2(\sqrt{A_c} \sin \psi, \phi)} > 0, \quad (4.83)$$

which emerges exclusively due to the self-sustained oscillations and equals zero if the static state is stable, as indicated by the Heaviside step function $\theta(\kappa \epsilon_d)$. The maximal value of the current $\delta \bar{I}_n(A_c)$ can be estimated as

$$\delta \bar{I}_n^{max} \approx \frac{\Delta_d^2 \sinh^2 \sqrt{A_c}}{\Delta_d^2 \sinh^2 \sqrt{A_c} + \Gamma_n^2 + \epsilon_d^2}. \quad (4.84)$$

Dependencies of the current \bar{I}_n as a function of $\tilde{\varepsilon}_d$ at $\tilde{\Delta}_d = 1$ and $\phi = \pi/3, 2\pi/3, \pi$ are presented in Figs. 4.8, 4.9. These graphs show that the nanomechanical instability discussed in this article leads to the emergence of significant diode and transistor effects. The effects are most pronounced at $\phi = \pi$ when in the static regime $A_c = 0$ where the Cooper pair exchange between the dot and the superconducting leads is completely blocked. In such a situation, a jump in the average current from zero to a finite value $\sim I_0$ (or vice-versa) occurs if the direction of the bias voltage changes (diode effect: for one direction of the bias voltage the current is present but for the opposite one — absent (blocked)), see Fig. 4.9 or if the position of the dot energy level ε_d controlled by the gate voltage (third electrode in a transistor), passes zero (transistor effect), see Fig. 4.8. Note that the discontinuity of the average current as a function of ε_d must be treated to the accuracy ξ .

4.1.9. Numerical results.

The analytical procedure described above is done in the assumption of the adiabatic limit, $\alpha = \omega/(2\Gamma_n) \ll 1$. However, in order to enlarge the range of parameters for which predicted effects are valid, the system of equations for the dot density matrix elements coupled to the equation for the QD displacement, Eqs. (4.21)-(4.22), was solved numerically.

Figure 4.10 demonstrates numerical solution results for the time evolution of the QD displacement after a small initial spontaneous fluctuation of the nanotube position, $x_0 = 0.01$, in three different regimes. The stable regime is represented in Fig. 4.10a. Figure 4.10b corresponds to the critical value of the dot energy level $\tilde{\varepsilon}_d = 0$ (the same as for $\phi = 2\pi n$, where n is an integer number) when the state of the mechanical subsystem is neither stable, nor unstable. Lastly, in the regime of presence of the mechanical instability, Fig. 4.10c, the amplitude of the dot oscillations starts to exponentially grow after a small shift from its equilibrium position. However, after some time, magnitude of the dot oscillations saturates and one has the stable regime of self-sustained oscillations of the nanotube. It emerges even without adding an external friction, $\gamma = 0$. The latter fact is associated with the self-saturation effect occurred for the considered hybrid system. We should note that Fig. 4.10 was obtained for the case of weak electromechanical coupling $\xi \ll 1$, in the adiabatic limit $\alpha \ll 1$, and for other parameters which are the same

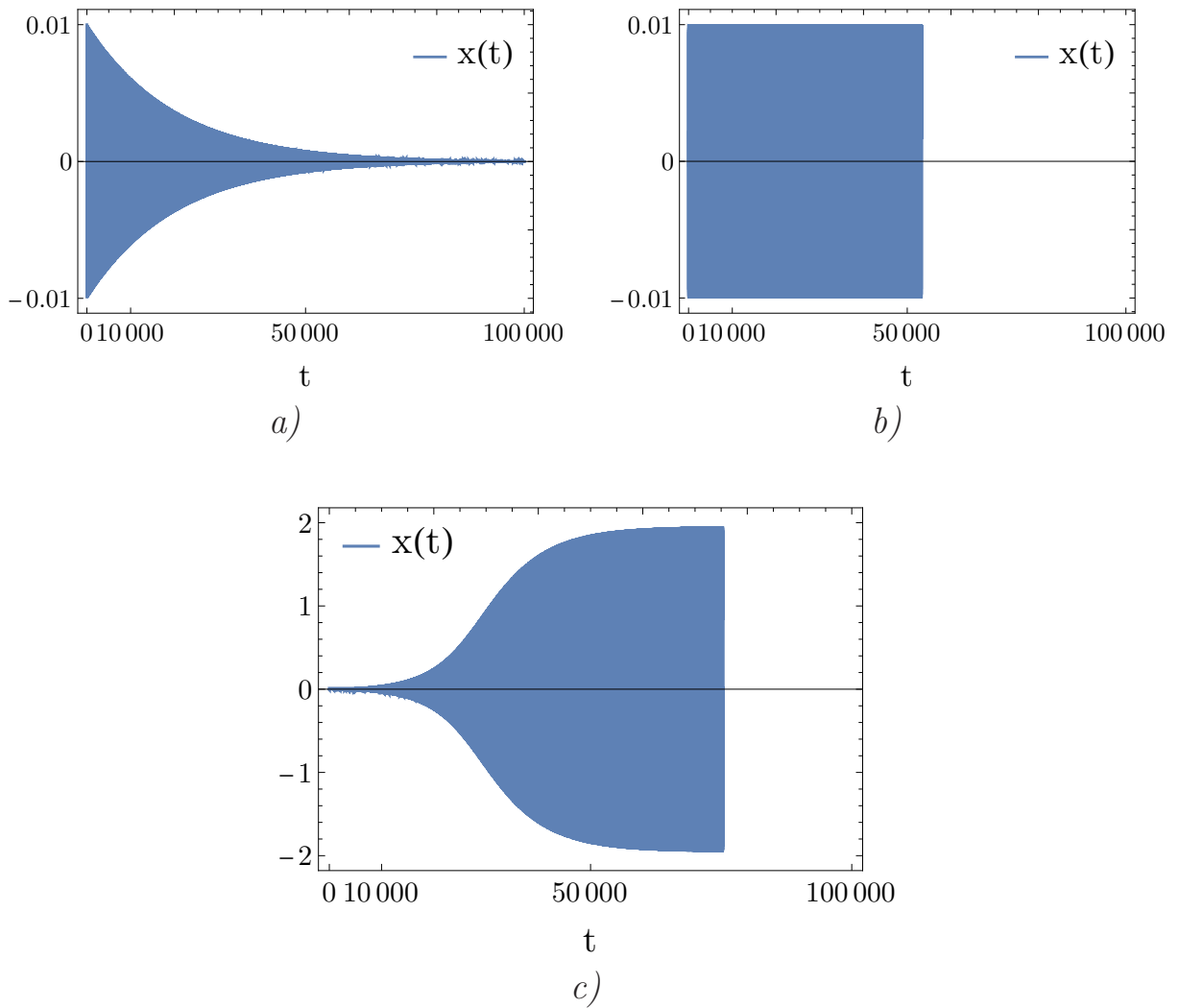


Fig. 4.10 Dependencies of the displacement x (in units of the tunneling length λ) of the QD in three different regimes realized for the system, on time (in units of ω). The figure (a) corresponds to the stable to an initial spontaneous fluctuation ($x_0 = 0.01$) from an equilibrium position, regime, $\tilde{\varepsilon}_d < 0$. The figure (b) corresponds to critical value, $\tilde{\varepsilon}_d = 0$ when the state of the mechanical subsystem is not stable or unstable, either. And the figure (c) demonstrates the time evolution of the QD oscillations in the regime when the mechanical instability occurs, $\tilde{\varepsilon}_d = +1/\sqrt{3}$. The latter case is presented in Figs. 4.4, 4.5 by the black curve. Other parameters used in numerical calculations:

$$\phi = \pi, \tilde{\Delta}_d = 1, \alpha = 0.05, \xi = 10^{-2}.$$

as for the black curve in Figs. 4.4-4.7 came up from analytical predictions. One can see that the amplitude $\sqrt{A_c}$ of the limit cycle given from Fig. 4.4 corresponds to the amplitude of oscillations procured from Fig. 4.10c, $\sqrt{A_c} \approx x^{max} \approx 2$. This is a manifestation of strong validity of the analytical calculations.

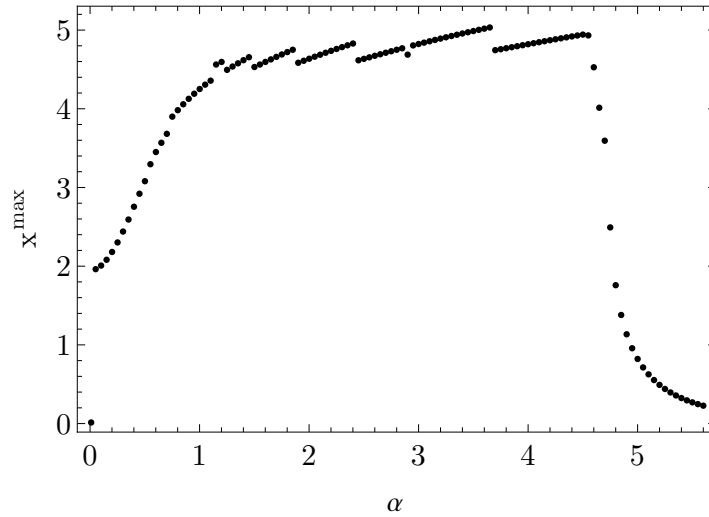


Fig. 4.11 Dependence of the amplitude $\sqrt{A_c}$ of QD self-sustained oscillations (normalized to the tunneling length λ) on the adiabaticity parameter α . One can note that the magnitude of the dot oscillation amplitude is maximal when $\omega \sim \Gamma_n$ and tends to zero in the diabatic regime. Other parameters used in numerical calculations: $\kappa = +1, \tilde{\varepsilon}_d = 1/\sqrt{3}, \phi = \pi, \tilde{\Delta}_d = 1, \xi = 10^{-2}$.

Figure 4.11 demonstrates dependence of the amplitude $\sqrt{A_c}$ (x^{max}) of nanotube self-sustained oscillations (normalized to the tunneling length λ) in the limit cycle on the adiabaticity parameter α . It was obtained from numerical solutions of the system of first-order differential equations for the matrix elements of the dot density operator, Eq. (4.22), coupled to the second-order one for the dot displacement, Eq. (4.21). One can note that the amplitude is maximal in the resonant case, when the frequency (in energy units) of the QD vibrations equals the energy difference between Andreev levels. The later is in an associated agreement with predictions for an electrical [169] and magnetic NEM system [119]. In addition, one should take heed that for the case of an electrical electromechanical coupling, in order to obtain a limit cycle, one need to take into account an thermodynamic friction (damping), $\gamma = 10^{-4} - 10^{-6}$ (for high-quality nanomechanical resonators). Moreover, the maximal values of the amplitude for mechanically *unstable* case is of order of magnitude as for the one in the adiabatic regime, more precisely, approximately twice bigger. Nevertheless, the amplitude is negligible small in the diabatic (anti-adiabatic) limit $\alpha \gg 1$ that means the *stability* of the equilibrium position of the nanotube in this regime. The adiabatic limit corresponds to the case when a nanotube displacement varies very little during one act of electron tunneling which is typically realized in experiments [137].

4.2. Ground-state cooling of nanomechanical vibrations by Andreev tunneling.

In this section a crucial influence of electron tunneling processes on a state of the mechanical subsystem is discussed. The effect of the ground-state cooling of vibrations of the nanotube is found. Also, a possibility to observe the cooling effect in an experiment is demonstrated.

4.2.1. Quantum-mechanical description of the mechanical subsystem.

In the previous section the nanoelectromechanical weak link composed of the carbon nanotube suspended above a trench in a normal metal electrode and positioned in a gap between two superconducting leads, was considered. Such a setup is a generalization of the experimentally implemented one [153], where a CNT suspended between normal and superconducting electrodes. The nanotube has been treated as a movable single-level quantum dot, in which the position-dependent superconducting order parameter is induced as a result of Cooper pair tunneling. It has been shown that in such a system self-sustained bending vibrations can emerge if a constant bias voltage is applied between normal and superconducting electrodes. Such a process of electron transport, which essentially involves Andreev conversion [149, 150] of normal electrons into Cooper pairs, we have called by the Andreev injection. As a consequence, the interplay between coherent two-electron (Cooper pair) and incoherent single-electron tunneling into/out of the movable part of the NEMS can result in pumping or cooling effect [151].

However, one can note from Eq. (4.80) that the direct eclectic current has a contribution $\propto x^2$. It means that it is crucial to take into account quantum fluctuations of the nanotube omitted within the semi-classical approach discussed in the previous section, 4.1. In this section we treat the bending vibrations of the nanotube quantum-mechanically which allow an investigation of the operation of such a NEM device in the cooling regime.

Figure 4.12 is an another schematic representation of the system under consideration. The Hamiltonian of the system consists of four terms,

$$H = H_d + H_v + H_l + H_t, \quad (4.85)$$

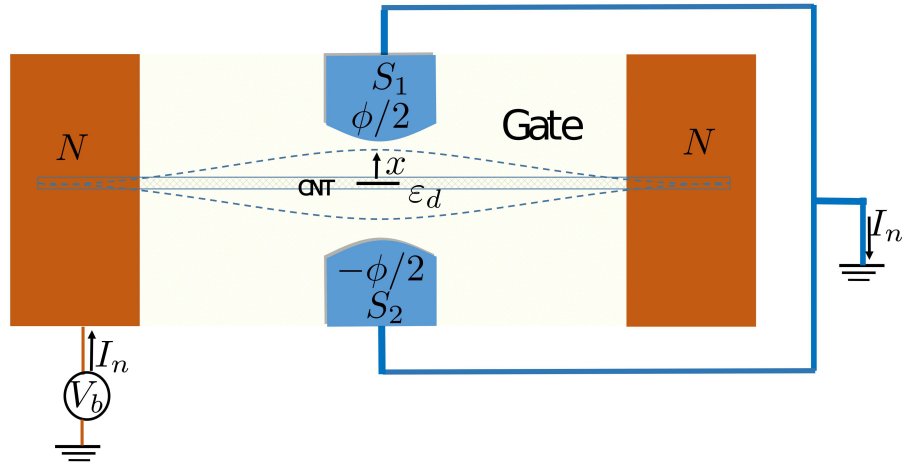


Fig. 4.12 Sketch of the nanoelectromechanical device under consideration. A carbon nanotube (CNT) is suspended in a gap between two edges of a normal electrode (N) and tunnel coupled to it. Also, the CNT oscillates in the x direction between two superconducting leads ($S_{1,2}$). This process affects the values of the tunneling barriers between the QD and superconducting electrodes. The normal electrode is biased by voltage V_b .

where the Hamiltonian H_d of the single-level QD, the Hamiltonian $H_l = H_l^n + H_l^s$ of the normal and superconducting electrodes, the tunnel Hamiltonian $H_t = H_t^n + H_t^s$ are done by Eqs. (4.3)-(4.6), respectively. It needs to be stressed that now the displacement \hat{x} is an operator. The Hamiltonian \hat{H}_v ,

$$\hat{H}_v = \frac{p^2}{2m} + \frac{m\omega^2 x^2}{2}, \quad (4.86)$$

describes the mechanical dynamic of the dot, p and x are the canonical conjugated momentum and coordinate, $[p, x] = -i\hbar$; m, ω are the mass and eigenfrequency of the dot, respectively.

4.2.2. Equations for Wigner distribution functions.

The time evolution of the system density matrix $\hat{\rho}$ is described by the Liouville-von Neumann equation Eq. (4.9). We use the reduced density matrix approximation according to which the full density matrix of the system $\hat{\rho}$ is factorized to the tensor product of the equilibrium density matrices of the normal

and superconducting leads, and the dot density matrix as:

$$\hat{\rho} = \hat{\rho}_n \otimes \hat{\rho}_s \otimes \hat{\rho}_d. \quad (4.87)$$

Here the reduced density operator of the QD $\hat{\rho}_d$ acts in the Hilbert space which can be presented as the tensor product of the vibrational space of the harmonic oscillator and the electronic space of the single-electron level on the QD.

By following the procedure introduced in subsection 4.1.2, we consider the stationary state of the system in the deep subgap case $\Delta_s \gg |eV_b| \gg \Delta_d, \Gamma_n$, where $\Delta_d = 2\pi\nu_s|t_0^s|^2$, $\Gamma_n = 2\pi\nu_n|t_0^n|^2$ ($\nu_{s(n)}$ is a density of states in the superconducting (normal) electrode). Using the standard procedure [45], one can trace out the lead degrees of freedom and obtain the following equation for the reduced density matrix $\hat{\rho}_d$,

$$-\iota [H_d^{\text{eff}} + H_v, \hat{\rho}_d] + \mathcal{L}_n\{\hat{\rho}_d\} + \mathcal{L}_\gamma\{\hat{\rho}_d\} = 0, \quad (4.88)$$

where the effective Hamiltonian H_d^{eff} is presented in Eq. (4.11) with the off-diagonal dot order parameter, Eq. (4.12), induced by superconducting proximity effect which is now is an operator,

$$\Delta_d(\hat{x}, \phi) = \Delta_d \cosh(\hat{x}/\lambda + i\phi/2). \quad (4.89)$$

The Lindbladian term $\mathcal{L}_n\{\hat{\rho}_d\}$ in Eq. (4.88) is induced by the incoherent electron exchange between the normal lead and the QD and in the high bias voltage regime, $|eV_b| \gg \varepsilon_0, \hbar\omega, T$, takes the form of Eq. (4.13). Also, in Eq. (4.88) we phenomenologically introduce the dissipation term $\mathcal{L}_\gamma\{\hat{\rho}_d\}$ [170],

$$\mathcal{L}_\gamma\{\hat{\rho}\} = -m\omega\gamma (n_B + 1/2) [x, [x, \hat{\rho}]] - \iota(\gamma/2) [x, \{p, \hat{\rho}\}], \quad (4.90)$$

where γ is the damping rate, n_B is the Bose-Einstein distribution function,

$$n_B = \frac{1}{e^{\hbar\omega/T} - 1}, \quad (4.91)$$

and T is temperature of the thermodynamic environment.

The QD density matrix $\hat{\rho}_d$ acts in the Hilbert space that can be presented as a tensor product of the vibrational space of the harmonic oscillator and the Fock

space of the single-level QD which is spanned on the state vectors $|0\rangle, d_{\uparrow}^{\dagger}(d_{\downarrow}^{\dagger})|0\rangle = |\uparrow(\downarrow)\rangle, d_{\uparrow}^{\dagger}d_{\downarrow}^{\dagger}|0\rangle = |\uparrow\downarrow\rangle \equiv |2\rangle$. It means the dot density matrix can be presented as:

$$\hat{\rho}_d = \hat{\rho}_d(x, x') = \begin{pmatrix} \hat{\rho}_0 & \hat{\rho}_{02} & 0 & 0 \\ \hat{\rho}_{20} & \hat{\rho}_2 & 0 & 0 \\ 0 & 0 & \hat{\rho}_{\uparrow} & 0 \\ 0 & 0 & 0 & \hat{\rho}_{\downarrow} \end{pmatrix}. \quad (4.92)$$

Thus, we get the following system of equations of motion for electronic components of the density matrix $\hat{\rho}_d$ ($\kappa = +1$),

$$\partial_t \rho_0 = -\imath [H_v, \rho_0] - 4\Gamma_n \rho_0 - \imath \Delta_d(x, \phi) \rho_{20} + \imath \rho_{02} \Delta_d^*(x, \phi) + \mathcal{L}_{\gamma} \{\hat{\rho}_0\}, \quad (4.93)$$

$$\partial_t \rho_{\uparrow} = -\imath [H_v, \rho_{\uparrow}] + 2\Gamma_n (\rho_0 - \rho_{\uparrow}) + \mathcal{L}_{\gamma} \{\hat{\rho}_{\uparrow}\}, \quad (4.94)$$

$$\partial_t \rho_{\downarrow} = -\imath [H_v, \rho_{\downarrow}] + 2\Gamma_n (\rho_0 - \rho_{\downarrow}) + \mathcal{L}_{\gamma} \{\hat{\rho}_{\downarrow}\}, \quad (4.95)$$

$$\partial_t \rho_{02} = -\imath [H_v, \rho_{02}] + 2\imath \varepsilon_d \rho_{02} - 2\Gamma_n \rho_{02} - \imath \Delta_d(x, \phi) \rho_2 + \imath \rho_0 \Delta_d(x, \phi) + \mathcal{L}_{\gamma} \{\hat{\rho}_{02}\} \quad (4.96)$$

$$\partial_t \rho_{20} = -\imath [H_v, \rho_{20}] - 2\imath \varepsilon_d \rho_{20} - 2\Gamma_n \rho_{20} - \imath \Delta_d^*(x, \phi) \rho_0 + \imath \rho_2 \Delta_d^*(x, \phi) + \mathcal{L}_{\gamma} \{\hat{\rho}_{20}\} \quad (4.97)$$

$$\partial_t \rho_2 = -\imath [H_v, \rho_2] + 2\Gamma_n (\rho_{\uparrow} + \rho_{\downarrow}) + \imath \rho_{20} \Delta_d(x, \phi) - \imath \Delta_d^*(x, \phi) \rho_{02} + \mathcal{L}_{\gamma} \{\rho_2\}. \quad (4.98)$$

Here ordering of the operators $\hat{\rho}_{ii}$ and $\hat{\Delta}_d(\hat{x}, \phi)$ is important. To find the equations in case of the opposite direction of the bias voltage, $\kappa = -1$, one needs to switch $0 \rightleftharpoons 2$, so that,

$$\partial_t \rho_0 = -\imath [H_v, \rho_0] + 2\Gamma_n (\rho_{\uparrow} + \rho_{\downarrow}) + \imath \rho_{02} \Delta_d(x, \phi) - \imath \Delta_d^*(x, \phi) \rho_{20} + \mathcal{L}_{\gamma} \{\rho_0\}. \quad (4.99)$$

$$\partial_t \rho_{\uparrow} = -\imath [H_v, \rho_{\uparrow}] + 2\Gamma_n (\rho_2 - \rho_{\uparrow}) + \mathcal{L}_{\gamma} \{\hat{\rho}_{\uparrow}\}, \quad (4.100)$$

$$\partial_t \rho_{\downarrow} = -\imath [H_v, \rho_{\downarrow}] + 2\Gamma_n (\rho_2 - \rho_{\downarrow}) + \mathcal{L}_{\gamma} \{\hat{\rho}_{\downarrow}\}, \quad (4.101)$$

$$\partial_t \rho_{02} = -\imath [H_v, \rho_{02}] - 2\imath \varepsilon_d \rho_{02} - 2\Gamma_n \rho_{02} - \imath \Delta_d^*(x, \phi) \rho_2 + \imath \rho_0 \Delta_d^*(x, \phi) + \mathcal{L}_{\gamma} \{\hat{\rho}_{02}\} \quad (4.102)$$

$$\partial_t \rho_{20} = -\imath [H_v, \rho_{20}] + 2\imath \varepsilon_d \rho_{20} - 2\Gamma_n \rho_{20} - \imath \Delta_d(x, \phi) \rho_0 + \imath \rho_2 \Delta_d(x, \phi) + \mathcal{L}_{\gamma} \{\hat{\rho}_{20}\} \quad (4.103)$$

$$\partial_t \rho_2 = -\imath [H_v, \rho_2] - 4\Gamma_n \rho_2 - \imath \Delta_d(x, \phi) \rho_{02} + \imath \rho_{20} \Delta_d^*(x, \phi) + \mathcal{L}_{\gamma} \{\hat{\rho}_0\}, \quad (4.104)$$

It is convenient to introduce the linear combinations of the density matrix elements as follows:

$$\begin{aligned}
R_v &= \rho_0 + \rho_\uparrow + \rho_\downarrow + \rho_2, \\
R_0 &= \rho_0 + \rho_2, \\
R_1 &= \rho_{20} + \rho_{02}, \\
R_2 &= \imath(\rho_{02} - \rho_{20}), \\
R_3 &= \rho_0 - \rho_2.
\end{aligned} \tag{4.105}$$

Then the equations for the density matrix elements of the QD, Eqs. (4.93)-(4.98), have the following form:

$$\begin{aligned}
\partial_t R_0 &= -\imath[H_v, R_0] + 2\Gamma_n(R_v - 2R_0 - \kappa R_3) + \imath[R_1, \Delta'(x, \phi)] - \imath[R_2, \Delta''(x, \phi)] \\
&\quad + \mathcal{L}_\gamma\{R_0\},
\end{aligned} \tag{4.106}$$

$$\begin{aligned}
\partial_t R_3 &= -\imath[H_v, R_3] - 2\Gamma_n(\kappa R_v + R_3) + \{R_1, \Delta''(x, \phi)\} + \{R_2, \Delta'(x, \phi)\} \\
&\quad + \mathcal{L}_\gamma\{R_3\},
\end{aligned} \tag{4.107}$$

$$\begin{aligned}
\partial_t R_1 &= -\imath[H_v, R_1] + 2\varepsilon_d R_2 - 2\Gamma_n R_1 + \imath[R_0, \Delta'(x, \phi)] - \{R_3, \Delta''(x, \phi)\} \\
&\quad + \mathcal{L}_\gamma\{R_1\},
\end{aligned} \tag{4.108}$$

$$\begin{aligned}
\partial_t R_2 &= -\imath[H_v, R_2] - 2\varepsilon_d R_1 - 2\Gamma_n R_2 - \imath[R_0, \Delta''(x, \phi)] - \{R_3, \Delta'(x, \phi)\} \\
&\quad + \mathcal{L}_\gamma\{R_2\},
\end{aligned} \tag{4.109}$$

$$\partial_t R_v = -\imath[H_v, R_v] + \imath[R_1, \Delta'(x, \phi)] - \imath[R_2, \Delta''(x, \phi)] + \mathcal{L}_\gamma\{R_v\}. \tag{4.110}$$

The state of the mechanical subsystem is completely described by the reduced density matrix,

$$\hat{\rho}_v = \text{Tr} \hat{\rho}_d, \tag{4.111}$$

where the tracing operation is taken over the electronic degrees of freedom on the dot. It is obvious that in the limiting case $\lambda \rightarrow \infty$ the electronic and vibronic subsystems are independent and the reduced vibronic density matrix has a form of equilibrium density matrix with the effective temperature that is determined by an environment temperature T .

It is convenient and natural to use the description in terms of the Wigner distribution function,

$$W_i(x,p) = \frac{1}{2\pi} \int d\xi e^{-ip\xi} \left\langle x + \frac{\xi}{2} | \hat{\rho}_i | x - \frac{\xi}{2} \right\rangle, \quad (4.112)$$

see also section 3.5. In general, a Wigner function gives probability distributions as:

$$\int dp W(x,p) = \langle x | \hat{\rho} | x \rangle, \quad (4.113)$$

$$\int dx W(x,p) = \langle p | \hat{\rho} | p \rangle, \quad (4.114)$$

and is a bounded function,

$$-2/\hbar \leq W(x,p) \leq 2/\hbar, \quad (4.115)$$

which is an evidence of the uncertainty principle. In addition, Eq. (4.112) can be rewritten as follows:

$$W_i(x,p) = \frac{1}{2\pi} \int d\xi e^{ix\xi} \left\langle p + \frac{\xi}{2} | \hat{\rho}_i | p - \frac{\xi}{2} \right\rangle. \quad (4.116)$$

Note that here and in what follows we introduce dimensionless variables: $x/x_0 \rightarrow x$, $px_0/\hbar \rightarrow p$, where x_0 is the amplitude of zero-point oscillations, all energy parameters are measured in units of $\hbar\omega$, the tunneling length λ is measured in units of x_0 , $\gamma/\omega \rightarrow \gamma$.

We are interested in a steady state regime of the mechanical subsystem in the limit of weak electromechanical coupling $1/\lambda \ll 1$. To find a form of Eqs. (4.106)-(4.110) in the Wigner-Moyal representation to leading order in this parameter, one can use the following expressions:

$$[H_v, \hat{R}_i] \rightarrow (x\partial_p - p\partial_x)W_i(x,p), \quad (4.117)$$

$$[\hat{x}, [\hat{x}, \hat{R}_i]] \rightarrow -\partial_p^2 W_i(x,p), \quad (4.118)$$

$$[\hat{x}, \{\hat{p}, \hat{R}_i\}] \rightarrow 2\imath\partial_p p W_i(x,p); \quad (4.119)$$

$$e^{\hat{x}/\lambda} \hat{R}_i \rightarrow e^{x/\lambda} W_i(x, p + \imath/(2\lambda)) \approx W_i(x,p) + \frac{\imath}{2\lambda} \partial_p W_i(x,p), \quad (4.120)$$

$$\hat{R}_i e^{\hat{x}/\lambda} \rightarrow e^{x/\lambda} W_i(x, p - \imath/(2\lambda)) \approx W_i(x,p) - \frac{\imath}{2\lambda} \partial_p W_i(x,p). \quad (4.121)$$

It results in that the steady-state equation for the Wigner function which describes the mechanical degree of freedom, $W_v(x,p)$, is given by the equation (up to terms of the second order in the parameter $1/\lambda$),

$$\{(x\partial_p - p\partial_x) + \mathcal{L}_\gamma\} W_v = -\frac{x}{\lambda^2}\Delta_d \cos(\phi/2)\partial_p W_1 + \frac{1}{\lambda}\Delta_d \sin(\phi/2)\partial_p W_2 \quad (4.122)$$

Here we assume $\gamma \sim (1/\lambda^2)$. This equation is coupled to the steady state equation for the vector-function $\vec{W} = (W_0, W_1, W_2, W_3)^T$ that takes the following form (up to terms of the first order in the parameter $1/\lambda$),

$$(x\partial_p - p\partial_x)\vec{W} + 2\hat{M}\vec{W} = \vec{F}, \quad (4.123)$$

$$\hat{M} = \begin{pmatrix} -2\Gamma_n & 0 & 0 & -\kappa\Gamma_n \\ 0 & -\Gamma_n & \varepsilon_d & 0 \\ 0 & -\varepsilon_d & -\Gamma_n & -\Delta_d \cos(\phi/2) \\ 0 & 0 & \Delta_d \cos(\phi/2) & -\Gamma_n \end{pmatrix},$$

$$\vec{F} = -2\Gamma_n W_v \begin{pmatrix} 1 \\ 0 \\ 0 \\ -\kappa \end{pmatrix} + \frac{\Delta_d}{\lambda} \sin(\phi/2) \begin{pmatrix} \partial_p W_2 \\ 2x W_3 \\ \partial_p W_0 \\ -2x W_1 \end{pmatrix}.$$

Furthermore, it is convenient to change from (x,p) to polar coordinates (A,φ) , so that, $x - \bar{x} = A \sin \varphi$ and $p = A \cos \varphi$, where $\bar{x} \sim (1/\lambda)$ stands for an equilibrium position of the dot. Then, equations (4.122)-(4.123) take the following form:

$$-\frac{\partial W_v}{\partial \varphi} + \bar{x}\hat{T}W_v + \gamma(n_B + 1/2)\hat{T}^2 W_v + \gamma(W_v + A \cos \varphi \hat{T}W_v) - \frac{\Delta_d}{\lambda} \sin(\phi/2)\hat{T}W_2 + \frac{\Delta_d A}{\lambda^2} \cos(\phi/2) \sin \varphi \hat{T}W_1 = 0; \quad (4.124)$$

$$-\frac{\partial \vec{W}}{\partial \varphi} + 2\hat{M}\vec{W} = \vec{F}, \quad (4.125)$$

$$\hat{M} = \begin{pmatrix} -2\Gamma_n & 0 & 0 & -\kappa\Gamma_n \\ 0 & -\Gamma_n & \varepsilon_d & 0 \\ 0 & -\varepsilon_d & -\Gamma_n & -\Delta_d \cos(\phi/2) \\ 0 & 0 & \Delta_d \cos(\phi/2) & -\Gamma_n \end{pmatrix},$$

$$\vec{F} = -\bar{x}\hat{T}\vec{W} - 2\Gamma_n W_v \begin{pmatrix} 1 \\ 0 \\ 0 \\ -\kappa \end{pmatrix} + \frac{\Delta_d}{\lambda} \sin(\phi/2) \begin{pmatrix} \hat{T}W_2 \\ 2A \sin \varphi W_3 \\ \hat{T}W_0 \\ -2A \sin \varphi W_1 \end{pmatrix}.$$

Here the differential operator \hat{T} is defined according to the expression:

$$\hat{T} \equiv \partial_p = \cos \varphi \frac{\partial}{\partial A} - \frac{\sin \varphi}{A} \frac{\partial}{\partial \varphi}. \quad (4.126)$$

Also, one can take a heed that $(x\partial_p - p\partial_x) = -\partial_\varphi$, $\partial_p^2 = (1/2A)\partial_A A \partial_A$ and $\partial_p p = (1/2A)\partial_A A^2$. Equations (4.124)-(4.125) have to be solved subject to the periodic boundary conditions,

$$W_v(A, \varphi + 2\pi) = W_v(A, \varphi), \quad \vec{W}(A, \varphi + 2\pi) = \vec{W}(A, \varphi). \quad (4.127)$$

We solve these equations by perturbation expansions,

$$W_i(A, \varphi) = W_i^{(0)}(A, \varphi) + W_i^{(1)}(A, \varphi) + \dots, \quad (4.128)$$

($i = v, 0, 1, 2, 3$), where $W_i^{(n)}$ is of n :th order in the parameter $1/\lambda \simeq 10^{-2} - 10^{-3}$ [161] (or the parameter of electromechanical coupling, $\Delta_d/\lambda \ll 1$).

It can be easily find from Eqs. (4.124)-(4.125) in zeroth order of the perturbation theory that the functions $W_v^{(0)}(A, \varphi)$, $\vec{W}^{(0)}(A, \varphi)$ do not depend on φ .

Hence, $W_v^{(0)}(A, \varphi) = W_v^{(0)}(A)$ and

$$W_0^{(0)} = \frac{\varepsilon_d^2 + \Gamma_n^2 + (\Delta_d^2/2) \cos(\phi/2)}{D^2} W_v^{(0)}, \quad (4.129)$$

$$W_1^{(0)} = \kappa \frac{\Delta_d \varepsilon_d \cos(\phi/2)}{D^2} W_v^{(0)}, \quad (4.130)$$

$$W_2^{(0)} = \kappa \frac{\Delta_d \Gamma_n \cos(\phi/2)}{D^2} W_v^{(0)}, \quad (4.131)$$

$$W_3^{(0)} = -\kappa \frac{\varepsilon_d^2 + \Gamma_n^2}{D^2} W_v^{(0)}, \quad (4.132)$$

where

$$D^2 = \varepsilon_d^2 + \Gamma_n^2 + \Delta_d^2 \cos^2(\phi/2). \quad (4.133)$$

From the requirement, $W_v^{(1)}(A, \varphi) = W_v^{(1)}(A)$, to first order in the perturbation theory, Eq. (4.124) determines an equilibrium position of the dot,

$$\bar{x} = \kappa \frac{\Delta_d^2}{\lambda D} \sin(\phi/2) \cos(\phi/2). \quad (4.134)$$

In the second order of the perturbation theory from Eq. (4.124) one gets:

$$-\frac{\partial W_v^{(2)}}{\partial \varphi} - \frac{\Delta_d}{\lambda} \sin(\phi/2) \hat{T} W_2^{(1)} + \frac{\Delta_d}{\lambda} \cos(\phi/2) A \sin \varphi \hat{T} W_1^{(0)} + \bar{x} \hat{T} W_v^{(1)} + \mathcal{L}_\gamma \{W_v^{(0)}\} = 0. \quad (4.135)$$

Then, let us average this equation over the φ variable in an usual way,

$$\langle W(A, \varphi) \rangle = \frac{1}{2\pi} \int_0^{2\pi} d\varphi W(A, \varphi). \quad (4.136)$$

By substituting Eq. (4.126) into Eq. (4.136), one finds after straightforward calculations the following expression:

$$\langle \hat{T} W(A, \varphi) \rangle = \frac{1}{A} \frac{\partial}{\partial A} (A \langle \cos \varphi W(A, \varphi) \rangle). \quad (4.137)$$

From these equations one can see that the first, third and fourth terms in the r.h.s. of Eq. (4.135) do not give an contribution, so that one obtains the following

equation for $W_v^{(0)}$,

$$-\frac{\Delta_0 \sin(\phi/2)}{\lambda A} \frac{\partial}{\partial A} \left(A \left\langle \cos \varphi W_2^{(1)} \right\rangle \right) + \frac{\gamma}{2A} \frac{\partial}{\partial A} \left(A^2 W_v^{(0)} \right) + \frac{\gamma (n_B + 1/2)}{2A} \frac{\partial}{\partial A} \left(A \frac{\partial W_v^{(0)}}{\partial A} \right) = 0. \quad (4.138)$$

Therefore, to get a closed equation for $W_v^{(0)}(A)$, one needs to know the function $W_2^{(1)}(A, \varphi)$. This function can be determined from Eqs. (4.125) which in the first order in the perturbation theory has a form:

$$-\frac{\partial \vec{W}^{(1)}}{\partial \varphi} + 2\hat{M}\vec{W}^{(1)} = \vec{F}, \quad (4.139)$$

where \hat{W} denotes an reduced vector-function $\hat{W} = (W_1, W_2, W_3)^T$ because of in the first-order approximation the equation for the Wigner function $W_0^{(1)}$ is decoupled from the other ones and is not relevant in what follows. Additionally,

$$\hat{M} = \begin{pmatrix} -\Gamma_n & \varepsilon_d & 0 \\ -\varepsilon_d & -\Gamma_n & -\Delta_d \cos(\phi/2) \\ 0 & \Delta_d \cos(\phi/2) & -\Gamma_n \end{pmatrix},$$

$$\vec{F} = -\bar{x}\hat{T}\vec{W}^{(0)} - 2\Gamma_n W_v^{(1)} \begin{pmatrix} 0 \\ 0 \\ -\kappa \end{pmatrix} + \frac{\Delta_d}{\lambda} \sin(\phi/2) \begin{pmatrix} 2A \sin \varphi W_3^{(0)} \\ \hat{T}W_0^{(0)} \\ -2A \sin \varphi W_1^{(0)} \end{pmatrix}.$$

The system of first-order differential equations, Eq. (4.139), can be solved exactly by using the Fourier representation since this equation contains functions which are periodic with the period of 2π , $W(A, \varphi + 2\pi) = W(A, \varphi)$,

$$W_i^{(1)}(A, \varphi) = \sum_{n=-\infty}^{+\infty} w(n) e^{in\varphi}, \quad w(n) = \frac{1}{2\pi} \int_0^{2\pi} W_i^{(1)}(\varphi) e^{-in\varphi} d\varphi. \quad (4.140)$$

Furthermore, because of the structure of Eq. (4.138), one can note that only the first harmonics ($n = \pm 1$) of the Fourier series, Eq. (4.140), give an contribution,

$$\begin{aligned} \langle \cos \varphi W_2^{(1)}(A, \varphi) \rangle &= \sum_n w_2(n) [\langle \cos \varphi \cos(n\varphi) \rangle + \iota \langle \cos \varphi \sin(n\varphi) \rangle] = \\ &= \sum_n w_2(n) \begin{cases} 0, & n \neq \pm 1, \\ 1/2, & n = \pm 1; \end{cases} = \frac{1}{2}(w_2(1) + w_2(-1)) = \text{Re}w_2(1). \end{aligned} \quad (4.141)$$

Then, straightforward calculations leads to the following form of Eq. (4.138),

$$\mathcal{D}_1 \frac{\partial}{\partial A} \left(A^2 W_v^{(0)} \right) + \mathcal{D}_2 \frac{\partial}{\partial A} \left(A \frac{\partial W_v^{(0)}}{\partial A} \right) = 0, \quad (4.142)$$

that is a stationary Fokker-Planck equation for the Wigner function $W_v^{(0)}(A)$, which describes the state of the mechanical subsystem, with the drift \mathcal{D}_1 and diffusive \mathcal{D}_2 coefficients,

$$\mathcal{D}_1 = -\kappa \frac{\Delta_d^2 \Gamma_n \varepsilon_d}{\lambda^2 D_1} \sin^2(\phi/2) + \gamma, \quad (4.143)$$

$$\mathcal{D}_2 = \frac{\Delta_d^2 \Gamma_n C}{\lambda^2 D_1} \sin^2(\phi/2) + \gamma (n_B + 1/2). \quad (4.144)$$

Here

$$D^2 = \varepsilon_d^2 + \Gamma_n^2 + \Delta_d^2 \cos^2(\phi/2), \quad (4.145)$$

$$D_1 = (D^2 - 1/4)^2 + \Gamma_n^2, \quad (4.146)$$

$$C = \frac{(D^2 + 1/4)(D^2 + \varepsilon_d^2 + \Gamma_n^2) - 4\Delta_d^2 \Gamma_n^2 \cos^2(\phi/2)}{4D^2}. \quad (4.147)$$

The solution of Eq. (4.142) at small (in comparison to λ) values of the amplitude has a form of the Boltzmann distribution function,

$$W_v^{(0)}(x, p) = (\beta/\pi) \exp[-\beta(x^2 + p^2)], \quad (4.148)$$

where the coefficient $\beta = \mathcal{D}_1/2\mathcal{D}_2$.

The expressions, Eqs. (4.143), (4.144), define the framework of validity of our consideration. It follows from Eqs. (4.143)-(4.147) that in the region which

is related to the maximal cooling effect as we will show in the next section, 4.2.3, (the range of the values of parameters (ϕ, ε_d) near the point $\varepsilon_d = 1/2, \phi = \pi$) the value of the level width is restricted from below, $\Gamma_n \geq \Gamma_n^{(0)} = \Delta_d^2/\lambda^2$.

4.2.3. Ground-state cooling of nanomechanical vibrations.

Nowadays, nanomechanical resonators with a significant value of the quality factor are achieved in experiments [164, 171]. For such a case, the electromechanical coupling dominates the coupling with the thermodynamic environment, $1/\lambda \gg \gamma$. Thus, let us consider the case $\gamma \rightarrow 0$. From Equations (4.143)-(4.144) it follows that the sign of the coefficient β is determined by the sign of $\kappa\varepsilon_d$. If $\kappa\varepsilon_d$ is positive, β becomes negative. This situation corresponds to the *mechanical instability* of the system and it was discussed in Ref. [3], see section 4.1. In what follows we consider the vibronic (stable) regime, when $\kappa = -1, \varepsilon_d > 0$ (the same for $\kappa = +1, \varepsilon_d < 0$).

The coefficient β determines the probability P_0 that the system is in its ground state. In terms of Wigner distribution functions this probability takes a form:

$$P_0 = 2\pi \int dx dp W_v^{(0)}(x,p) W_0(x,p) = \frac{2\beta}{\beta + 1}, \quad (4.149)$$

where

$$W_0(x,p) = (1/\pi) \exp[-(x^2 + p^2)], \quad (4.150)$$

is the Wigner function of the harmonic oscillator ground state. Note that according to Heisenberg's uncertainty principle the maximal value of parameter β is equal to unity, $\beta \leq \beta_{\max} = 1$.

Dependencies of the probability P_0 as a function of the superconducting phase difference ϕ for different values of the quantum dot energy level ε_d are demonstrated in Fig. 4.13.

We can see that the maximal effect of cooling takes place in the region $\phi \simeq \pi, \varepsilon_d \simeq 1/2$, the degree of cooling reaches the significant values, $P_0 \simeq 0.95$. One can estimate it as

$$P_0 = \frac{2\varepsilon_d}{\varepsilon_d + \varepsilon_d^2 + \Gamma_n^2 + 1/4}, \quad (4.151)$$

and, therefore, note that the maximal cooling effect occurs in the anti-adiabatic regime, $\Gamma_n \simeq 0.2 < 1$. More precisely, the extrema of the function β are the

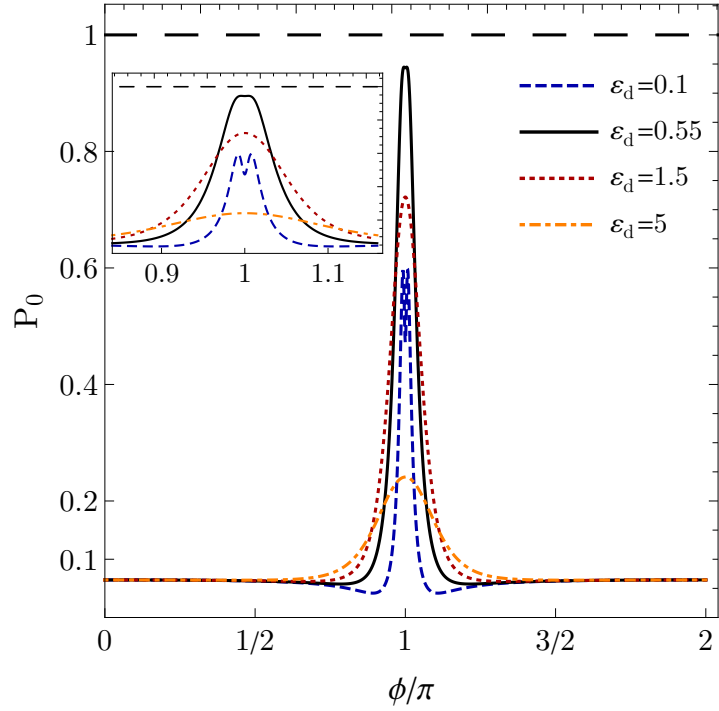


Fig. 4.13 The ground state occupation probability P_0 versus the superconducting phase difference ϕ for different values of the quantum dot energy level: $\varepsilon_d = 0.1$ (blue dashed curve), 0.56 (black thick), 1.5 (red dotted), 5 (orange dot-dashed). The black dotted line indicates the maximal value of the occupation probability. Inset: zoomed central region where the cooling reaches its maximum at $\phi = \pi$. Other parameters: $\Gamma_n = 0.2$; $\Delta_d = 25$; $\lambda = 100$; $\gamma = 10^{-5}$, $T = 15\hbar\omega$.

following:

$$\phi_{extr,n} = \pi n; \quad n \in \mathbb{Z}, \quad (4.152)$$

$$\phi_{extr,\pm} = 2 \arccos \frac{\pm \sqrt{\sqrt{(\varepsilon_d^2 + \Gamma_n^2)(16\Gamma_n^2 + 1)} - 2(\varepsilon_d^2 + \Gamma_n^2)}}{\sqrt{2}\Delta_d}, \quad (4.153)$$

and associated with the ones seen in Fig. 4.13.

Additionally, we calculate the probability distribution P_n . The probability to find the mechanical subsystem being in a state n is defined as:

$$P_n = 2\pi \int dx dp W_v^{(0)}(x,p) W_n(x,p), \quad (4.154)$$

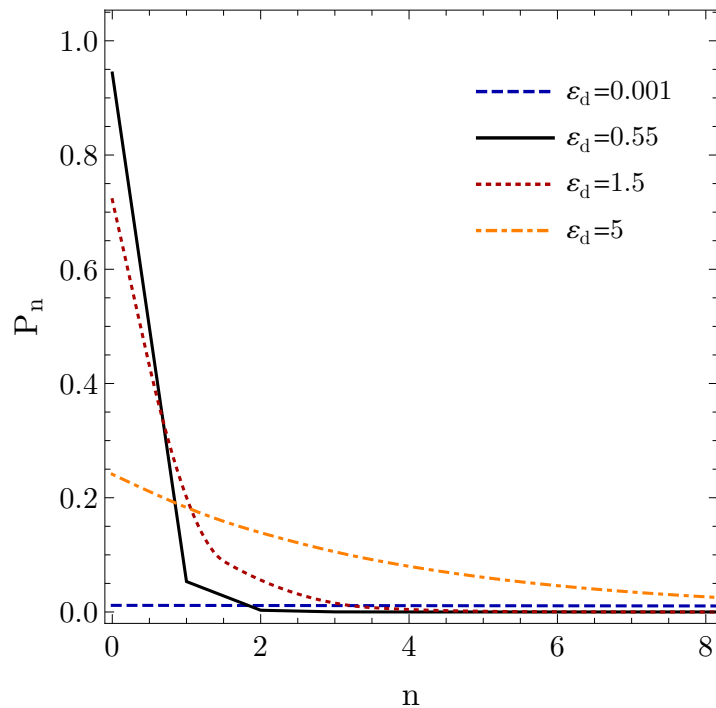


Fig. 4.14 The probability distribution P_n for different values of the quantum dot energy level: $\varepsilon_d = 0.001$ (blue dashed curve), 0.56 (black thick), 1.5 (red dotted), 5 (orange dot-dashed) for $\phi = \pi$. The black dotted line indicates the maximal value of the ground-state occupation probability. Other parameters are the same as in Fig. 4.13: $\Gamma_n = 0.2$; $\Delta_d = 25$; $\lambda = 100$; $\gamma = 10^{-5}$, $T = 15\hbar\omega$.

where now $W_n(x,p)$ stands for the Wigner function of the harmonic oscillator corresponded to n th Fock state,

$$W_n(x,p) = \frac{(-1)^n}{\pi} e^{-(x^2+p^2)} L_n[2(x^2 + p^2)], \quad (4.155)$$

where $L_n(x)$ denotes an n th Laguerre polynomial. Thus, $n = 0$ ($L_0(x) = 1$) gives an special case of Eq. (4.150). Straightforward calculations leads to the following expression for the probability P_n ,

$$P_n = \frac{2\beta(1-\beta)^n}{(1+\beta)^{n+1}} = \left(\frac{1-\beta}{1+\beta}\right)^n P_0, \quad (4.156)$$

where P_0 is defined by Eq. (4.149).

4.2.4. Non-monotonic behaviour of electric current.

The effect of cooling of the mechanical vibrations can be explored by dc current measurements. The Wigner distribution function gives the possibility to calculate various physical quantities. The electric current through the system can be defined in a standard way as a change of the number of electrons in the normal lead, see Eq. (4.78). Thus, one can obtain the following expression for the electric current in terms of Wigner functions, analogous to Eq. (4.79),

$$I/I_0 = \kappa \int_0^{2\pi} d\varphi \int_0^\infty dAA[W_v(A,\varphi) + \kappa W_3(A,\varphi)], \quad (4.157)$$

where $I_0 = e\Gamma_n/\hbar$. In the zeroth order of perturbation theory over the parameter of the electromechanical coupling, using Eqs. (4.129) and (4.148), we get the expression for the static current (see the first term in the r.h.s. of Eq. (4.1.8)),

$$I_n^{(0)} = I_0 \frac{\Delta_d^2 \cos^2(\phi/2)}{\Gamma_n^2 + \varepsilon_d^2 + \Delta_d^2 \cos^2(\phi/2)}. \quad (4.158)$$

From this equation one can see that the current $I_n^{(0)}$ is equal to zero at $\phi = \pi$ despite the fact of maximal effect of cooling in this regime we are interested the most. Therefore, we need to consider next-order corrections. From Equation (4.157) one notes that in order to find the next perturbation order terms, one need to know the functions $W_v^{(1),(2)}$ and $W_3^{(1),(2)}$, at least. This fact leads to the requirement to include in Eqs. (4.122),(4.123) a contribution from the next order of the perturbation theory.

However, one can avoid to do that because of the fact that due to the geometry of our system, the normal current is equal to the sum of the partial currents corresponding to the superconducting electrodes, $I_n = I_1^{(s)} + I_2^{(s)}$. Here the supercurrent in the j superconducting lead is determined by the change of the number of Cooper pairs and can be presented as:

$$I_j^{(s)} = \frac{2e}{\hbar} \text{Tr} \left(\frac{\partial H_d^{\text{eff}}}{\partial \phi_j} \hat{\rho}_d \right), \quad (4.159)$$

where one should take into account that in more general case the expression for the dot order parameter is following:

$$\Delta_d(x, \phi) = \frac{1}{2} \Delta_d (e^{-x/\lambda - i\phi_1} + e^{x/\lambda - i\phi_2}). \quad (4.160)$$

Then,

$$I_j = ie\omega \Delta_d \text{Tr} \left\{ e^{(-1)^j x/\lambda} (e^{i\phi_j} \rho_{02} - e^{-i\phi_j} \rho_{20}) \right\}. \quad (4.161)$$

In terms of Wigner functions the expression for the electric current takes a form:

$$I_n = e\omega \int dx dp [\Delta_d \sin(\phi/2) \sinh(x/\lambda) W_1 + \Delta_d \cos(\phi/2) \cosh(x/\lambda) W_2], \quad (4.162)$$

which is convenient to be re-written in the polar coordinates (angle-action representation) up to the second-order terms in the perturbation theory as

$$I_n = e\omega \Delta_d \int_0^{2\pi} d\varphi \int_0^\infty dAA \left\{ \sin(\phi/2) \left[\frac{A \sin \varphi}{\lambda} W_1^{(0)} + \frac{A \sin \varphi}{\lambda} W_1^{(1)} \right] + \cos(\phi/2) \left[W_2^{(0)} + W_2^{(2)} + \frac{A^2 \sin^2 \varphi}{2\lambda^2} W_2^{(0)} \right] \right\}. \quad (4.163)$$

From this equation one can find that zeroth-order terms give Eq. (4.158), the contribution of the first-order corrections equals to zero, and the non-zero second-order contribution (the second term in the integrand) at $\phi = \pi$ is

$$I_n^{(2)} = e\omega 2\pi \frac{\Delta_d}{\lambda} \int_0^\infty dAA^2 \text{Im} w_1(1). \quad (4.164)$$

Thus, at $\phi = \pi$ the current is determined by the mechanical fluctuations and in the leading order (second) of the electromechanical coupling parameter it reads as

$$I_n = I_0 \left(\frac{\Delta_d}{\lambda} \right)^2 \frac{(\Gamma_n^2 + \varepsilon_d^2 + 1/4) \langle x^2 \rangle + \varepsilon_d/2}{(\Gamma_n^2 + \varepsilon_d^2 - 1/4)^2 + \Gamma_n^2}, \quad (4.165)$$

where the $\langle \dots \rangle$ denote the average value in the phase space with $W_v^{(0)}(x, p)$ and

$$\langle x^2 \rangle = (2\beta)^{-1}. \quad (4.166)$$

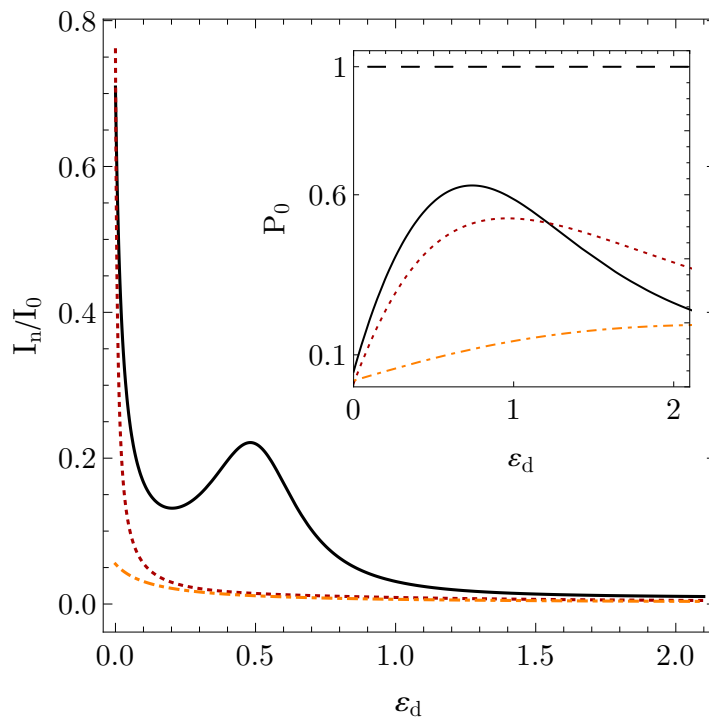


Fig. 4.15 The dependence of the electric current (normalized to I_0) on the quantum dot level energy ε_d at $\phi = \pi$ for different values of Γ_n : $\Gamma_n = 0.2$ (black thick curve), $\Gamma_n = 1$ (red dotted), $\Gamma_n = 3$ (orange dot-dashed). Inset: the ground state occupation probability versus the QD level energy. Other parameters:

$$\Delta_d = 5, \lambda = 50, \gamma = 5 \times 10^{-5}, T = 15.$$

Figure 4.15 presents the dependence of the electric current on the quantum dot level energy ε_d for different values of Γ_n at $\phi = \pi$. We can see the pronounced drop of the current which corresponds to the cooling regime as one can note from the inset where the ground-state probability increase occurs in this case. This maximum-minimum structure disappears in the heating regime ($P_0 \lesssim 0.5$). Also, one can see the maximum of the current in the case of $2\varepsilon_d = \Gamma_n$ at $\Gamma_n \rightarrow 0$. It is a resonant peak and has therefore a different from cooling nature and is discussed, for example, in Ref. [151] for a hybrid N-QD-S device. Thus, the above-mentioned facts can serve as a criterion that the system is in the cooling regime.

Conclusions

In this chapter the nanomechanical weak link that involves a carbon nanotube suspended between two normal leads and biased by a constant voltage is considered. The nanotube, which is treated as a single-level quantum dot, performs bending vibrations in a gap between two superconducting electrodes. The

coupling between the electronic and mechanical degrees of freedom is induced due to the superconducting proximity effect which exhibits in the appearance of the position-dependent dot order parameter.

On the one hand, in the first section we demonstrate that in such a system, the static, straight configuration of the nanotube is *unstable* regarding the occurrence of self-sustained bending vibrations in a wide range of parameters if a bias voltage is applied between the normal and superconducting leads. It is shown that the occurrence of this mechanical instability crucially depends on the direction of the bias voltage and the relative position of the QD level. We have also shown that the appearance of self-sustained mechanical vibrations strongly affects the dc current through the system, leading to transistor and diode effects. The latter can be used for the direct experimental observation of the predicted phenomena.

On the other hand, in the second section, using the density matrix approximation, we find that at certain direction of the applied bias voltage, the stationary state of the mechanical subsystem has a Boltzmann form. Moreover, the probability to find the system in the ground state has been demonstrated to be $P_0 \lesssim 1$. The latter is related to the cooling regime of the considered system. Additionally, the probability depends on the superconducting phase difference and the relative position of the QD energy level in a key manner. Also, we have discussed that the direct electric current behaviour mirrors the stationary state of the system.

Thus, the clear possibility to govern the operating mode of the device by changing the bias and gate voltages is demonstrated and the schemes for an experimental detection of the predicted effects are proposed.

The main results of this chapter are published in Refs. [3, 4, 9, 172].

CONCLUSIONS

In the works this dissertation based on, phenomena which emerge due to an electromechanical coupling in nano-structures based on a movable quantum dot, are investigated.

The main results are the following:

1. The electron transport through an single-molecule transistor with coherent vibrons was theoretically investigated. It has been shown that current-voltage characteristics of such a nanoscale transistor are step-like functions of the bias voltage similarly to the polaronic ones. However, the lifting of this coherent-oscillation induced blockade occurs at voltages much lower than the ones predicted within Franck-Condon theory.
2. The possibility to generate quantum entanglement between charge qubit states and mechanical coherent ones in a nanoelectromechanical system was shown. The experimentally simple protocol of the bias voltage manipulation, which results in the formation of entangled states incorporating "cat states", was proposed.
3. The non-trivial behavior of a hybrid nanoelectromechanical device, which emerges due to a fundamentally new type of electromechanical coupling based on the quantum delocalization of Cooper pairs, has been theoretically investigated. The range of existence of the mechanical instability in such a system was theoretically found. Moreover, the instability results in the generation of self-sustained mechanical oscillations under the self-saturation effect.
4. The regime when the stationary state of the mechanical subsystem of the hybrid nanoelectromechanical system has a Boltzmann form determined by parameters of the device, was investigated. In this case the probability to find the system in the ground state was shown to be sufficiently large which corresponds to the ground-state cooling effect in the system.
5. It has been theoretically demonstrated that the mechanical vibrations in the hybrid nanoelectromechanical device strongly affect the direct electric current through the one. It allows to probe experimentally the presence and characteristics of the predicted self-sustained oscillations as well as the cooling effect.

Acknowledgements

The candidate deeply acknowledges the very best supervision of Sergei I. Kulinich and Ilya V. Krive. Also, the candidate greatly acknowledges all the support and advisement of Leonid Y. Gorelik.

Moreover, the candidate's warm thanks are to Sergey N. Shevchenko for the all-round support.

Nevertheless, the candidate says a hundred of thanks to O.A. Ilinskaya, A.V. Parafilo, A.D. Shkop, H.C. Park and R.I. Shekhter for the helpful discussions and collaboration together with the useful advises.

The candidate sincerely thanks Sergei V. Koniakhin for the all-round help, too.

In addition, the candidate appreciates the support of the Department of Theoretical Physics headed by Dr. Victor V. Slavin, in particular, special candidate's thanks go to A.N. Kalinenko, of B. Verkin Institute for Low Temperature Physics and Engineering of the NAS of Ukraine (Kharkiv, Ukraine) as well as the Center for Theoretical Physics of Complex Systems headed by Prof. Sergej Flach, of the Institute of Basic Sciences (Daejeon, Republic of Korea).

BIBLIOGRAPHY

- [1] **O.M. Bahrova**, S.I. Kulinich, and I.V. Krive. “Polaronic effects induced by non-equilibrium vibrons in a single-molecule transistor”. *Low Temperature Physics* **46.7** (2020), pp. 671–676. DOI: 10.1063/10.0001362. arXiv: 2111.15216 [cond-mat.mes-hall].
- [2] **O.M. Bahrova**, L.Y. Gorelik, and S.I. Kulinich. “Entanglement between charge qubit states and coherent states of nanomechanical resonator generated by ac Josephson effect”. *Low Temp. Phys.* **47.4** (2021), pp. 287–293. DOI: 10.1063/10.0003739. arXiv: 2112.00204 [cond-mat.mes-hall].
- [3] **O. M. Bahrova** et al. “Nanomechanics driven by the superconducting proximity effect”. *New Journal of Physics* **24.3** (2022), p. 033008. DOI: <https://doi.org/10.1088/1367-2630/ac5758>.
- [4] **O.M. Bahrova** et al. “Cooling of nanomechanical vibrations by Andreev injection”. *Low Temp. Phys. [Fiz. Nizk. Temp. vol.48, No.6, pp. 535-541]* **48.6** (2022), pp. 476–482. DOI: 10.1063/10.0010443.
- [5] **O.M. Bahrova** and I. V. Krive. “How to control transport of spin-polarized electrons via magnetic field in a molecular transistor”. *Physics and Scientific&Technological progress: student scientific conference*. Kharkiv, 2018, p. 3.
- [6] **O. M. Bahrova**, S. I. Kulinich, and I. V. Krive. “Polaronic effects induced by coherent vibrons in a single-molecule transistor”. *I International Advanced Study Conference Condensed matter & Low Temperature Physics*. Ukraine, Kharkiv, p. 183.
- [7] A.D. Shkop and **O.M. Bahrova**. “Coulomb and vibration effects in spin-polarized current through a single-molecule transistor”. *XI Conference of Young Scientists “Problems of Theoretical Physics”*. Kyiv, Ukraine, pp. 15–16.
- [8] **O.M. Bahrova**, L.Y. Gorelik, and S.I. Kulinich. “Schrödinger-cat states generation via mechanical vibrations entangled with a charge qubit”. *II International Advanced Study Conference Condensed matter & Low Temperature Physics*. Kharkiv, Ukraine, p. 201.

- [9] **O.M. Bahrova** et al. “Self-sustained mechanical oscillations promoted by superconducting proximity effect”. *The International Symposium on Novel maTerials and quantum Technologies*, p. 134.
- [10] **O.M. Bahrova** et al. “Nanomechanics provoked by Andreev injection”. *29th International Conference on Low Temperature Physics*.
- [11] I. V. Krive et al. “Resonant tunneling of electrons in quantum wires (Review)”. *Low Temperature Physics* **36.2** (2010), pp. 119–141. DOI: <https://doi.org/10.1063/1.3319350>.
- [12] Hermann Grabert and Michel H. Devoret, eds. *Single Charge Tunneling. Coulomb Blockade Phenomena In Nanostructures*. Springer US, 1992, p. 335. DOI: <https://doi.org/10.1007/978-1-4757-2166-9>.
- [13] Supriyo Datta. *Electronic transport in mesoscopic systems*. Cambridge, UK New York: Cambridge University Press, 1997. ISBN: 9780521416047.
- [14] Yuli Nazarov and Yaroslav Blanter. *Quantum Transport*. Cambridge University Press, 2013. 590 pp. ISBN: 978-0-521-83246-5.
- [15] Dmitry Ryndyk. *Theory of Quantum Transport at Nanoscale*. Springer International Publishing, 2019. 260 pp. ISBN: 9783319795775.
- [16] R. Landauer. “Spatial Variation of Currents and Fields Due to Localized Scatterers in Metallic Conduction”. *IBM Journal of Research and Development* **1.3** (1957), pp. 223–231. DOI: 10.1147/rd.13.0223.
- [17] M. Büttiker. “Role of quantum coherence in series resistors”. *Physical Review B* **33.5** (1986), pp. 3020–3026. DOI: <https://doi.org/10.1103/PhysRevB.33.3020>.
- [18] Henk van Houten and Carlo Beenakker. “Quantum Point Contacts”. *Physics Today* **49.7** (1996), pp. 22–27. DOI: <https://doi.org/10.1063/1.881503>.
- [19] Москалец М. В. *Основы мезоскопической физики: Учебное пособие*. Харьков: НТУ «ХПИ», 2010, p. 180.
- [20] Hongkun Park et al. “Nanomechanical oscillations in a single- C_{60} transistor”. *Nature* **407.6800** (2000), pp. 57–60. DOI: 10.1038/35024031.

- [21] S. C. ten Kate et al. “Large even-odd spacing and g -factor anisotropy in PbTe quantum dots” (2022). DOI: 10.48550/arXiv.2205.06753.
- [22] Renaud Leturcq et al. “Franck–Condon blockade in suspended carbon nanotube quantum dots”. *Nature Physics* **5.5** (2009), pp. 327–331. DOI: <https://doi.org/10.1038/nphys1234>.
- [23] Dongsung T. Park et al. “Significant energy relaxation of quantum dot emitted hot electrons”. *Physical Review Research* **3.3** (2021), p. 033015. DOI: 10.1103/PhysRevResearch.3.033015.
- [24] Xinhe Wang et al. “Stressed carbon nanotube devices for high tunability, high quality factor, single mode GHz resonators”. *Nano Research* **11.11** (2018), pp. 5812–5822. DOI: <https://doi.org/10.1007/s12274-018-2085-x>.
- [25] F. R. Braakman et al. “Long-distance coherent coupling in a quantum dot array”. *Nature Nanotechnology* **8.6** (2013), pp. 432–437. DOI: <https://doi.org/10.1038/nnano.2013.67>.
- [26] Gianluca Rastelli and Michele Governale. “Single atom laser in normal-superconductor quantum dots”. *Physical Review B* **100.8** (2019), p. 085435. DOI: <https://doi.org/10.1103/PhysRevB.100.085435>.
- [27] Wen-Yao Wei et al. “Observation of Collective Coulomb Blockade in a Gate-controlled Linear Quantum-dot Array” (2016). DOI: <https://doi.org/10.48550/arXiv.1603.04625>.
- [28] Yuli V. Nazarov, ed. *Quantum Noise in Mesoscopic Physics*. Springer Netherlands, 2003, p. 524. DOI: <https://doi.org/10.1007/978-94-010-0089-5>.
- [29] G. Rastelli et al. “Interplay of magneto-elastic and polaronic effects in electronic transport through suspended carbon-nanotube quantum dots”. *Comptes Rendus Physique* **13.5** (2012), pp. 410–425. DOI: <https://doi.org/10.1016/j.crhy.2012.03.001>.
- [30] Yigal Meir and Ned S. Wingreen. “Landauer formula for the current through an interacting electron region”. *Physical Review Letters* **68.16** (1992), pp. 2512–2515. DOI: <https://doi.org/10.1103/PhysRevLett.68.2512>.

- [31] Antti-Pekka Jauho, Ned S. Wingreen, and Yigal Meir. “Time-dependent transport in interacting and noninteracting resonant-tunneling systems”. *Physical Review B* **50.8** (1994), pp. 5528–5544. DOI: <https://doi.org/10.1103/PhysRevB.50.5528>.
- [32] Ned S. Wingreen, Antti-Pekka Jauho, and Yigal Meir. “Time-dependent transport through a mesoscopic structure”. *Physical Review B* **48.11** (1993), pp. 8487–8490. DOI: <https://doi.org/10.1103/PhysRevB.48.8487>.
- [33] Ned S. Wingreen, Karsten W. Jacobsen, and John W. Wilkins. “Inelastic scattering in resonant tunneling”. *Physical Review B* **40.17** (1989), pp. 11834–11850. DOI: <https://doi.org/10.1103/PhysRevB.40.11834>.
- [34] L.I. Glazman and R.I. Shekhter. “Inelastic resonant tunneling of electrons through a potential barrier. Sov.Phys. JETP **67,163**”. *Sov. Phys. JETP* **67.1** (1988), p. 163.
- [35] S.M. Lindsay and M.A. Ratner. “Molecular Transport Junctions: Clearing Mists”. *Advanced Materials* **19.1** (2007), pp. 23–31. DOI: <https://doi.org/10.1002/adma.200601140>.
- [36] Michael Galperin, Mark A. Ratner, and Abraham Nitzan. “Molecular transport junctions: vibrational effects”. *Journal of Physics: Condensed Matter* **19.10** (2007), p. 103201. DOI: <https://doi.org/10.1088/0953-8984/19/10/103201>.
- [37] Yu. G. Naidyuk and I. K. Yanson. *Point-Contact Spectroscopy*. Springer New York, 2005. DOI: <https://doi.org/10.1007/978-1-4757-6205-1>.
- [38] Pawel Utko et al. “Nanoelectromechanical coupling in fullerene peapods probed by resonant electrical transport experiments”. *Nature Communications* **1.1** (2010). DOI: [10.1038/ncomms1034](https://doi.org/10.1038/ncomms1034).
- [39] Menno Poot and Herre S.J. van der Zant. “Mechanical systems in the quantum regime”. *Physics Reports* **511.5** (2012), pp. 273–335. DOI: <https://doi.org/10.1016/j.physrep.2011.12.004>.
- [40] B. Babić et al. “Intrinsic Thermal Vibrations of Suspended Doubly Clamped Single-Wall Carbon Nanotubes”. *Nano Letters* **3.11** (2003), pp. 1577–1580. DOI: <https://doi.org/10.1021/nl0344716>.

- [41] Jens Koch and Felix von Oppen. “Franck-Condon Blockade and Giant Fano Factors in Transport through Single Molecules”. *Physical Review Letters* **94.20** (2005), p. 206804. DOI: <https://doi.org/10.1103/PhysRevLett.94.206804>.
- [42] L. G. Lang and Y. A. Firsov. “Kinetic Theory of Semiconductors with Low Mobility”. *Sov. Phys. JETP* **16** (1963), p. 1301.
- [43] A.D. Shkop **O. M. Bahrova**, S. I. Kulinich, and I. V. Krive. “Interplay of Vibration and Coulomb Effects in Transport of Spin-Polarized Electrons in a Single-Molecule Transistor”. *Superlattices and Microstructures* **137** (2021), p. 106353. DOI: 10.1016/j.spmi.2019.106356. arXiv: 2103.12001 [cond-mat.mes-hall].
- [44] D. Fedorets. “Quantum description of shuttle instability in a nanoelectromechanical single-electron transistor”. *Physical Review B* **68.3** (2003), p. 033106. DOI: 10.1103/PhysRevB.68.033106.
- [45] Tomáš Novotný, Andrea Donarini, and Antti-Pekka Jauho. “Quantum Shuttle in Phase Space”. *Physical Review Letters* **90.25** (2003), p. 256801. DOI: <https://doi.org/10.1103/PhysRevLett.90.256801>.
- [46] Urban Lundin and Ross H. McKenzie. “Temperature dependence of polaronic transport through single molecules and quantum dots”. *Physical Review B* **66.7** (2002), p. 075303. DOI: <https://doi.org/10.1103/PhysRevB.66.075303>.
- [47] Gerald D. Mahan. *Many-Particle Physics*. Springer US, 2013. 785 pp. ISBN: 978-1-4757-5714-9. DOI: <https://doi.org/10.1007/978-1-4757-5714-9>.
- [48] G. A. Skorobogatko et al. “Magnetopolaronic effects in electron transport through a single-level vibrating quantum dot”. *Low Temperature Physics* **37.12** (2011), pp. 1032–1037. DOI: <https://doi.org/10.1063/1.3674185>.
- [49] I. M. Ryzhik I. S. Gradshteyn. *Table of Integrals, Series, and Products*. Boston: Elsevier Science & Techn., 2014. 1206 pp. ISBN: 9781483265643.
- [50] Felix von Oppen and Jens Koch. “Novel Quantum Transport Effects in Single-Molecule Transistors”. *Advances in Solid State Physics*. Springer Berlin Heidelberg, 2008, pp. 99–109. DOI: https://doi.org/10.1007/978-3-540-38235-5_8.

- [51] A. N. Pasupathy et al. “Vibration-Assisted Electron Tunneling in C_{140} Transistors”. *Nano Letters* **5.2** (2005), pp. 203–207. DOI: 10.1021/nl048619c.
- [52] Yu D. Zubov et al. “Transport properties and enhanced figure of merit of quantum dot-based spintronic thermoelectric device”. *Journal of Physics Condensed Matter* **30.31**, 315303 (2018), p. 315303. DOI: 10.1088/1361-648X/aacc07.
- [53] A. D. Shkop and **O. M. Bahrova**. “Effects of magnetopolaronic blockade in transport of spin-polarized electrons”. *IX International Conference on Low Temperature Physics*. Kharkiv, Ukraine.
- [54] A. D. Shkop and **O. M. Bahrova**. “Effects of the Franck-Condon blockade in tunneling of spin-polarized electrons in a molecular transistor”. *Journal of V.N. Karazin Kharkiv National University, series "Physics"* **27** (2018), p. 53.
- [55] A.D. Shkop, **O.M. Bahrova**, and I.V. Krive. “Effects of Coulomb interaction and Franck-Condon blockade in tunneling of spin-polarized electrons in a molecular transistor”. *X International Conference on Low Temperature Physics*. Kharkiv, Ukraine, p. 155.
- [56] A. D. Shkop. “Thermoelectric Effects in Tunneling of Spin-Polarized Electrons in a Molecular Transistor”. *Journal of Low Temperature Physics* **208.3-4** (2022), pp. 248–270. DOI: 10.1007/s10909-022-02758-0.
- [57] Jonas N. Pedersen, Jesper Q. Thomassen, and Karsten Flensberg. “Non-collinear magnetoconductance of a quantum dot”. *Physical Review B* **72.4** (2005), p. 045341. DOI: <https://doi.org/10.1103/PhysRevB.72.045341>.
- [58] D. M. Kennes, D. Schuricht, and V. Meden. “Efficiency and power of a thermoelectric quantum dot device”. *EPL (Europhysics Letters)* **102.5** (2013), p. 57003. DOI: <https://doi.org/10.1209/0295-5075/102/57003>.
- [59] Jaeuk U. Kim, Ilya V. Krive, and Jari M. Kinaret. “Nonequilibrium Plasmons in a Quantum Wire Single-Electron Transistor”. *Physical Review Letters* **90.17** (2003), p. 176401. DOI: <https://doi.org/10.1103/PhysRevLett.90.176401>.

- [60] A. Mitra, I. Aleiner, and A. J. Millis. “Phonon effects in molecular transistors: Quantal and classical treatment”. *Physical Review B* **69**.24 (2004), p. 245302. DOI: <https://doi.org/10.1103/PhysRevB.69.245302>.
- [61] Weici Liu et al. “Full Counting Statistics of Electrons through Interaction of the Single Quantum Dot System with the Optical Field”. *Nanomaterials* **9**.3 (2019), p. 394. DOI: <https://doi.org/10.3390/nano9030394>.
- [62] Weici Liu et al. “Negative Differential Conductance Assisted by Optical Fields in a Single Quantum Dot with Ferromagnetic Electrodes”. *Nanomaterials* **9**.6 (2019), p. 863. DOI: <https://doi.org/10.3390/nano9060863>.
- [63] D. Boese and H. Schoeller. “Influence of nanomechanical properties on single-electron tunneling: A vibrating single-electron transistor”. *Europh. Lett.* **54**.5 (2001), pp. 668–674. DOI: <https://doi.org/10.1209/epl/i2001-00367-8>.
- [64] Kevin D. McCarthy, Nikolay Prokof’ev, and Mark T. Tuominen. “Incoherent dynamics of vibrating single-molecule transistors”. *Physical Review B* **67**.24 (2003), p. 245415. DOI: <https://doi.org/10.1103/PhysRevB.67.245415>.
- [65] Yiwen Chu et al. “Creation and control of multi-phonon Fock states in a bulk acoustic-wave resonator”. *Nature* **563**.7733 (2018), pp. 666–670. DOI: <https://doi.org/10.1038/s41586-018-0717-7>.
- [66] Г. Бейтмен and А. Эрдейи. *Высшие трансцендентные функции*. Vol. 2. Москва: Наука, 1966, p. 297.
- [67] Jean-Pierre Gazeau. *Coherent States in Quantum Physics*. Wiley, 2009. DOI: [10.1002/9783527628285](https://doi.org/10.1002/9783527628285).
- [68] A.I. Baz, Y.B. Zeldovich, and A.M. Perelomov. *Scattering Reactions and Decays in Non-Relativistic Quantum Mechanics*. Jerusalem: Israel Programm for Scientific Transaction, 1969.
- [69] A. Zazunov, D. Feinberg, and T. Martin. “Phonon Squeezing in a Superconducting Molecular Transistor”. *Physical Review Letters* **97**.19 (2006), p. 196801. DOI: <https://doi.org/10.1103/PhysRevLett.97.196801>.
- [70] S. M. Girvin. “Schrodinger Cat States in Circuit QED”. *arXiv:1710.03179 [quant-ph]* (2017). DOI: <https://doi.org/10.48550/arXiv.1710.03179>.

- [71] K. L. Ekinci and M. L. Roukes. “Nanoelectromechanical systems”. *Review of Scientific Instruments* **76.6** (2005), p. 061101. DOI: <https://doi.org/10.1063/1.1927327>.
- [72] Y. Nakamura, Yu. A. Pashkin, and J. S. Tsai. “Coherent control of macroscopic quantum states in a single-Cooper-pair box”. *Nature* **398.6730** (1999), pp. 786–788. DOI: <https://doi.org/10.1038/19718>.
- [73] G. Wendin and V. S. Shumeiko. “Quantum bits with Josephson junctions (Review Article)”. *Low Temperature Physics* **33.9** (2007), pp. 724–744. DOI: <https://doi.org/10.1063/1.2780165>.
- [74] Yu. A. Pashkin et al. “Josephson charge qubits: a brief review”. *Quantum Information Processing* **8.2-3** (2009), pp. 55–80. DOI: [10.1007/s11128-009-0101-5](https://doi.org/10.1007/s11128-009-0101-5).
- [75] Antti Ranni et al. “Real-time observation of Cooper pair splitting showing strong non-local correlations”. *Nature Communications* **12.1** (2021). DOI: <https://doi.org/10.1038/s41467-021-26627-8>.
- [76] Bas Hensen et al. “A silicon quantum-dot-coupled nuclear spin qubit”. *Nature Nanotechnology* **15.1** (2019), pp. 13–17. DOI: <https://doi.org/10.1038/s41565-019-0587-7>.
- [77] E. Dupont-Ferrier et al. “Coherent Coupling of Two Dopants in a Silicon Nanowire Probed by Landau-Zener-Stückelberg Interferometry”. *Physical Review Letters* **110.13** (2013), p. 136802. DOI: <https://doi.org/10.1103/PhysRevLett.110.136802>.
- [78] Oleh V. Ivakhnenko, Sergey N. Shevchenko, and Franco Nori. “Nonadiabatic Landau–Zener–Stückelberg–Majorana transitions, dynamics, and interference”. *Physics Reports* **995** (Jan. 2023), pp. 1–89. DOI: [10.1016/j.physrep.2022.10.002](https://doi.org/10.1016/j.physrep.2022.10.002).
- [79] Yan Xue et al. “Split-ring polariton condensates as macroscopic two-level quantum systems”. *Physical Review Research* **3.1** (2021), p. 013099. DOI: [10.1103/PhysRevResearch.3.013099](https://doi.org/10.1103/PhysRevResearch.3.013099).
- [80] Sanjib Ghosh and Timothy C. H. Liew. “Quantum computing with exciton-polariton condensates”. *npj Quantum Information* **6.1** (2020). DOI: <https://doi.org/10.1038/s41534-020-0244-x>.

- [81] S.N. Shevchenko, S. Ashhab, and Franco Nori. “Landau–Zener–Stückelberg interferometry”. *Physics Reports* **492.1** (2010), pp. 1–30. DOI: <https://doi.org/10.1016/j.physrep.2010.03.002>.
- [82] Sergey N. Shevchenko. *Mesoscopic Physics meets Quantum Engineering*. WSPC, 2019. 176 pp. ISBN: 978-981-12-0139-4. DOI: <https://doi.org/10.1142/11310>.
- [83] Sahel Ashhab, Olga A. Ilinskaya, and Sergey N. Shevchenko. “Nonlinear Landau-Zener-Stückelberg-Majorana problem. in preparation”. *Physical Review A* **106.6** (Dec. 2022), p. 062613. DOI: [10.1103/physreva.106.062613](https://doi.org/10.1103/physreva.106.062613).
- [84] A. V. Parafilo and M. N. Kiselev. “Landau–Zener transitions and Rabi oscillations in a Cooper-pair box: beyond two-level models”. *Low Temperature Physics* **44.12** (2018), pp. 1325–1330. DOI: <https://doi.org/10.1063/1.5078628>.
- [85] S. Schmid, L. Guillermo Villanueva, and M. L. RoukesLee. *Fundamentals of Nanomechanical Resonators*. Springer International Publishing, 2016. 184 pp. ISBN: 9783319286891.
- [86] K. J. Satzinger et al. “Quantum control of surface acoustic-wave phonons”. *Nature* **563.7733** (2018), pp. 661–665. DOI: <https://doi.org/10.1038/s41586-018-0719-5>.
- [87] A. Bienfait et al. “Phonon-mediated quantum state transfer and remote qubit entanglement”. *Science* **364.6438** (2019), pp. 368–371. DOI: [10.1126/science.aaw8415](https://doi.org/10.1126/science.aaw8415).
- [88] Yiwen Chu et al. “Quantum acoustics with superconducting qubits”. *Science* **358.6360** (2017), pp. 199–202. DOI: [10.1126/science.aao1511](https://doi.org/10.1126/science.aao1511).
- [89] M.-H. Chou et al. “Measurements of a quantum bulk acoustic resonator using a superconducting qubit”. *Applied Physics Letters* **117.25** (2020), p. 254001. DOI: <https://doi.org/10.1063/5.0023827>.
- [90] M. D. LaHaye et al. “Nanomechanical measurements of a superconducting qubit”. *Nature* **459.7249** (2009), pp. 960–964. DOI: <https://doi.org/10.1038/nature08093>.

- [91] L. Tian. “Entanglement from a nanomechanical resonator weakly coupled to a single Cooper-pair box”. *Physical Review B* **72.19** (2005), p. 195411. DOI: <https://doi.org/10.1103/PhysRevB.72.195411>.
- [92] L. Y. Gorelik et al. “Coherent transfer of Cooper pairs by a movable grain”. *Nature* **411.6836** (2001), pp. 454–457. DOI: <https://doi.org/10.1038/35078027>.
- [93] A. Isacsson et al. “Mechanical Cooper Pair Transportation as a Source of Long-Distance Superconducting Phase Coherence”. *Physical Review Letters* **89.27** (2002), p. 277002. DOI: <https://doi.org/10.1103/PhysRevLett.89.277002>.
- [94] Connor T. Hann et al. “Hardware-Efficient Quantum Random Access Memory with Hybrid Quantum Acoustic Systems”. *Physical Review Letters* **123.25** (2019), p. 250501. DOI: <https://doi.org/10.1103/PhysRevLett.123.250501>.
- [95] Joschka Roffe. “Quantum error correction: an introductory guide”. *Contemporary Physics* **60.3** (2019), pp. 226–245. DOI: <https://doi.org/10.1080/00107514.2019.1667078>.
- [96] M. H. Devoret and R. J. Schoelkopf. “Superconducting Circuits for Quantum Information: An Outlook”. *Science* **339.6124** (2013), pp. 1169–1174. DOI: [10.1126/science.1231930](https://doi.org/10.1126/science.1231930).
- [97] Weizhou Cai et al. “Bosonic quantum error correction codes in superconducting quantum circuits”. *Fundamental Research* **1.1** (2021), pp. 50–67. DOI: <https://doi.org/10.1016/j.fmre.2020.12.006>.
- [98] Daniel Gottesman, Alexei Kitaev, and John Preskill. “Encoding a qubit in an oscillator”. *Phys. Rev. A* **64.1** (2001), p. 012310. DOI: [10.1103/PhysRevA.64.012310](https://doi.org/10.1103/PhysRevA.64.012310).
- [99] Marios H. Michael et al. “New Class of Quantum Error-Correcting Codes for a Bosonic Mode”. *Physical Review X* **6.3** (2016), p. 031006. DOI: <https://doi.org/10.1103/PhysRevX.6.031006>.
- [100] L. Hu et al. “Quantum error correction and universal gate set operation on a binomial bosonic logical qubit”. *Nature Physics* **15.5** (Feb. 2019), pp. 503–508. DOI: <https://doi.org/10.1038/s41567-018-0414-3>.

- [101] L. Y. Gorelik et al. “Shuttle Mechanism for Charge Transfer in Coulomb Blockade Nanostructures”. *Physical Review Letters* **80**.20 (1998), pp. 4526–4529. DOI: <https://doi.org/10.1103/PhysRevLett.80.4526>.
- [102] Gleb A. Skorobagatko, Ilya V. Krive, and Robert I. Shekhter. “Polaronic effects in electron shuttling”. *Low Temperature Physics* **35**.12 (2009), pp. 949–956. DOI: <https://doi.org/10.1063/1.3276063>.
- [103] A. V. Parafilo et al. “Nanoelectromechanics of superconducting weak links (Review Article)”. *Low Temp. Phys.* **38** (2012), pp. 273–282. DOI: [10.1063/1.3699628](https://doi.org/10.1063/1.3699628).
- [104] R. I. Shekhter et al. “Electronic spin working mechanically (Review Article)”. *Low Temperature Physics* **40**.7 (2014), pp. 600–614. DOI: <https://doi.org/10.1063/1.4887060>.
- [105] R. I. Shekhter et al. “Shuttling of electrons and Cooper pairs”. *Journal of Physics: Condensed Matter* **15**.12 (2003), R441–R469. DOI: <https://doi.org/10.1088/0953-8984/15/12/201>.
- [106] R. I. Shekhter et al. “Nanomechanical Shuttle Transfer of Electrons”. *Journal of Computational and Theoretical Nanoscience* **4**.5 (2007), pp. 860–895. DOI: <https://doi.org/10.1166/jctn.2007.2378>.
- [107] Robert I. Shekhter et al. “Nonequilibrium and quantum coherent phenomena in the electromechanics of suspended nanowires (Review Article)”. *Low Temperature Physics* **35**.8 (2009), pp. 662–678. DOI: <https://doi.org/10.1063/1.3224725>.
- [108] D. Fedorets et al. “Vibrational instability due to coherent tunneling of electrons”. *Europhysics Letters (EPL)* **58**.1 (2002), pp. 99–104. DOI: <https://doi.org/10.1209/epl/i2002-00611-3>.
- [109] D. Fedorets et al. “Quantum Shuttle Phenomena in a Nanoelectromechanical Single-Electron Transistor”. *Physical Review Letters* **92**.16 (2004), p. 166801. DOI: [10.1103/PhysRevLett.92.166801](https://doi.org/10.1103/PhysRevLett.92.166801).
- [110] O. A. Ilinskaya. “On a new mechanism of friction in nanoelectromechanical systems”. *Low Temperature Physics* **44**.8 (2018), pp. 816–818. DOI: [10.1063/1.5049164](https://doi.org/10.1063/1.5049164).

- [111] A. V. Parafilo et al. “Spin-mediated photomechanical coupling of a nanoelectromechanical shuttle”. *Phys. Rev. Lett.* **117** (2016), p. 057202. DOI: 10.1103/PhysRevLett.117.057202. arXiv: 1602.03766 [cond-mat.mes-hall].
- [112] J. Atalaya and L. Y. Gorelik. “Spintronics-based mesoscopic heat engine”. *Physical Review B* **85.24** (2012), p. 245309. DOI: 10.1103/PhysRevB.85.245309.
- [113] S.I. Kulinich et al. “Single-Electron Shuttle Based on Electron Spin”. *Physical Review Letters* **112.11** (2014), p. 117206. DOI: <https://doi.org/10.1103/PhysRevLett.112.117206>.
- [114] O. A. Ilinskaya et al. “Shuttling of Spin Polarized Electrons in Molecular Transistors”. *Synthetic Metals* **216** (2015), pp. 83–87. DOI: <https://doi.org/10.1016/j.synthmet.2015.11.001>. arXiv: 1507.05813 [cond-mat.mes-hall].
- [115] O. A. Ilinskaya et al. “Magnetically controlled single-electron shuttle”. *Low Temperature Physics* **41.1** (2015), pp. 70–74. DOI: 10.1063/1.4904445.
- [116] O. A. Ilinskaya, R. I. Shekhter, and M. Jonson. “Polaronic suppression of shuttle vibrations”. *Low Temperature Physics* **49.1** (Jan. 2023), pp. 71–75. DOI: <https://doi.org/10.1063/10.0016477>.
- [117] O. A. Ilinskaya et al. “Spin-polaronic effects in electric shuttling in a single molecule transistor with magnetic leads”. *Physica E Low-Dimensional Systems and Nanostructures* **122**, 114151 (2020), p. 114151. DOI: 10.1016/j.physe.2020.114151. arXiv: 2003.01066 [cond-mat.mes-hall].
- [118] O. A. Ilinskaya et al. “Coulomb effects on thermally induced shuttling of spin-polarized electrons”. *Low Temperature Physics* **45.9** (2019), pp. 1032–1040. DOI: 10.1063/1.5121274.
- [119] O. A. Ilinskaya et al. “Coulomb-promoted spintromechanics in magnetic shuttle devices”. *Phys. Rev. B* **100.4**, 045408 (2019), p. 045408. DOI: 10.1103/PhysRevB.100.045408. arXiv: 1902.09067 [cond-mat.mes-hall].

- [120] O. A. Ilinskaya et al. “Mechanically Induced Thermal Breakdown in Magnetic Shuttle Structures”. *New Journal of Physics* **20.6** (2018), p. 063036. DOI: <https://doi.org/10.1088/1367-2630/aac750>. arXiv: 1806.00633 [`cond-mat.mes-hall`].
- [121] P. Vincent et al. “Driving self-sustained vibrations of nanowires with a constant electron beam”. *Physical Review B* **76.8** (2007), p. 085435. DOI: <https://doi.org/10.1103/PhysRevB.76.085435>.
- [122] Dominik V. Scheible and Robert H. Blick. “Silicon nanopillars for mechanical single-electron transport”. *Applied Physics Letters* **84.23** (2004), pp. 4632–4634. DOI: 10.1063/1.1759371.
- [123] Chulki Kim, Jonghoo Park, and Robert H. Blick. “Spontaneous Symmetry Breaking in Two Coupled Nanomechanical Electron Shuttles”. *Physical Review Letters* **105.6** (2010), p. 067204. DOI: <https://doi.org/10.1103/PhysRevLett.105.067204>.
- [124] Chulki Kim, Marta Prada, and Robert H. Blick. “Coulomb Blockade in a Coupled Nanomechanical Electron Shuttle”. *ACS Nano* **6.1** (2012), pp. 651–655. DOI: <https://doi.org/10.1021/nn204103m>.
- [125] Mo Zhao and Robert H. Blick. “Stochastic model of nanomechanical electron shuttles and symmetry breaking”. *Physical Review E* **93.6** (2016), p. 063306. DOI: 10.1103/PhysRevE.93.063306.
- [126] K. W. Chan et al. “Single-electron shuttle based on a silicon quantum dot”. *Applied Physics Letters* **98.21** (2011), p. 212103. DOI: <https://doi.org/10.1063/1.3593491>.
- [127] Andriy V. Moskalenko et al. “Nanomechanical electron shuttle consisting of a gold nanoparticle embedded within the gap between two gold electrodes”. *Physical Review B* **79.24** (2009), p. 241403. DOI: <https://doi.org/10.1103/PhysRevB.79.241403>.
- [128] G. A. Steele et al. “Strong Coupling Between Single-Electron Tunneling and Nanomechanical Motion”. *Science* **325.5944** (2009), pp. 1103–1107. DOI: DOI:10.1126/science.1176076.

- [129] S. Etaki et al. “Self-sustained oscillations of a torsional SQUID resonator induced by Lorentz-force back-action”. *Nature Communications* **4.1** (2013). DOI: 10.1038/ncomms2827.
- [130] Takafumi Fujita et al. “Coherent shuttle of electron-spin states”. *npj Quantum Information* **3.1** (2017). DOI: 10.1038/s41534-017-0024-4.
- [131] K. Jensen, Kwanpyo Kim, and A. Zettl. “An atomic-resolution nanomechanical mass sensor”. *Nature Nanotechnology* **3.9** (2008), pp. 533–537. DOI: <https://doi.org/10.1038/nnano.2008.200>.
- [132] F R Braakman and M Poggio. “Force sensing with nanowire cantilevers”. *Nanotechnology* **30.33** (2019), p. 332001. DOI: <https://doi.org/10.1088/1361-6528/ab19cf>.
- [133] C. Urgell et al. “Cooling and self-oscillation in a nanotube electromechanical resonator”. *Nature Physics* **16.1** (2019), pp. 32–37. DOI: <https://doi.org/10.1038/s41567-019-0682-6>.
- [134] D. R. Schmid et al. “Magnetic damping of a carbon nanotube nano-electromechanical resonator”. *New Journal of Physics* **14.8** (2012), p. 083024. DOI: <https://doi.org/10.1088/1367-2630/14/8/083024>.
- [135] D. R. Schmid et al. “Liquid-induced damping of mechanical feedback effects in single electron tunneling through a suspended carbon nanotube”. *Applied Physics Letters* **107.12** (2015), p. 123110. DOI: <https://doi.org/10.1063/1.4931775>.
- [136] Jeffrey A. Weldon et al. “Sustained Mechanical Self-Oscillations in Carbon Nanotubes”. *Nano Letters* **10.5** (2010), pp. 1728–1733. DOI: <https://doi.org/10.1021/nl100148q>.
- [137] Kyle Willick and Jonathan Baugh. “Self-driven oscillation in Coulomb blockaded suspended carbon nanotubes”. *Phys. Rev. Research* **2** (3 2020), p. 033040. DOI: 10.1103/PhysRevResearch.2.033040.
- [138] V. Meden. “The Anderson–Josephson quantum dot—a theory perspective”. *Journal of Physics: Condensed Matter* **31.16** (2019), p. 163001. DOI: <https://doi.org/10.1088/1361-648X/aafd6a>.
- [139] A. V. Parafilo et al. “Manifestation of polaronic effects in Josephson currents”. *Low Temp. Phys.* **39** (2013), pp. 685–694. DOI: 10.1063/1.4818791.

- [140] I. V. Krive et al. “The influence of electro-mechanical effects on resonant electron tunneling through small carbon nanopeapods”. *New Journal of Physics* **10.4** (2008), p. 043043. DOI: <https://doi.org/10.1088/1367-2630/10/4/043043>.
- [141] A. V. Parafilo et al. “Polaronic effects and thermally enhanced weak superconductivity”. *Physical Review B* **89.11** (2014), p. 115138. DOI: [10.1103/PhysRevB.89.115138](https://doi.org/10.1103/PhysRevB.89.115138).
- [142] R. I. Shekhter et al. “Nanoelectromechanics of shuttle devices”. *Nanoelectromechanics* **1** (2013), pp. 1–25. DOI: <https://doi.org/10.48550/arXiv.1303.0740>.
- [143] Tomáš Novotný, Alessandra Rossini, and Karsten Flensberg. “Josephson current through a molecular transistor in a dissipative environment”. *Physical Review B* **72.22** (2005), p. 224502. DOI: <https://doi.org/10.1103/PhysRevB.72.224502>.
- [144] Jonas Sköldbberg et al. “Spectrum of Andreev Bound States in a Molecule Embedded Inside a Microwave-Excited Superconducting Junction”. *Physical Review Letters* **101.8** (2008), p. 087002. DOI: <https://doi.org/10.1103/PhysRevLett.101.087002>.
- [145] A. V. Parafilo et al. “Nano-mechanics driven by Andreev tunneling”. *Physical Review B* **102.23** (2020), p. 235402. DOI: <https://doi.org/10.1103/PhysRevB.102.235402>. arXiv: 2009.02679 [[cond-mat.mes-hall](https://arxiv.org/abs/2009.02679)].
- [146] J Barański and T Domański. “Enhancements of the Andreev conductance due to emission/absorption of bosonic quanta”. *Journal of Physics: Condensed Matter* **27.30** (2015), p. 305302. DOI: <https://doi.org/10.1088/0953-8984/27/30/305302>.
- [147] B. Baran and T. Domański. “Quasiparticles of a periodically driven quantum dot coupled between superconducting and normal leads”. *Physical Review B* **100.8** (2019), p. 085414. DOI: <https://doi.org/10.1103/PhysRevB.100.085414>.

- [148] Ali G. Moghaddam, Michele Governale, and Jürgen König. “Driven superconducting proximity effect in interacting quantum dots”. *Physical Review B* **85.9** (2012), p. 094518. DOI: <https://doi.org/10.1103/PhysRevB.85.094518>.
- [149] A.F. Andreev. “The Thermal Conductivity of the Intermediate State in Superconductors”. *Sov. Phys. JETP* **19.5** (1964), p. 1228.
- [150] I. O. Kulik. “Macroscopic Quantization and the proximity effect in S-N-S junctions”. *Sov. Phys. JETP* **30.5** (1970), p. 944.
- [151] P. Stadler, W. Belzig, and G. Rastelli. “Ground-State Cooling of a Mechanical Oscillator by Interference in Andreev Reflection”. *Physical Review Letters* **117.19** (2016), p. 197202. DOI: [10.1103/PhysRevLett.117.197202](https://doi.org/10.1103/PhysRevLett.117.197202).
- [152] P. Stadler, W. Belzig, and G. Rastelli. “Charge-vibration interaction effects in normal-superconductor quantum dots”. *Physical Review B* **96.4** (2017), p. 045429. DOI: [10.1103/PhysRevB.96.045429](https://doi.org/10.1103/PhysRevB.96.045429).
- [153] J. Gramich, A. Baumgartner, and C. Schönenberger. “Resonant and Inelastic Andreev Tunneling Observed on a Carbon Nanotube Quantum Dot”. *Physical Review Letters* **115.21** (2015), p. 216801. DOI: [10.1103/PhysRevLett.115.216801](https://doi.org/10.1103/PhysRevLett.115.216801).
- [154] Anton V. Parafilo et al. “Pumping and Cooling of Nanomechanical Vibrations Generated by Cooper-Pair Exchange. to be published”. *Journal of Low Temperature Physics* **210.1-2** (Nov. 2022), pp. 150–165. DOI: [10.1007/s10909-022-02905-7](https://doi.org/10.1007/s10909-022-02905-7). arXiv: 2202.07924 [cond-mat.mes-hall].
- [155] В. Б. Берестецкий, Е. М. Лифшиц, and Л.П. Питаевский. *Релятивистская квантовая теория*. Vol. 1. 2 vols. Наука, 1968, p. 480.
- [156] О. М. Єрмолаєв and Г. І. Рашба. *Вступ до статистичної фізики і термодинаміки*. ХНУ, 2004, p. 516. ISBN: 966–623–283–9.
- [157] Alexey Bezryadin and Paul M. Goldbart. “Superconducting Nanowires Fabricated Using Molecular Templates”. *Advanced Materials* **22.10** (2010), pp. 1111–1121. DOI: <https://doi.org/10.1002/adma.200904353>.
- [158] Kohei Masuda et al. “Thermal and quantum phase slips in niobium-nitride nanowires based on suspended carbon nanotubes”. *Applied Physics Letters* **108.22** (2016), p. 222601. DOI: <https://doi.org/10.1063/1.4952721>.

- [159] Patricio Arrangoiz-Arriola et al. “Resolving the energy levels of a nanomechanical oscillator”. *Nature* **571**.7766 (2019), pp. 537–540. DOI: <https://doi.org/10.1038/s41586-019-1386-x>.
- [160] Danko Radić. *Nanomechanical cat-states generated by dc-voltage driven Cooper pair box qubit*. (video conference).
- [161] A. F. Morpurgo et al. “Gate-Controlled Superconducting Proximity Effect in Carbon Nanotubes”. *Science* **286**.5438 (1999), pp. 263–265.
- [162] A. V. Rozhkov and Daniel P. Arovas. “Interacting-impurity Josephson junction: Variational wave functions and slave-boson mean-field theory”. *Phys. Rev. B* **62** (10 Sept. 2000), pp. 6687–6691. DOI: [10.1103/PhysRevB.62.6687](https://doi.org/10.1103/PhysRevB.62.6687).
- [163] Henrik Bruus and Karsten Flensberg. *Many-Body Quantum Theory in Condensed Matter Physics: An Introduction*. OXFORD UNIV PR, 2004. 466 pp. ISBN: 0198566336.
- [164] J. Moser et al. “Nanotube mechanical resonators with quality factors of up to 5 million”. *Nature Nanotechnology* **9**.12 (2014), pp. 1007–1011. DOI: [10.1038/nnano.2014.234](https://doi.org/10.1038/nnano.2014.234).
- [165] J. C. Cuevas, A. Martín-Rodero, and A. Levy Yeyati. “Hamiltonian approach to the transport properties of superconducting quantum point contacts”. *Physical Review B* **54**.10 (1996), pp. 7366–7379. DOI: [10.1103/PhysRevB.54.7366](https://doi.org/10.1103/PhysRevB.54.7366).
- [166] Qing-feng Sun et al. “Electron transport through a mesoscopic hybrid multiterminal resonant-tunneling system”. *Physical Review B* **61**.7 (2000), pp. 4754–4761. DOI: <https://doi.org/10.1103/PhysRevB.61.4754>.
- [167] Bogoliubov N. N. and Mitropolsky Y. A. *Asymptotic methods in the theory of non-linear oscillations*. London: Gordon and Breach, 1985.
- [168] A. M. Kosevich and A. C. Kovalev. *Vvedenie v nelineinuyu fizicheskuyu mehaniku (Vvedenie v nelineinuyu fizicheskuyu mehaniku)*. Kyiv: Nauk. dumka, 1989, p. 303. ISBN: 5-12-000865-8.
- [169] A. Isacsson et al. “Shuttle instability in self-assembled Coulomb blockade nanostructures”. *Physica B: Condensed Matter* **255**.1-4 (1998), pp. 150–163. DOI: [https://doi.org/10.1016/S0921-4526\(98\)00463-3](https://doi.org/10.1016/S0921-4526(98)00463-3).

- [170] Heinz-Peter Breuer and Francesco Petruccione. *The Theory of Open Quantum Systems*. Oxford University Press, 2007. ISBN: 9780199213900.
- [171] Edward A. Laird et al. “A High Quality Factor Carbon Nanotube Mechanical Resonator at 39 GHz”. *Nano Letters* **12.1** (2011), pp. 193–197. DOI: 10.1021/nl203279v.
- [172] **O.M. Bahrova** et al. “Ground-state cooling of mechanical vibrations in a hybrid nano-electromechanical device”. *Quantum Thermodynamics Conference 2022*.
- [173] A. Baas et al. “Optical bistability in semiconductor microcavities”. *Physical Review A* **69.2** (2004), p. 023809. DOI: 10.1103/PhysRevA.69.023809.
- [174] M. Amthor et al. “Optical bistability in electrically driven polariton condensates”. *Physical Review B* **91.8** (Feb. 2015), p. 081404. DOI: 10.1103/PhysRevB.91.081404.
- [175] R. Avriller, B. Murr, and F. Pistolesi. “Bistability and displacement fluctuations in a quantum nanomechanical oscillator”. *Physical Review B* **97.15** (2018), p. 155414. DOI: 10.1103/PhysRevB.97.155414.
- [176] W. Belzig and P. Samuelsson. “Full counting statistics of incoherent Andreev transport”. *Europhys. Lett.* **64, 253** (2003) (2003). DOI: 10.1209/epl/i2003-00314-9. arXiv: cond-mat/0305249 [cond-mat.supr-con].
- [177] Marius Grundmann Bimberg and Nikolai N. Ledentsov. *Quantum Dot Heterostructures*. John Wiley & Sons, 1999. 340 pp. ISBN: 0-471-97388-2.
- [178] Alexandre Blais, Steven M. Girvin, and William D. Oliver. “Quantum information processing and quantum optics with circuit quantum electrodynamics”. *Nature Physics* **16.3** (2020), pp. 247–256. DOI: <https://doi.org/10.1038/s41567-020-0806-z>.
- [179] Alan M. Cassell et al. “Directed Growth of Free-Standing Single-Walled Carbon Nanotubes”. *Journal of the American Chemical Society* **121.34** (1999), pp. 7975–7976. DOI: <https://doi.org/10.1021/ja992083t>.
- [180] Andrew N. Cleland. *Foundations of Nanomechanics*. Springer Berlin Heidelberg, 2003. DOI: <https://doi.org/10.1007/978-3-662-05287-7>.

- [181] A. Cottet and W. Belzig. “Dynamical Spin-Blockade in a quantum dot with paramagnetic leads”. *Europhys. Lett.* **66** (2004), p. 405. DOI: 10.1209/epl/i2004-10009-9. arXiv: cond-mat/0401456 [`cond-mat.mes-hall`].
- [182] John H. Davies. *The Physics of Low-dimensional Semiconductors*. Cambridge University Press, 1997. DOI: <https://doi.org/10.1017/CBO9780511819070>.
- [183] Guang-Wei Deng et al. “Strongly Coupled Nanotube Electromechanical Resonators”. *Nano Letters* **16.9** (2016), pp. 5456–5462. DOI: <https://doi.org/10.1021/acs.nanolett.6b01875>.
- [184] L. Y. Gorelik et al. “Spin-controlled nanoelectromechanics in magnetic NEM-SET systems”. *New Journal of Physics* **7** (2005), pp. 242–242. DOI: <https://doi.org/10.1088/1367-2630/7/1/242>.
- [185] Markus Grassl and Martin Rötteler. “Quantum Error Correction and Fault Tolerant Quantum Computing”. *Encyclopedia of Complexity and Systems Science*. Ed. by Robert A. Meyers. Springer New York, 2009, pp. 7324–7342. DOI: 10.1007/978-0-387-30440-3_435.
- [186] Hui Gu et al. “Biomarkers-based Biosensing and Bioimaging with Graphene for Cancer Diagnosis”. *Nanomaterials* **9.1** (2019), p. 130. DOI: <https://doi.org/10.3390/nano9010130>.
- [187] P. Harrison. *Quantum Wells, Wires and Dots*. 2nd ed. Chichester: John Wiley&Sons, 2005. ISBN: 978-0-470-01079-2.
- [188] R. Härtle et al. “Cooling by heating in nonequilibrium nanosystems”. *Physical Review B* **98.8** (2018), p. 081404. DOI: 10.1103/PhysRevB.98.081404.
- [189] Ryoma Hayakawa, Toyohiro Chikyow, and Yutaka Wakayama. “Vertical resonant tunneling transistors with molecular quantum dots for large-scale integration”. *Nanoscale* **9.31** (2017), pp. 11297–11302. DOI: <https://doi.org/10.1039/C7NR02463K>.
- [190] C. Holmqvist, W. Belzig, and M. Fogelström. “Non-equilibrium charge and spin transport in superconducting-ferromagnetic-superconducting point contacts”. *Philosophical Transactions of the Royal Society of London. A*.

- Mathematical, Physical and Engineering Sciences* **376**.2125 (2018). Id/No 20150229, p. 13. DOI: 10.1098/rsta.2015.0229.
- [191] J. Hwang et al. “A single-molecule optical transistor”. *Nature* **460**.7251 (2009), pp. 76–80. DOI: 10.1038/nature08134.
- [192] Yoseph Imry. *Introduction to mesoscopic physics*. New York: Oxford University Press, 1997. ISBN: 9781602560949.
- [193] Jens Koch, Felix von Oppen, and A. V. Andreev. “Theory of the Franck-Condon blockade regime”. *Physical Review B* **74**.20 (2006), p. 205438. DOI: <https://doi.org/10.1103/PhysRevB.74.205438>.
- [194] P. Krantz et al. “A quantum engineer’s guide to superconducting qubits”. *Applied Physics Reviews* **6**.2 (2019), p. 021318. DOI: 10.1063/1.5089550.
- [195] Thilo Krause et al. “Thermodynamics of the polaron master equation at finite bias”. *The Journal of Chemical Physics* **142**.13 (2015), p. 134106. DOI: <https://doi.org/10.1063/1.4916359>.
- [196] Edward A. Laird et al. “Quantum transport in carbon nanotubes”. *Reviews of Modern Physics* **87**.3 (2015), pp. 703–764. DOI: 10.1103/RevModPhys.87.703.
- [197] Lijun Liu et al. “Recent progress of graphene oxide-based multifunctional nanomaterials for cancer treatment”. *Cancer Nanotechnology* **12**.1 (2021). DOI: 10.1186/s12645-021-00087-7.
- [198] G. Micchi, R. Avriller, and F. Pistolesi. “Mechanical Signatures of the Current Blockade Instability in Suspended Carbon Nanotubes”. *Physical Review Letters* **115**.20 (2015), p. 206802. DOI: <https://doi.org/10.1103/PhysRevLett.115.206802>.
- [199] Michael A. Nielsen and Isaac Chuang. *Quantum computation and quantum information*. American Association of Physics Teachers, 2002.
- [200] A. V. Parafilo et al. “Thermoelectric effects in electron chiral tunneling in metallic carbon nanotubes”. *Superlattices and Microstructures* **88** (2015), pp. 72–79. DOI: 10.1016/j.spmi.2015.08.029.
- [201] Hee Chul Park et al. “Coulomb blockade of spin-dependent shuttling”. *Low Temperature Physics* **39**.12 (2013), pp. 1071–1077. DOI: <https://doi.org/10.1063/1.4830420>.

- [202] Mickael L. Perrin et al. “Single-Molecule Resonant Tunneling Diode”. *The Journal of Physical Chemistry C* **119.10** (2015), pp. 5697–5702. DOI: <https://doi.org/10.1021/jp512803s>.
- [203] Uri Peskin. “Quantum transport in the presence of contact vibrations”. *The Journal of Chemical Physics* **151.2** (2019), p. 024108. DOI: <https://doi.org/10.1063/1.5100142>.
- [204] Vladimir Popov. “Resonant Tunneling and Two-dimensional Gate Transistors”. *Different Types of Field-Effect Transistors - Theory and Applications*. InTech, 2017. DOI: 10.5772/intechopen.69069.
- [205] S. Sarpmaz et al. “Tunneling in Suspended Carbon Nanotubes Assisted by Longitudinal Phonons”. *Physical Review Letters* **96.2** (2006), p. 026801. DOI: <https://doi.org/10.1103/PhysRevLett.96.026801>.
- [206] P. Stadler, W. Belzig, and G. Rastelli. “Control of vibrational states by spin-polarized transport in a carbon nanotube resonator”. *Physical Review B* **91.8** (2015), p. 085432. DOI: 10.1103/PhysRevB.91.085432.
- [207] Jan von Delft and D.C. Ralph. “Spectroscopy of discrete energy levels in ultrasmall metallic grains”. *Physics Reports* **345.2-3** (2001), pp. 61–173. DOI: [https://doi.org/10.1016/S0370-1573\(00\)00099-5](https://doi.org/10.1016/S0370-1573(00)00099-5).
- [208] Heng Wang and Guido Burkard. “Creating arbitrary quantum vibrational states in a carbon nanotube”. *Physical Review B* **94.20** (2016), p. 205413. DOI: <https://doi.org/10.1103/PhysRevB.94.205413>.
- [209] Hua Zhang et al. “Recent advances of two-dimensional materials in smart drug delivery nano-systems”. *Bioactive Materials* **5.4** (2020), pp. 1071–1086. DOI: <https://doi.org/10.1016/j.bioactmat.2020.06.012>.
- [210] А. В. Свідзинський. *Математичні методи теоретичної фізики*. 3-е вид. 2 т. Луцьк: Вежа, 2004, с. 620. ISBN: 978-966-02-5132-8.

Appendix A

List of the candidate's publications related to the dissertation

1. **O.M. Bahrova**, S.I. Kulinich, I.V. Krive, Polaronic effects induced by non-equilibrium vibrons in a single-molecule transistor, *Low Temp. Phys.* **46**, No. 7, 671, (2020) [*Fiz. Nizk. Temp.*, **46**, 799 (2020)], DOI: 10.1063/10.0001362
2. **O.M. Bahrova**, L.Y. Gorelik, S.I. Kulinich, Entanglement between charge qubit states and coherent states of nanomechanical resonator generated by ac Josephson effect, *Low Temp. Phys.*, **47**, No. 4, 287, (2021) [*Fiz. Nizk. Temp.*, **47**, 315 (2021)], DOI: 10.1063/10.0003739
3. **O.M. Bahrova**, L.Y. Gorelik, S.I. Kulinich, R.I. Shekhter, H.C. Park, Nanomechanics driven by the superconducting proximity effect, *New J. Phys.*, **24**, 033008 (2022), DOI: 10.1088/1367-2630/ac5758
4. **O.M. Bahrova**, L.Y. Gorelik, S.I. Kulinich, R.I. Shekhter, H.C. Park, Cooling of nanomechanical vibrations by Andreev injection, *Low Temp. Phys.*, **48**, No. 6, 476 (2022) [*Fiz. Nizk. Temp.*, **48**, 535 (2022)], DOI: 10.1063/10.0010443
5. **O.M. Bahrova**, I.V. Krive, How to control transport of spin-polarized electrons via magnetic field in a molecular transistor, Physics and Scientific&Technological progress: student scientific conference, p.3, (2018).
6. **O. M. Bahrova**, S. I. Kulinich, I. V. Krive, Polaronic effects induced by coherent vibrons in a single-molecule transistor, I International Advanced Study Conference Condensed matter & Low Temperature Physics, June 8-14, 2020, Ukraine, Kharkiv, Abstracts, p. 183, (2020).
7. A.D. Shkop, **O.M. Bahrova**, Coulomb and vibration effects in spin-polarized current through a single-molecule transistor, XI Conference of Young Scientists "Problems of Theoretical Physics", December 21-23, 2020, Ukraine, Kyiv, Abstracts, p.15-16, (2020).
8. **O.M. Bahrova**, L.Y. Gorelik, S.I. Kulinich, Schrödinger-cat states generation via mechanical vibrations entangled with a charge qubit, II International Advanced Study Conference Condensed matter & Low Temperature Physics, June 6–12, 2021, Ukraine, Kharkiv, Abstracts, p.201, (2021).

9. **O.M. Bahrova**, L.Y. Gorelik, S.I. Kulinich, H.C. Park, R.I. Shekhter, Self-sustained mechanical oscillations promoted by superconducting proximity effect, The International Symposium on Novel maTerials and quantum Technologies, December 14–17, 2021, Abstracts, p.134, (2021).
10. **O.M. Bahrova**, L.Y. Gorelik, S.I. Kulinich, H.C. Park, R.I. Shekhter, Nanomechanics provoked by Andreev injection, 29th International Conference on Low Temperature Physics, August 18-24, 2022, Abstracts, p.1554 & 1771, (2022).

Appendix B

Information on the approbation of the dissertation results

- Physics and Scientific&Technological progress: student scientific conference (Kharkiv, Ukraine, April 10-12, 2018);
- I International Advanced Study Conference Condensed matter & Low Temperature Physics (Kharkiv, Ukraine, June 8-14, 2020);
- XI Conference of Young Scientists “Problems of Theoretical Physics” (Kyiv, Ukraine (online), December 21-23, 2020);
- II International Advanced Study Conference Condensed matter & Low Temperature Physics (Kharkiv, Ukraine, June 6–12, 2021);
- The International Symposium on Novel maTerials and quantum Technologies, (Kanagawa, Japan (online), December 14–17, 2021);
- Quantum Thermodynamics Conference 2022, (Belfast, United Kingdom (online), June 27-July 1, 2022);
- 29th International Conference on Low Temperature Physics, (Sapporo, Japan (online), August 18-24, 2022);